Bruno Muniz e Souza

Thermodynamics Simulations and Kinetics Modeling of $MgSO_4.7H_2O$ Thermal Decomposition

Tese de Doutorado

Thesis presented to the Programa de Pós-graduação em Engenharia de Materiais e de Processos Químicos e Metalúrgicos of PUC-Rio in partial fulfillment of the requirements for the degree of Doutor em Engenharia de Materiais e de Processos Químicos e Metalúrgicos.

Advisor: Prof. Eduardo de Albuquerque Brocchi
Co-advisor: Prof. Rodrigo Fernandes Magalhães de Souza

Rio de Janeiro
Abril de 2022

Bruno Muniz e Souza

Thermodynamics Simulations and Kinetics Modeling of $MgSO_4.7H_2O$ Thermal Decomposition

Thesis presented to the Programa de Pós-graduação em Engenharia de Materiais e de Processos Químicos e Metalúrgicos of PUC-Rio in partial fulfillment of the requirements for the degree of Doutor em Engenharia de Materiais e de Processos Químicos e Metalúrgicos.
Approved by the Examination Committee.

Prof. Dr. Eduardo de Albuquerque Brocchi
Advisor and President
Engenharia Química e de Materiais – PUC-Rio

Prof. Dr. Rodrigo Fernandes Magalhães de Souza
Co-advisor
Engenharia Química e de Materiais – PUC-Rio

Prof. Dr. Brunno Ferreira dos Santos
Engenharia Química e de Materiais – PUC-Rio

Prof. Dr. Francisco José Moura
Engenharia Química e de Materiais – PUC-Rio

Dra. Iranildes Daniel dos Santos
Instituto Tecnológico Vale

Prof. Dr. Felipe Sombra dos Santos
Escola de Química – UFRJ

Rio de Janeiro, 19 de abril de 2022

Bruno Muniz e Souza

Graduated in Chemical Engineering at the Federal Rural University of Rio de Janeiro in 2013 and obtained his M.Sc Degree in. Materials and Chemical and Metallurgical Process Engineering from the Pontifical Catholic University of Rio de Janeiro in 2016.

Bibliographic data

Souza, Bruno Muniz e

Thermodynamics simulations and kinetics modeling of $MgSO_4.7H_2O$ thermal decomposition / Bruno Muniz e Souza; advisor: Eduardo de Albuquerque Brocchi ; co-advisor: Rodrigo Fernandes Magalhães de Souza. – 2022.

180 f. ; 29,7 cm

Thesis (doctorate)–Pontifical Catholic University of Rio de Janeiro, Department of Chemical and Materials Engineering, 2022.

Includes bibliography

1. Chemical and Materials Engineering – Theses. 2. Magnesium sulfate. 3. Thermal decomposition. 4. Kinetic modeling. 5. Reducing agent. 6. Moisturizing effect. I. Brocchi, Eduardo de Albuquerque. II. Souza, Rodrigo Fernandes Magalhães de. III. Pontifical Catholic University of Rio de Janeiro. Department of Chemical and Materials Engineering. IV. Title.

CDD: 620.11

To my loves, Fabiola and Alice.

My thanks

To my advisor, Professor Eduardo de Albuquerque Brocchi, for the trust placed in me during this journey.

To my co-supervisor, Professor Rodrigo Fernandes Magalhães de Souza, for his dedication and constant support and for the friendship developed during our time together.

To my parents, Jorge and Márcia, for all their dedication during my life and for showing me the importance of studies.

To my friends, for being present at all times and being a fundamental part of my day-to-day.

To the other professors of the Department of Chemical and Materials Engineering, for the knowledge transmitted to me during my journey in this institution.

To the employees of the Chemical and Materials Engineering Department, Carmem Façanha, Leonardo Rabello, Rosely Gonçalves and Matheus de Oliveira, for their attention.

To the technicians of the Chemical and Materials Engineering Department, Henrique Meira da Silva and Vitor Hugo da Cunha, for the technical support provided to me and my project.

To the Pontifical Catholic University of Rio de Janeiro for the opportunity to study at an institution that values excellence in its teaching and research, while supporting students when necessary.

To Vale S.A., for the technical support, which made it possible to conceive and carry out this work

This study was financed in party by the Coordenação de Aperfeiçoamento de Pessoal de Nível Superior – Brasil (CAPES) – Finance Code 001.

Abstract

Souza, Bruno Muniz; Brocchi, Eduardo de Albuquerque (advisor), de Souza, Rodrigo Fernandes Magalhães (Co-Advisor). **Thermodynamics Simulations and Kinetics Modeling of $MgSO_4.7H_2O$ Thermal Decomposition.** Rio de Janeiro, 2022. 180 p. Tese de Doutorado - Departamento de Engenharia Química e de Materiais, Pontifícia Universidade Católica do Rio de Janeiro.

Magnesium sulfate is present in several industrial and mining wastes. It and its derivatives could be reused in various industrial areas, ceasing to be a waste to become part of a process. Its oxide, MgO, can be used in some functions, as a pH regulator, depending on its reactivity. Due to this, its formation must occur at temperatures below the decomposition temperatures of $MgSO_4$. Therefore, this work evaluated aspects of the decomposition of $MgSO_4$ through two articles. Article 1 (Thermodynamics Simulations and Kinetics Modeling of the Thermal Decomposition of $MgSO_4.7H_2O$: Part 1 – Reducing Agent Effect), evaluated the kinetic effect of using carbon, through four different reducing agents, on the thermal decomposition of $MgSO_4*7H_2O$, while article 2 (Thermodynamics Simulations and Kinetics Modeling of the Thermal Decomposition of $MgSO_4.7H_2O$: Part 2 – Hydration Effect) analyzed the influences of the heating rate of the tests and the degree of hydration of the magnesium sulfate used. The thermogravimetric tests carried out throughout these articles used samples with a mass of approximately 10 mg of the mixture (sulfate + reducing agent) and these mixtures had a stoichiometric ratio of 1:1. The experiments carried out in article 1 used reducing agents, charcoal, green coke, breeze coke, and graphite as reducing agents. In article 2, the sulfates analyzed were anhydrous, monohydrate, and heptahydrate and the heating rates used were 5 $K.min^{-1}$, 10 $K.min^{-1}$, 15 $K.min^{-1}$, and 20 $K.min^{-1}$. All data obtained from thermogravimetric tests were processed through mathematical modeling to obtain kinetic data. In article 1, the use of reducing agents proved efficient, reducing the activation energy of magnesium sulfate decomposition from 22.731 $kJ.mol^{-1}$ (pure sulfate) to 340.391 $kJ.mol^{-1}$ (green coke), 196.120 $kJ.mol^{-1}$ (graphite), 191,100 $kJ.mol^{-}$

[1] (coke breeze) and 162,302 kJ.mol^{-1} (charcoal). In article 2, the heating rate was not shown to be a determining factor for the decomposition of $MgSO_4$, in relation to the hydration of magnesium sulfate, the results indicated that a small portion of H_2O in the system can positively influence the decomposition since the average Ea values were 404.5 KJ.mol^{-1} (mono), 407 KJ.mol^{-1} (anhydrous) and 433.3 KJ.mol^{-1} (hepta).

Keywords: Magnesium sulfate, thermal decomposition, kinetic modeling, reducing agent, hydration effect.

Resumo

Souza, Bruno Muniz; Brocchi, Eduardo de Albuquerque; de Souza, Rodrigo Fernandes Magalhães. **Simulação Termodinâmica e Modelagem Cinética da Decomposição Térmica do $MgSO_4.7H_2O$.** Rio de Janeiro, 2022. 180 p. Tese de Doutorado - Departamento de Engenharia Química e de Materiais, Pontifícia Universidade Católica do Rio de Janeiro.

O sulfato de magnésio está presente em diversos rejeitos industriais e de mineração. Ele e seus derivados poderiam ser reaproveitados em várias áreas industriais, deixando de ser um rejeito para se tornar parte de um processo. Seu óxido, MgO, pode ser utilizado em algumas funções, como regulador de pH, dependendo de sua reatividade. Devido a isto sua formação deve ocorrer em temperaturas abaixo das temperaturas de decomposição do $MgSO_4$. Assim sendo este trabalho avaliou aspectos da decomposição do $MgSO_4$ através de dois artigos. O artigo 1 (Thermodynamics Simulations and Kinetics Modeling of the Thermal Decomposition of $MgSO_4.7H_2O$: Part 1 – Reducing Agent Effect), avaliou o efeito cinético da utilização do carbono, através de quatro diferentes agentes redutores, na decomposição térmica do $MgSO_4*7H_2O$, enquanto que o artigo 2 (Thermodynamics Simulations and Kinetics Modeling of the Thermal Decomposition of $MgSO_4.7H_2O$: Part 2 – Hydration Effect) analisou as influências da taxa de aquecimento dos ensaios e do grau de hidratação do sulfato de magnésio utilizado. Os ensaios termogravimétricos realizados ao longo destes artigos, utilizaram amostras com massa de aproximadamente 10 mg de mistura (sulfato + agente redutor) e estas misturas tiveram uma relação estequiométrica de 1:1. Os experimentos realizados no artigo 1, utilizaram como agentes redutores agentes redutores, carvão vegetal, coque verde, coque breeze e grafite. No artigo 2, os sulfatos analisados foram o anidro, o monohidratado e o heptahidratado e as taxas de aquecimento utilizadas foram de 5 $K.min^{-1}$, 10 $K.min^{-1}$, 15 $K.min^{-1}$ e 20 $K.min^{-1}$. Todos os dados obtidos dos ensaios termogravimétricos foram processados através de modelagem matemática para se obter os dados cinéticos. No artigo 1 a utilização dos agentes redutores se mostrou eficiente reduzindo a energia de ativação da

decomposição do sulfato de magnésio de 22,731 kJ.mol^{-1} (sulfato puro) para 340,391 kJ.mol^{-1} (coque verde), 196,120 kJ.mol^{-1} (grafite), 191,100 kJ.mol^{-1} (coque breeze) e 162,302 kJ.mol^{-1} (carvão vegetal). No artigo 2, a taxa de aquecimento não se mostrou como um fator determinante para a decomposição do $MgSO_4$, já em relação a hidratação do sulfato de magnésio, os resultados indicaram que uma pequena parcela de H_2O no sistema pode influenciar positivamente a decomposição, visto que os valores de Ea médio foram de 404,5 KJ.mol^{-1} (mono), 407 KJ.mol^{-1} (anidro) e 433,3 KJ.mol^{-1} (hepta).

Palavras-chave: Sulfato de magnésio, decomposição térmica, modelagem cinética, agente redutor, efeito da hidratação.

Summary

Figure list

Table list

1. Introduction

1.1. Context

The United Nations (UN) Environment Program's International Resource Panel presented in its report Global Resources Outlook 2019: Natural Resources for the Future We Want, the evolution of the world extraction of the four main groups of natural resources. The report shows a growth in world extraction from 27.1 billion tons in 1970 to 92.1 billion tons in 2017. According to data presented between the years 1970 and 2000, world extraction showed a growth of 2.3 % per year, between 2000 and 2017 this growth increased to 3.2% per year (OBERLE et al., 2020).

According to the projections presented by the UN, the world population in 1970 was 3.7 billion while the population in 2017 was 7.5 billion, an increase of approximately 2.2% per year. However, when looking at growth after 2000, this rate drops to 1.3% per year (UN DEPARTMENT OF ECONOMICS AND SOCIAL AFFAIRS, 2019; UNITED NATIONS, 2019). Comparing the data on the growth of the world population and the data on the growth of the world extraction, it is possible to identify that in the year 1970 7300 kg of natural resources were extracted per inhabitant, this number rose to 12300 kg/inhabitant. This growth is in line with ALI *et al*., (2017), who indicated in their work that greater amounts of metals will be needed than those currently extracted so that more sustainable development is possible.

The United Nations Environment Program also presents data on the extraction of metallic minerals in its survey. This extraction totaled 2.6 billion tons in 1970, while in 2017 9.1 tons were extracted, this variation represents an increase of 2.7% per year to the amount extracted and an increase of approximately 0.5% to the total number of resources extracted (OBERLE et al., 2020).

Despite the constant growth in the extraction of natural resources, over the years this extraction has been going through a process of concentration. If in 1970 ten countries were responsible for 64% of world extraction, in 2017 these countries accounted for 68% of the total amount.

Among these countries, China stands out, accounting for more than 33% of world extraction. India, the United States, and Brazil, respectively, complete the four highest world extraction rates (OBERLE et al., 2020).

Leader in world extraction, China is responsible for the production of approximately 85% of the world's magnesium. This great concentration makes the world extremely dependent on a single country and consequently vulnerable to any decision that may be taken by it. In September 2021, to reduce the emission of gases caused by burning coal, some Chinese provinces reduced the production of magnesium, causing an increase in the amount of the metal trapped by up to five times (BURTON, 2021; DALY, 2021; RAM, 2021; THE ECONOMIST, 2021).

The increase in the value of the magnesium as a consequence of a momentary shortage caused by the decrease in production. Since magnesium is an important part of aluminum alloys, this shortage has left several sectors on alert, from sectors such as packaging manufacturing to the automotive sector (BURTON, 2021; DALY, 2021; RAM, 2021; THE ECONOMIST, 2021). This super dependence generates economic instability for companies and generates tension for thousands of employees.

Due to this dependence and a low magnesium recycling rate (only 13%), the European Union has placed magnesium among the critical and essential raw materials for development (EUROPEAN COMMISSION, 2020). In the literature it is possible to find some works addressing the recycling of magnesium, however most of them address the recycling of metallic magnesium (BROWN, 2000; JAVAID et al., 2006; OSLANEC; IŽDINSKÝ; SIMANČÍK, 2008; YAM et al., 2020; ZHU et al., 2016).

Another possibility to reduce this dependence is the use of residues containing magnesium, industrial or mining, as a source of magnesium. The processing of several other metals of interest generates some form of magnesium in their residue. In the literature, it is possible to find some works dealing with these ores, such as ores of aluminum, tin, iron, lithium, nickel, gold, titanium, vanadium, and zinc (BARBOSA; GONZÁLEZ; DEL CARMEN RUIZ, 2015; BROCCHI; MOURA, 2008; CHENG et al., 2010; DA SILVA,

2018; GUAN et al., 2016; HARVEY; HANNAH; VAUGHAN, 2011; JENA; DRESLER; REILLY, 1995; LI et al., 2018; LIU; NAIDU, 2014; MACCARTHY et al., 2016; MOODLEY et al., 2012; OZGA; RIESENKAMPF, 1996; SUK; KOTELNIKOV; KOVALSKII, 2009; WANDERLEY, 2018; WANG et al., 2016b; ZHANG et al., 2019).

As one of the countries with the highest extraction rates in the world, Brazil has large reserves of a series of ores, such as aluminum, tin, iron, nickel, titanium, and vanadium (U.S. GEOLOGICAL SURVEY, 2021). Although the mining search is always for reserves with the highest content of the metals of interest, some naturally present very low contents, such as the Brazil domestic reserves of vanadium, which present contents between 1% and 1.5% and, these values are the highest vanadium content in the world (DA SILVA, 2018). Another metal that has a low reserve content in the country is nickel, with values between 0.29% and 2% (ANM, 2020).

The low metals content found in these reserves imply huge amounts of tailings. In Brazil, the gross extraction of nickel reserves totaled approximately 5.5 million tonnes of ores. with an average content of 1.38% (ANM, 2020). In the literature, it is possible to find works that show nickel ores with MgO contents of up to 29% (FAN et al., 2012; GARCES-GRANDA; LAPIDUS; RESTREPO-BAENA, 2018; MACCARTHY et al., 2016; STOPIC; FRIEDRICH, 2016; WHITTINGTON; MUIR, 2000; XIAO et al., 2020)

In addition to magnesium, nickel ores typically contain other metals in large amounts, such as iron, cobalt, aluminum, and silicon. They may also contain other elements in smaller amounts, such as manganese, chromium, calcium, potassium, phosphorus, and sulfur. (FAN et al., 2012; MACCARTHY et al., 2016; MCDONALD; WHITTINGTON, 2008; STOPIC; FRIEDRICH, 2016; STOPIC; FRIEDRICH; FUCHS, 2003; WHITTINGTON, 2000; ZHAI et al., 2009). Due to the complexity in ore processing, caused by a large number of chemical components and by their low concentrations, hydrometallurgical processing by acid leaching is a good option and presents a growth, in its use in relation to other methods (OXLEY; BARCZA, 2013).

In acid leaching, the leaching agent reacts with the ore, causing its decomposition and resulting in an aqueous solution containing the metal ions present in the ore (WANDERLEY, 2018). Among the leaching agents, sulfuric acid is widely used in the processing of nickel ores (KAYA; TOPKAYA, 2011; STOPIC; FRIEDRICH, 2016; WANDERLEY, 2018). Its use results in a solution with a high content of SO_4^{-2}.

This aqueous solution undergoes different processes to recover the metals of interest at high concentration levels. In nickel ores processing, it is also possible to obtain iron, aluminum, copper, and cobalt with desired concentrations (AGATZINI-LEONARDOU et al., 2009; WANDERLEY et al., 2020). The other metals present in the ore structure in lower content and without economic interest, are removed from the acid solution through a pH neutralization. Magnesium oxide is among the neutralizing agents used for this process (STOPIC; FRIEDRICH, 2016). The use of magnesium oxide becomes interesting since the oxide can be obtained through the decomposition of magnesium sulfate. The compound is formed by ions present in the tailings of nickel ores processing (MELLO et al., 2020).

1.2. Justification and relevance

The use of magnesium oxide as a pH regulating agent is only possible if it presents characteristics that result in an appropriate reactivity for the system to be neutralized. These characteristics are influenced by the reactional conditions of oxide formation. This makes the study of this reaction system important, since temperature and reaction atmosphere are among the factors that influence the reactivity if MgO (SOUZA et al., 2020).

The decomposition reaction of magnesium sulfate to the formation of magnesium oxide can be carried out under different operating conditions and therefore it is interesting to have a broad literary base. When analyzing the thermodynamic conditions of the thermal decomposition of $MgSO_4$, the literature presents a good variety of studies (PLEWA; STEINDOR, 1987; SCHEIDEMA, 2015; SCHEIDEMA; TASKINEN, 2011; SOUZA et al., 2020). Concerning the thermodynamic analyzes of the reducing thermal decomposition of $MgSO_4$, the subject, despite not having a theoretical

amplitude close to that of the decomposition without the reducing agent, presents a range of works that provide a good theoretical basis.

If there is a good number of works in the literature addressing the thermodynamics of magnesium sulfate decomposition, the analysis of the kinetic data does not present the same literary coverage. The few works available in the literature with a kinetic approach concerning the decomposition of $MgSO_4$, do not present any comparison between more than two different reaction systems. (HULBERT, 1968; L'VOV; UGOLKOV, 2004; MELLO et al., 2020; PLEWA; STEINDOR, 1987).

Therefore, the present work aims to contribute to the increase of the theoretical basis regarding the kinetic and thermodynamic analysis of magnesium sulfate decomposition, through the analysis of different variables and the comparison between them.

1.3. Objective

1.3.1. General

Given the context presented during the introduction and to contribute to the literature, this work aimed to evaluate, kinetically and thermodynamically, factors that can positively influence the thermal decomposition of magnesium sulfate and to analyze the behavior of the proposed systems for these decompositions. This evaluation was carried out with a focus on studying the influence of the following factors: the presence of reducing agents, the use of different heating rates, and the degree of hydration of the decomposed magnesium sulfate.

This study was proposed to evaluate the reaction system gradually, and therefore the experiments were carried out to describe an evaluative line.

1.3.2. Specifics

- Carry out thermogravimetric tests, within a temperature range and with a single heating rate, to evaluate the influence of four different carbon sources on the thermal decomposition behavior of magnesium sulfate heptahydrate.

- Carry out non-isothermal thermogravimetric tests to analyze the influence of different heating rates in the tests and different levels of hydration of magnesium sulfates.
- Apply the data obtained in thermogravimetric tests to a mathematical model to obtain kinetic parameters and thereby contribute to the discussions proposed in this work.

These objectives were worked on and presented throughout two articles that make up this thesis.

.

2. Literature review

2.1. Magnesium

Eighth most abundant element in the earth's crust and third in seawater, magnesium does not occur in pure form in nature but is naturally present in seawater, minerals, and brines. The metal belongs to the alkaline earth group, has a grayish appearance, good reactivity, and produces an intense white glow during burning (AL-TABBAA, 2013; HABASHI, 1997; YAROSHEVSKY, 2006). Metallic magnesium was first isolated in 1808 through the electrolysis of magnesium chloride. In 1886, magnesium was produced industrially for the first time, also by electrolysis (HABASHI, 1997)

Its characteristics and properties make it used in several sectors, such as the aerospace industry where it is used due to the low density, structural strength, and electromagnetic shielding that it adds to metallic alloys (HAN et al., 2020; MEHRA; MAHAPATRA; HARSHA, 2018; VEDABOURISWARAN; ARAVINDAN, 2018), in the automobile industry due to its good castability and damping capacity (LUO; SACHDEV, 2012; PAN; YANG; CHEN, 2016) and in medicine since it is important in the prevention of osteoporosis, helping in bone calcification and influencing human metabolism (AINA et al., 2012; MARCHI et al., 2007; SABATIER et al., 2011).

Tang *et al.* (2017) and Liu *et al.* (2013) indicated that magnesium compounds can be used for phosphorus recovery in wastewater and sewage. Zhao *et al.* (2020) pointed to the use of magnesium present in steel slag to capture CO_2. In addition to the specific uses of magnesium, it can be used to replace other elements, such as aluminum, bromine, lithium, thorium, yttrium, zinc (U.S. GEOLOGICAL SURVEY, 2021)

Magnesium occurs naturally in several forms: carbonate, being the form responsible for the main sources of production; chloride, found mostly in seawater; sulfate, the only form that does not present anhydrous compounds; and even rarely in the oxide and hydroxide forms (HABASHI, 1997).

The main source of magnesium in Brazil is magnesite, another ore widely used in the world as a source of magnesium is dolomite (MME, 2020; SILVA, 2018). Magnesite ($MgCO_{3)}$ has approximately 29% of the mass related to magnesium, while dolomite [$CaMg(CO_3)_2$] has 13% magnesium in its structure. According to the Webmineral database, there are more than 230 minerals cataloged containing at least 10% by mass composed of magnesium in their structures, several of which contain other metals and serve as a source for processing these metals (WEBMINERAL, 2022).

Despite magnesium being one of the most abundant metals in the world, usable deposits are concentrated in a few places. This particularity makes it essential to search for processes that allow the reuse of waste containing magnesium (ALI et al., 2017; EUROPEAN COMMISSION, 2020; THE WORLD BANK, 2017; U.S. GEOLOGICAL SURVEY, 2021). Magnesium recycling was during the second world war the main source of metal in Europe, after the second war the number of companies dedicated to magnesium recycling was reduced (BROWN, 2000).

According to the study carried out by the European Union, the current magnesium recycling rate is 13% and represents the dimension of the challenge (EUROPEAN COMMISSION, 2020). Even in China, the country responsible for the highest rates of extraction and production of magnesium compounds in the world, work is being carried out in search of procedures that favor the recycling and reuse of waste containing magnesium (DALY, 2021; GAO et al., 2021; JIAO et al., 2019; THE ECONOMIST, 2021).

2.2. Magnesium sulfate

Magnesium sulfate can be used in a wide range of industries. Having its use in food industries, extractive metallurgy, cosmetics industries, agriculture, pharmaceutical industries, pulp, and paper industries, the manufacture of products such as detergents and rubbers, and in the treatment of functional constipation (COSTA, 2020; CURRY; VAN OSS, 2020; DUPONT; CAMPAGNE; CONSTANT, 2014; LI et al., 2010; YANFEI et al., 2015). In the chemical industry, magnesium sulfate can be used as a precursor for other compounds such as MgO (SOUZA et al., 2020).

$MgSO_4$ has an interesting solubility curve that shows two different behaviors between 293 K and 513 K. Between 293 K and 363 K, the solubility increases with increasing temperature, however, from 363 K onwards, this trend is reversed and the solubility starts to decrease with increasing temperature (COSTA, 2020; LI et al., 2010).

Wang *et al.* (1999) used in your study $MgSO_4$ in your anhydrous and monohydrate forms how catalysts for the formation of a diamond from high graphite pressures. Chipera and Vaniman (2007), report in their work on the possibility of the existence of a large amount of hydrated magnesium sulfate on Mars, indicating a possible source of hydrogen on Mars. Scheidema (2015) Magnesium sulfate can be crystallized from solution and decomposed into magnesium oxide and sulfur dioxide.

Habashi (1997) highlights that magnesium sulfate is a hygroscopic compound and absorbs water until the formation of the heptahydrate form, so it does not occur naturally in the anhydrous form. The author indicates that there are five stable sulfate hydrates: $MgSO_4*12H_2O$, $MgSO_4*7H_2O$, $MgSO_4*6H_2O$, $MgSO_4*5/4H_2O$, and $MgSO_4*H_2O$. Having five stable hydrates, magnesium sulfate only occurs naturally in the forms of Epsomite (heptahydrate) and Kieserite (monohydrate), the other forms are achieved through crystallization and dehydration (SCHEIDEMA; TASKINEN; METSÄRINTA, 2011).

Habashi (1997) indicates that anhydrous magnesium sulfate can be formed between 673 and 773 K. In the literature, some works present experiments on the dehydration of sulfates. Genceli *et al.* (2007) studied the dehydration of $MgSO_4*11H_2O$ in an atmosphere of helium gas and a heating rate of 5 $K.m^{-1}$, the authors reached complete dehydration at 498 K. Brancato *et al.* (2018) performed the complete dehydration of $MgSO_4*7H_2O$ up to 573 K with a heating rate of 1 $K.m^{-1}$ and an inert nitrogen atmosphere. Souza et al. (2020) obtained anhydrous sulfate by dehydrating sulfate heptahydrate at temperatures between 373 K and 623 K, in an inert nitrogen atmosphere and with a heating rate of 15 $K.m^{-1}$.

Okrimenko *et al.* (2020) analyzed the possibility of heat storage through hydrated salts. The authors highlighted that among the hydrated salts, the hydrated sulfates are among those with the highest heat storage potential. The total dehydration of magnesium sulfate heptahydrate has a theoretical storage energy density of 2.8 $GJ.m^{-3}$.

Brancato *et al.* (2018) and Okhrimenko *et al.* (2020) identified that the complete dehydration of $MgSO_4*7H_2O$ occurs in three steps, changing from heptahydrate to hexahydrate, from hexahydrate to monohydrate, and from monohydrate to anhydrous form.

2.3. Magnesium oxide

Magnesium oxide is the most consumed magnesium compound in the world in recent years (CURRY; VAN OSS, 2020; U.S. GEOLOGICAL SURVEY, 2021). MgO is a basic oxide and stands out for having the lowest solubility among alkaline earth metal oxides, this characteristic makes this oxide have good potential to be used as a reusable catalyst (BARTLEY et al., 2012).

In the literature, several works present ways of using the compound, among them are: Asencios *et al.* (2012) showed that MgO can be used as a catalyst, Pilarska *et al.* (2017) pointed out the use as an antibacterial and anticorrosive agent, as a fire-resistant and insulating material and as an active adsorbent of solid and gaseous impurities, Al-Tabbaa (2013) indicated the compound as an important component for the formation of types of cement, Caldas (2019) points to the use during the formation of iron ore pellets.

Scheidema (2015) highlighted that magnesium oxide can be used as a neutralizing agent. This use is important because it allows the recirculation of MgO to the flowcharts from which $MgSO_4$ was removed, so MgO can replace the use of other pH regulators (FREITAS et al., 2009; MO; DENG; TANG, 2010; SCHEIDEMA; TASKINEN, 2011).

Some works such as Souza *et al.* (2020), Cardoso (2018) and Scheidema *et al.* (2011), indicate that the MgO obtained by the

decomposition of $MgSO_4$, can be used as a neutralizing agent. However, for it to be used with this function, the oxide must have specific characteristics, such as porosity and high surface areas. These characteristics are of paramount importance for the compound to have a high reactivity (MO; DENG; TANG, 2010). Jin and Al-Tabbaa (2014) and Scheidema and Taskinen (2011) highlighted that in decompositions with temperatures above 1273 K, the oxides formed do not present the necessary characteristics for this use.

Aphane *et al.* (2009) analyzed the surface area of MgO obtained from $MgCO_3$, with temperatures of 823, 1273, and 1473 K. The experiments revealed that the oxide obtained at 823 K had a surface area of 21.17 $m^2.g^{-1}$, for the oxide obtained at 1273 K the surface area was 11.72 $m^2.g^{-1}$ and the oxide formed at 1473 K obtained a surface area of 4.32 $m^2.g^{-1}$.

Bartley *et al.* (2012) investigated the production of MgO from the decomposition of four precursors, $(MgCO_3)_4Mg(OH)_2$, $Mg(OH)_2$, $MgCO_3$, and MgC_2O_4. The authors highlighted that the reactivity of the oxides formed was dependent on the conditions of their formation. The authors obtained an oxide with a high surface area from the precursors, in all cases, the oxides had a surface area greater than 200 $m^2.g^{-1}$.

Dong *et al.* (2017) obtained MgO from $Mg(OH)_2$ from a brine. The oxide was produced at 773 K and a time of 2 hours and reached a surface area of 78.8 $m^2.g^{-1}$.

2.4. Waste containing magnesium

Being present in several minerals used in other processes, it is natural that the residues of these processes contain plausible amounts of magnesium for use and recovery. According to the nature of the ore processing, this residue may present a mixture of metals or only magnesium, it may be a solid residue or an aqueous solution.

2.4.1. Solid waste

Özdemir et al. (2009) analyzed tailings from magnesite beneficiation plants in Turkey. The authors reported that these tailings were only stored in the plants, instead of being reused. An analysis of the chemical composition of these tailings indicated content of up to 39% of MgO. Costa (2020) investigated a residue from the flotation of zinc ores, the characterization of this tailing indicated that content of 81.7% by weight of dolomite [$CaMg(CO_3)_2$], after magnetic separation, the content of $CaMg(CO_3)_2$ increased to 90.3% by weight of the non-magnetic portion.

Brocchi and Moura (2008) studied the chlorination of tin slag. The authors identified the presence of magnesium in the composition of this slag and the results found indicated that the metal remained in the slag after chlorination by carbon tetrachloride.

Dong *et al.* (2018) analyzed the chemical composition of the tailings of brine from a desalination plant in Singapore and detected the presence of magnesium. Cipollina *et al.* (2015) analyzed a brine from a desalination industry in the city of Trapani, in the Sicily region of Italy. The authors point out that in brines the concentration of magnesium can reach up to 40 $kg.m^{-3}$, a concentration up to 30 times greater than that of seawater.

Moodley *et al.* (2012) analyzed the carbochlorination of two titania slags, a rutile sample, and a synthetic rutile sample and identified the presence of magnesium in all samples, however, magnesium was completely chlorinated during the experiments. Wang *et al.* (2016b) examined the carbochlorination of a titania slag from Sichuan, China, and, through the analysis of the chemical composition performed before and after the procedure, verified the presence of magnesium in both samples.

Jena *et al.* (1995) identified the presence of magnesium in the slag from the processing of titanomagnetite ores with vanadium. Zhang *et al.* (2019) analyzed a slag from the processing of a vanadium ore from a Chinese steel mill. During this analysis, the authors identified magnesium in the slag, which was also present in the solution after leaching. Da Silva (2018) analyzed the mineral tailings from a vanadium production line and performed the characterization of these tailings to determine their

composition. This characterization determined that magnesium corresponds to approximately 10% of the sample.

Damayanti and Khaerunissa (2016) analyzed the chemical composition of tailings from Indonesian bauxite ore and identified the presence of magnesium in the oxide form, Khairul *et al.* (2019) also reported the presence of magnesium in bauxite tailings. Li *et al.* (2018) investigated the recovery of gold and silver in cyanide tailings containing magnesium, after chlorination of the tailings, the authors detected that more than 75% of the magnesium remains in the tailings.

2.4.2. Aqueous waste

Paul *et al.* (2012) analyzed tailings from six textile industries in Solapur, India. The chemical analyzes of the tailings identified the presence of magnesium in the tailings of the six industries. Tolonen *et al.* (2015) identified the presence of magnesium in mine water samples.

Ozga and Riesenkampf (1996) described the presence of magnesium in zinc ores through two compounds, a zinc magnesium oxide, (Zn,Mg)O, and a ferrite, (Zn,Mg,Fe)Fe_2O_4. Booster *et al.* (2000) reported the presence of dissolved magnesium in zinc mineral processing solutions and analyzed the possibility of separation through selective precipitation. Kim and Azimi (2022) indicated magnesium as one of the constituents of the liquor from steel slag leaching and analyzed its precipitation.

Among the works reporting the existence of magnesium in aqueous residues, the numerous works related to residues from the processing of lateritic nickel ores stand out. McCarthy *et al.* (2016) performed one analysis chemical and detected the presence of magnesium in one sample of lateritic nickel ore from the region of Australia's western and our products from the leaching stages performed during ore processing.

Xue-Yi *et al.* (2010) reported that 95% of the magnesium present in a lateritic ore sample from the Tubay region, Philippines, is dissolved by sulfuric acid and remains in the leached solution. Guan *et al.* (2016) studied different nickel and cobalt recovery processes present in the liquor resulting

from the leaching of lateritic ores. The methods proposed by the authors obtained a higher degree of recovery of 98% of Ni and Co, with that the leached solution contained only magnesium and calcium at the end of the processing. Harvey *et al.* (2011), reported the use of magnesium oxide during the Ni and Co recovery process by precipitation.

2.5. Magnesium recovery

Since magnesium is present in a series of residues, from different processes and at different stages, it is possible to find in the literature a vast number of studies reporting processes in search of the recovery of magnesium and its compounds.

Brown (2000) points out that the low density of solid magnesium compounds brings greater challenges to their recycling, making larger quantities indispensable to reduce the cost of recycling. The reuse of aqueous waste is an alternative to this difficulty.

Several works have been carried out to develop techniques for the reuse of magnesium present in tailings and disposal, from tailings from the manufacture of magnesium itself, through waste from the seawater desalination process, to waste from machining processes (COURTIAL; CABRILLAC; DUVAL, 1994; MAHMUD et al., 2022; OSLANEC; IŽDINSKÝ; SIMANČÍK, 2008; YAM et al., 2020).

Highfield *et al.* (2012) studied the recovery of Mg from a serpentine sample [$(Mg,Al)_3(Si,Fe)_2O_5(OH)_4$]. The recovery of magnesium as $MgSO_4*7O_2O$ resulted in a rate of 50 to 60%, whereas the recovery in the form of [$(NH_4)_2Mg_2(SO_4)_3$] had a recovery rate of 90%.

Özdemir *et al.* (2009) in their work analyzed the recovery of magnesium from the tailings of magnesite beneficiation plants, through leaching by hydrochloric acid. Magnesium recovery was carried out in the form of $MgCl_2*6H_2O$ and obtained a rate of 92%. $MgCl_2*6H_2O$ was crystallized to a purity of 91% by evaporating the leaching solution. The authors also indicated that the final residue of this process consisted of 93%

SiO_2, 2.3% MgO, and 3.4% H_2O and can still be used in the ceramic, cement, and glass industries.

Cipollina *et al.* (2015) studied the recovery of magnesium present in brines through reactive precipitation, with NaOH as an alkaline reagent. Magnesium recovery occurs in the form of $Mg(OH)_2$, it obtained purity of greater than 98% and a recovery of 100% of the magnesium present in the brine. Li *et al.* (2019b) analyzed in their work the separation of magnesium and lithium in brine (15 $g.L^{-1}$ of Mg, 80 $g.L^{-1}$ of Na, and 0.2 $g.L^{-1}$ of Li). The authors performed an extraction of almost 100% of the magnesium present in the brine.

Kim and Azimi (2022) studied the selective precipitation of magnesium present in steel slag in the form of magnesium hydroxide. Through the use of NaOH as a precipitating agent, this precipitation occurred at 9.6 pH. The recovery of Mg was 100% and the precipitated $Mg(OH)_2$ obtained a purity degree of greater than 90%.

Among the works present in the literature on the processing of lateritic nickel ores, some analyze the recovery of magnesium present in these systems. Karidakis *et al.* (2005) and Wanderley *et al.* (2020) indicate that a typical lateritic nickel ores processing flowchart has as final residue an acidic solution containing only aqueous magnesium sulfate.

Karidakis *et al.* (2005) studied the recovery of magnesium from leaching liquor. The authors present a recovery process through the addition of calcium hydroxide [$Ca(OH)_2$], in this process the magnesium is precipitated in the form of the hydroxide $Mg(OH)_2$.

Liu *et al.* (2012) investigated the recovery of magnesium present in low-grade nickel ore. The recovery was carried out after a roasting procedure, at 673 K and 2h, with ammonium sulfate followed by a leaching step with water and reached a rate of 62.15%.

Meng *et al.* (2015) studied the separation of Mg from the other compounds present in the liquor from the leaching of nickel ore and serpentine. The authors performed the separation by means of alkaline

oxidation and acid leaching and obtained a degree of recovery of 99% of magnesium. Magnesium was recovered in the form of MgO with a content of 91.9%.

2.5.1. Ore leaching liquor wastes

The processing of a series of ores has, without its flowcharts, acid leaching steps, to carry out the digestion of the metals present in the structure of the ores, among these, we can highlight ores of nickel, cobalt, zinc, vanadium, titanium, copper, silicon, boron, uranium and niobium (BROCCHI; MOURA, 2008; DA SILVA, 2018; FERNANDES et al., 2007; LEMOS; ANGORA; MASSON, 2007; LI et al., 2010; LÜDKE, 2018; WANDERLEY, 2018; ZHANG; ZHU; CHENG, 2011).

Sulfuric acid (H_2SO_4) is one of the most used acids in the industry and is also heavily used in the processing of ores as a leaching agent (AGATZINI-LEONARDOU et al., 2009; NKOSI et al., 2017; ROSITA et al., 2020; SAHOO; NAIK; DAS, 2001; SOUZA et al., 2007; STOPIC; FRIEDRICH; FUCHS, 2003; UROSEVIC et al., 2015; YÖRÜKOĞLU; OBUT; GIRGIN, 2003; ZHAI et al., 2009). The acid has three characteristics that make it very versatile: it is soluble in water, it is a strong oxidant, and it is highly corrosive.

In the leaching step, the use of sulfuric acid has the function of carrying out the complete digestion of the compounds present in the ores, according to unbalanced equations 1 and 2, thus breaking their structures and forming acidic aqueous solutions containing the dissolved metals (KHOO; HAQUE; BHATTACHARYA, 2017; STOPIC; FRIEDRICH; FUCHS, 2003; WANDERLEY, 2018; WHITTINGTON, 2000; YANG et al., 2021). In addition to the presence of ions from the ores, the solution also contains the SO_4^{2-} ion.

$$MeO + H_2SO_4 \rightarrow Me(SO_4)_{(aq)} + H_2O \quad (1)$$

$$Me(SO_4)_{(aq)} = Me^{+} + SO_4^{2-} \quad (2)$$

After the leaching step, the metals of interest can be recovered by some techniques, which vary according to the composition of the aqueous

solution and the needs presented by it. Among the techniques used for the recovery of the metals of interest is precipitation by pH variation (INEICH et al., 2017; MACINGOVA; LUPTAKOVA, 2012), ion exchange (DĄBROWSKI et al., 2004; KOVACHEVA; DJINGOVA, 2002; YANFEI et al., 2015), by solvent extraction (CHENG et al., 2011; KONGOLO et al., 2003; ZHANG et al., 2019).

After the stages of recovery of the metals of interest, some metals, which are not the focus of the production line, remain in the aqueous solution and are discarded as waste from the processes. Several wastes, whether extraction or industrial, contain magnesium and sulfate in ionic forms, so these ions can be synthesized as magnesium sulfate (GAO et al., 2021; MA et al., 2016; ROCHE; PRASAD, 2009; SCHEIDEMA; TASKINEN; METSÄRINTA, 2011; WANDERLEY et al., 2020). Enabling its use in other processes and reducing the number of tailings present in dams.

2.5.2. Magnesium sulfate wasts

Since different residues containing magnesium and sulfate are discarded or stored, it is natural that the literature presents a variety of works addressing the reuse of these residues.

Karidakis et al. (2005) report two different processes for recovering magnesium in the form of sulfates from leaching liquor. For the formation of magnesium sulfate monohydrate ($MgSO_4*H_2O$), the process presented is a non-evaporative crystallization by heating the liquor through an autoclave. For the formation of sulfate heptahydrate ($MgSO_4*7H_2O$), the method is crystallization using evaporation.

Wanderley *et al.* (2020) studied the recovery of magnesium present in the liquor from the leaching of a lateritic mineral. They carried out the recovery of magnesium in the form of $MgSO_4*H_2O$ by the crystallization process and without decomposition of the crystals. The authors constructed a sulfate solubility curve between 303 K and 503 K. The best result achieved was the recovery of 80% of magnesium in five hours, 503 K, and a pH of 5.7.

Costa (2020) carried out the processing of a residue from the flotation stage of zinc ore, the author subjected the residue to magnetic separation and an acid leaching of the non-magnetic portion, to recover the Mg present in it. After these steps, the yield of Mg extraction was approximately 72%, with leaching based on H_2SO_4, the temperature of 323 K, and a time of 35 min. Mg was recovered as $MgSO_4*7H_2O$.

Hajbi *et al.* (2015), reported the crystallization of $MgSO_4$ in two different degrees of hydration, $MgSO_4*7H_2O$ and $MgSO_4*6H_2O$. This crystallization was carried out from the waste of a desalination industry and by the isothermal evaporation process, at 298K.

Li *et al.* (2010) reported in their work, a mass fraction of $MgSO_4$ in the leached solution was between 10 to 20% and carried out the crystallization of $MgSO_4*H_2O$ at 453 K. The results indicate that after 4 h of process, crystallization does not show a significant increase, so the recovery achieved was approximately 45%.

Gao *et al.* (2021), in their study, indicated that up to 363 K, increasing the initial temperature of crystallization of magnesium sulfate resulted in an increase in its crystallization rate. At this temperature and with a crystallization time of 10h, the authors obtained a crystallization rate of 84.25%, magnesium sulfate was obtained with a purity of 99.2%.

2.6. Decomposition of sulfates

Studies evaluating the decomposition of sulfates have been present in the literature for at least seventy years. They show which aspects were analyzed and tell the evolution of these processes.

Brownell (1951) studied the reaction of calcium, strontium, and barium sulfates with silica. In his study, the author analyzed the decomposition of these sulfates at different temperatures up to 1573 K, to make corrections in the necessary amounts of each sulfate during the reactions. For strontium and barium sulfates, a relevant degree of decomposition does not occur until 1573 K. For calcium sulfate, the author identified that decomposition occurred at a relevant rate above 1523 K.

Ostrofft and Sanderson (1959) evaluated the decomposition of eleven different sulfates, $MnSO_4$, $FeSO_4$, $CoSO_4$, $NiSO_4$, $CuSO_4$, $ZnSO_4$, $CdSO_4$, $PbSO_4$, $MgSO_4$, $CaSO_4$, and $SrSO_4$. The authors used thermogravimetric analysis and differential thermal analysis to determine the decomposition temperatures of the anhydrous sulfates. The authors only found intermediate products in the decomposition of copper and zinc sulfates.

Gallagher et al. (1970) determined that the reaction atmosphere influences the decomposition behavior of iron(II), heptahydrate, and monohydrate sulfates. In the presence of O_2, iron(II) sulfate is converted into iron(III) sulfate before the decomposition of the sulfate, while in an inert atmosphere of N_2 the two processes occur at the same time. The authors identified that the presence of moisture decreased the decomposition temperature.

Narayan et al. (1988) when studying the thermal decomposition of zinc sulfate indicated some factors that influence the decomposition, being the sample size, the container material, the hydration of the compound, and the carrier gas. To reduce the effects of heat and mass transfers, the sample size must be smaller, the decomposition temperatures were higher for the experiments using dehydrated compounds, the carrier gas influences the decomposition by changing the partial pressure of the products and the material of the container can current as a process catalyst.

Siriwardane *et al.* (1999) evaluated the decomposition of copper, iron(II), iron(III), nickel, and zinc sulfates in an N_2 atmosphere and a vacuum. The experiments showed that in a vacuum the decomposition temperatures were lower than in experiments in an N_2 atmosphere.

Okumura et al. (2003) analyzed the isothermal reductive decomposition of calcium sulfate at temperatures of 1669 and 1819 K. The tests were carried out with reactional atmospheres of CO and CO/CO_2, in addition to N_2 as an inert gas. The highest conversion rate of $CaSO_4$ to CaO was 91% and was reached at a temperature of 1819 K and an atmosphere composed of 2% CO, 30% CO_2, and the remainder N_2. The decompositions

formed CaO in the assays without the presence of CO_2 and formed CaS with the presence of the compound.

Hoteit et al., (2007) evaluated the influences of temperature and the presence of carbon monoxide on the decomposition of $CaSO_4$. The experiments were carried out with a temperature between 1073 and 1223 K and concentrations of 2%, 1%, and 0.5% CO. The results showed that the conversion rate increases with increasing temperature. Increasing the concentration of CO influences two aspects of the system, it increases the initial rate of the reaction, but it decreases the final conversion of decomposition. The best conversion was 52% and was achieved at 1223 K and 0.5% CO.

Kanari *et al.* (2018) also evaluated the thermal decomposition of iron(II) sulfates, heptahydrate, and monohydrate. The authors evaluated the decomposition in $Cl_2 + O_2$, O_2, and N_2 atmospheres. In an N_2 atmosphere, the sulfate heptahydrate was completely dehydrated to 573 K. In the oxidizing atmosphere and at the same temperature, $FeSO_4*7H_2O$ was transformed into $Fe^{III}SO_4*OH$. Starting at 773 K, both $FeSO_4$ and $Fe^{III}SO_4*OH$ were decomposed to form Fe_2O_3.

Souza *et al.* (2019) analyzed the decomposition of $KAl(SO_4)_2*12H_2O$ in the presence of a solid reducing agent, charcoal, in an atmosphere of N_2. Dehydration occurred before the start of decomposition with and without the catalyst. The experiments indicated that the presence of the reducing agent at the initial temperature of decomposition was decreased by 170 K, from 1023 K to 853 K.

Kurban *et al.* (2022) while investigating the decomposition behavior of $ZnSO_4*H_2O$ with or without the presence of a catalyst, Pd/Al_2O_3, reported that although the catalyst does not decrease the initial decomposition temperature, it does decrease the final decomposition temperature. The presence of the catalyst also modifies the behavior of the decomposition, transforming the decomposition that was in two steps to one in a single step.

Brownell (1951) evaluated the reaction of anhydrous magnesium sulfate with silica. The author identified that from 1173 K onwards considerable sulfate decomposition occurs, thus making the reaction with silica impossible. Ostrofft and Sanderson (1959) obtained a decomposition temperature for anhydrous $MgSO_4$ of 1168 K.

Plewa and Steindor (1987) experimentally demonstrated that above 898 K magnesium sulfate is not stable and in the presence of CO, $MgSO_4$ decomposes from 823 K. The authors identified that between 913 and 948 K, the rate of decomposition is controlled by the chemical reaction.

Scheidema and Taskinen (2011) indicated that, according to the thermodynamic data, the presence of reducing agents can reduce the decomposition temperature of $MgSO_4$ by up to 500 K. The thermodynamic values indicated the decomposition of pure sulfate at 1358 K and in the presence of CO, S_2 and H_2, at 865 K, 896 K, and 879 K respectively.

Scheidema *et al.* (2011) reported that the rate of magnesium sulfate decomposition is influenced by particle size and temperature. According to the authors, the decomposition of $MgSO_4$ occurs between 1173 K and 1373 K and its products are MgO, SO_2, and O_2.

Ding *et al.* (2011) analyzed the decomposition of $MgSO_4$ in the presence of natural gas, with the proposal to form H_2S, CO_2, and MgO. The authors identified that the presence of H_2O can initiate the thermodynamic reduction of sulfate.

Scheidema and Taskinen (2011) through thermogravimetric tests determined the decomposition temperatures of $MgSO_4$ according to atmospheric compositions. With an atmosphere of 100% N_2, the temperature was 1373 K, with 10% CO and 90% N_2 it was 1343 K, and with 5% H_2 and 95% N_2, it was 1223 K.

Scheidema (2015) highlighted that the decomposition of $MgSO_4$ is a strongly endothermic reaction. The decomposition products generate different products according to the temperature of the system, for

temperatures below 973 K, SO_3 is the product, while above this temperature the products are SO_2 and O_2.

Regarding the decomposition of hydrated magnesium sulfates, several studies indicate that complete dehydration of sulfates occurs before the start of decomposition, regardless of the degree of hydration (OKHRIMENKO et al., 2017, 2020; PAULIK; PAULIK; ARNOLD, 1981; SOUZA et al., 2020; ZHENG et al., 2020).

2.7. Thermogravimetric Analysis

Thermogravimetric analyzes are experiments of mass variation in relation to temperature. These analyzes can be performed in different reaction atmospheres or under vacuum, can be isothermal and non-isothermal, and can be used for different evaluations. In the literature, there are works related to thermal decomposition, analysis of catalysts, and combustion of biological waste, among others (NURUNNABI et al., 2006; SANCHEZ et al., 2009; SOUZA et al., 2020).

According to Ionashiro (2004), the first thermogravimetric analyses date from the beginning of the 20th century, and the first thermobalance was developed by Kotara Honda, in 1915, and operated in an almost isothermal way since the equipment took 10 to 14 hours to reach a variation of 1000 K Current thermogravimetric reach heating rates of up to 1000 $K.min^{-1}$ (NETZSCH, 2022).

Kato *et al.* (1994) performed an activation of a nickel ferrite in an H_2 atmosphere, a flow rate of 50 $cm^3.min^{-1}$ at 573 K. In addition to this activation, the authors used a thermogravimetric analyzer to decompose the activated ferrite in a CO_2 atmosphere and 573K.

Kanari and Gaballah (1999) analyzed the chlorination of MgO through a thermogravimetric analyzer. The experiments used three different gas compositions, Cl_2 + air, Cl_2 + N_2, and Cl_2 + CO, and temperatures below 1273 K.

Okumura *et al.* (2003) used a thermogravimetric analyzer to evaluate the decomposition of calcium sulfate, with different reaction atmospheres. The tests used CO + N_2 and CO + CO_2 + N_2 atmospheres, and temperatures of 1123 K and 1273 K.

Monteiro (2017) used the thermogravimetric analyzer to evaluate the stability of a biomass powder and a cobalt ferrite, Fe_2CoO_4, individually and together. The tests used an inert atmosphere and a temperature ranging from 293 K to 1273 K.

Denisenko et al. (2017) evaluated the decomposition of europium sulfates, $Eu_2(SO_4)_3*8H_2O$, and $EuSO_4$. The experiments used an atmosphere of N_2 and air and a temperature range between 298 K and 773 K.

Kurban *et al.* (2022) analyzed the thermal decomposition of $ZnSO_4$ to evaluate the effect of a catalyst. The tests took place in an inert atmosphere of N_2 and temperatures ranging from 298 K to 1273 K.

Grigorova and Paunova (2022) used a thermogravimetric analyzer to study the reduction of a waste mixture of metallurgical products. The assays simultaneously reduced residues with several metals: Fe, Zn, Pb, Cu, and Cd.

Hulbert (1968) analyzed through isothermal thermogravimetric analysis the decomposition of $MgSO_4$ between 1193 K and 1353 K and indicated that the increase in mass delays the decomposition process.

Genceli *et al.* (2007) used thermogravimetric analysis to evaluate the behavior of $MgSO_4*11H_2O$ during the temperature range from 300 K to 573 K with a heating rate of 5 $K.min^{-1}$ and He reaction atmosphere.

Okhrimenko *et al.* (2017) evaluated dehydration of $MgSO_4*7H_2O$ at low temperature and water vapor pressure. The experiments were carried out in a temperature range of 308 to 333 K and initially took place in a vacuum.

Brancato *et al.* (2018) evaluated the behavior of pure $MgSO_4*7H_2O$ and macrocellular foams filled with $MgSO_4*7H_2O$ with the aid of a thermogravimetric analyzer, with a temperature range between 298 K and 573 K, heating rate of 1 $K.min^{-1}$ and with N_2 flow of 50 $ml.min^{-1}$.

Souza *et al.* (2020) used thermogravimetric analysis to evaluate the decomposition behavior of $MgSO_4*7H_2O$ with and without the presence of charcoal. The operating range of the experiments was from 300 K to 1400 K, in an N_2 atmosphere and a heating rate of 15 $K.min^{-1}$.

2.8. Reducing Agents

Hoteit et al. (2007) indicate that an atmosphere with low oxygen concentrations is favorable for a decrease in temperatures. Thus, the use of compounds that remove oxygen from the reaction atmosphere becomes important, these compounds are known as reducing agents.

Kuusik *et al.* (1985) evaluated the influence of the use of carbon monoxide as a reducing agent on the decomposition of $CaSO_4$. The authors analyzed the use of an atmosphere with 5, 10, and 20% CO and concluded that the concentration of the reducing agent influenced the decomposition temperature of the sulfate and the compounds formed. Increasing the concentration of the reducing agent decreased the decomposition temperature of the sulfate.

Complementing the analysis performed by Kuusik *et al.* (1985), Scheidema *et al.* (2011) evaluated the effect of the concentration of the reducing agent (S_2) on the formation of MgO, from the decomposition at 1173 K. The concentrations evaluated were: 1x, 2x and 4x the stoichiometric concentration. The authors identified that the surface area of MgO was higher in the experiments with the stoichiometric concentration.

Reducing agents can be solid or gaseous (HLABELA et al., 2010; SOUZA et al., 2020). Several types of compounds can be used as reducing agents, for example, pure agents such as H_2 and S_2 (SCHEIDEMA; TASKINEN, 2011); metallic sulfides (HUANG et al., 2015); composite catalysts (MELLO et al., 2020; SOTO-DÍAZ et al., 2019); carbon compounds

such as charcoal, CO and CO_2 (JIANG et al., 2013; XIA et al., 2022; YANG et al., 2010).

The use of carbon as a reducing agent presents a good option since there are numerous carbon compounds. This great variety of compounds means that carbon can be used as a reducing agent for different analyses. For evaluations of solid-solid systems, carbon can be used in the form of charcoal, graphite, and coke. (LV et al., 2018; SOUZA et al., 2019; XIAO et al., 2020), for solid-gas and gas-gas systems carbon can be present as CO, CO_2, and CH_4 (XIA et al., 2022; ZHANG et al., 2013).

2.9. Kinetic Modeling

Rodrigues (2015) describes kinetic modeling as having the use of conservation and constitutive equations to describe the kinetic behavior of chemical reactions and the processes of heat and mass transfer. Kinetic models seek to be accurate and well detailed in these descriptions.

2.9.1. Kinetic modeling in thermogravimetric curves

For thermogravimetric curves, kinetic modeling can obtain kinetic parameters for both isothermal and dynamic methods. Monteiro (2017)highlights that for the modeling of isothermal methods, several thermogravimetric graphs are needed, while for dynamic methods a single curve is capable of providing the data necessary for modeling.

Vachuška and Vobořil (1971), developed an algorithm to be applied to data from non-isothermal thermogravimetric curves, taking into account the thermal effects of reactions that result in a deviation of the programmed heating for the samples. The authors used this algorithm to determine the values of Ea and the reaction order. The method was tested on data from the literature on gypsum dehydration and calcium oxalate monohydrate dehydration. The results obtained were compared with the values in the literature and obtained results with excellent agreement.

Dharwadkar et al. (1978) performed kinetic modeling on a set of data from the thermogravimetric analysis of the thermal decomposition of

$CdCO_3$. The authors performed the modeling based on the article by Avrami (1941) and obtained correlation coefficient values greater than 0.996.

Sakakibara *et al.* (1989), analyzed three different mathematical models to describe the behavior of a thermogravimetric curve. The methods evaluated by the authors were: a Difference-Differential method developed by Freeman and Carroll (1958), an integral method developed by Coats and Redfern (1964) and a differential method developed by Achar *et al.* (1966), developed specifically for TG curves. The authors determined that although the method proposed by Freeman and Carroll was the most used, it was the most limited method for evaluating thermogravimetric curves.

Laureiro *et al.* (1989), in their work, analyzed the decomposition of chromium trioxide, through thermogravimetric analysis. The authors identified three decomposition steps and found the activation energy of the third step, Cr_2O_5 decomposition. The activation energy was calculated by the method of Achar *et al.* (1966) and obtained a value of 254 $kJ.mol^{-1}$.

Rode and Hlavacek (1995), used kinetic modeling to determine the reaction rate of TiN synthesis, from isothermal thermogravimetric analysis data. The authors used four different laws to determine the kinetic parameters, in all models the R^2 values were greater than 0.979.

Pomiro *et al.* (2014) used kinetic modeling to determine the parameters of Eu_2O_3 carbochlorination. The data were obtained by isothermal thermogravimetric tests and through them, the order of the reactions, the correlation coefficients, and the equilibrium constants was calculated. The model proved to be efficient since the R^2 values were greater than 0.998.

2.9.2. Sulfate decomposition kinetics

Johnson and Gallagher (1971) studied the kinetics of decomposition of aluminum sulfate and aluminum ammonium sulfate. The data used to determine the activation energies of these decompositions were obtained in isothermal experiments with temperatures between 908 and 943 K. The

authors determined the Ea values as 288.89 kJ.mol^{-1} and 309.82 kJ.mol^{-1}, respectively for aluminum sulfate and aluminum ammonium sulfate.

Hlabela *et al.* (2010) determined the kinetic parameters of the reduction of barium sulfate to barium sulfite in the presence of carbon monoxide, using isothermal thermogravimetric assays. The authors determined the values of n and Ea for each experiment and calculated the degree of reliability of the model at 95%.

Rego et al. (2021) used two kinetic models to perform kinetic modeling of the decomposition of aluminum sulfate [$Al_2(SO_4)_3$*$18H_2O$], potassium alum [$KAl(SO_4)_2$*$12H_2O$], and of potassium sulfate (K_2SO_4). The authors determined the values of n, Ea, and R_2 by the two models. Both methods obtained excellent adjustments, reaching R_2 values greater than 0.995.

Kurban *et al.* (2022) concluded through data from a thermogravimetric analysis that the thermal decomposition of pure zinc sulfate monohydrate occurs in two stages. In the presence of a Pd/Al_2O_3 catalyst, the decomposition occurs in a single step. Through the kinetic modeling performed by the authors, they determined the order of reactions and activation energies for each of the steps. The model used was developed by Speyer (1994)and obtained R^2 values greater than 0.97 in all stages.

2.9.3. Kinetics of magnesium sulfate decomposition

Hulbert (1968) in their work studied the kinetics of the isothermal decomposition of magnesium sulfate between 1193 K and 1353 K. The anhydrous sulfate used was obtained from the dehydration of $MgSO_4$*$7H_2O$, carried out at 673 K. The author performed decomposition experiments at 1193, 1223, 1273, 1293, and 1333 K. For the determination of the activation energy, the data obtained by the decomposition at 1293 K were considered, and the author obtained an activation energy of 311.7 ± 12.5 kJ.mol^{-1}.

Plewa and Steindor (1987) determined the activation energy of $MgSO_4$ decomposition in the presence of CO. In their study, the authors

performed isothermal experiments between 913 and 938 K to determine the activation energy. The value found was 209.7 ± 8.6 $kJ.mol^{-1}$.

L'vov and Ugolkov (2004) investigated the decomposition of $MgSO_4$ and $BaSO_4$ in a vacuum. The data used for the modeling were obtained by isothermal thermogravimetric tests. The experimental values of the Ea parameter for $MgSO_4$ and $BaSO_4$ were, respectively, 335.7 ± 1.7 and 411 ± 4 $kJ.mol^{-1}$.

Mello *et al.* (2020) evaluated the efficiency of the Pd/Al_2O_3 catalyst in the decomposition of $MgSO_4*7H_2O$. Using the model proposed by Speyer (1994), the authors determined the values of Ea, n and obtained values of R^2 greater than 0.98 in both decompositions.

2.10. Literary Contribution

The search for kinetic data referring to the decomposition of sulfates present in the literature indicated that there is not a wide range of works proposed to determine these parameters. Among these works, a small part performs the determination of kinetic parameters in processes involving reducing agents.

Looking directly at the works on the decomposition of magnesium sulfate, the literature indicates the existence of fewer than ten works with kinetic data. These few works, for the most part, do not use reducing agents in their analyses, only one work presents the kinetic data of the decomposition of magnesium sulfate in the presence of a reducing agent.

The present work proposes to make a literary contribution in this regard, seeking to determine the kinetic data for the decomposition of magnesium sulfate with different degrees of hydration, with different operating conditions, and with the presence of different reducing agents.

3. Materials and methods

3.1. Chemicals

During this work, the thermogravimetric analyzes were consolidated in an inert atmosphere, using 99.9% nitrogen from Linde. For the tests concerning the impact of the use of different oxidizing agents on the decomposition of $MgSO_4$, ground charcoal, green coke, coke breeze fines, and graphite were used.

Throughout the experiments related to the analysis of the influence of hydration degrees and heating rates, magnesium sulfates with three different degrees of hydration were used: anhydrous magnesium sulfate >97% from Merck, magnesium sulfate monohydrate 97 % from Merck, and magnesium sulfate heptahydrate >99% from Merck.

3.2. Thermodynamics assessment

All reaction systems used thoughout the work were thermodynamically evaluates using the HSC Chemistry 10 program (ROINE, 2021). The analyses of the equilibrium compositions vs. temperature of the reaction systems were carried out, considering the possible species present both in the solid phase and in the gas phase. Through this assessment, the products obtained in each stage of the experiments and the behavior of the system from the formation of these new components were determined.

3.3. Experimental procedure

After the thermodynamic assessment, the operational conditions used in this research were defined. The operating ranges of the thermogravimetric tests were defined and used for experiments with and without the presence of reducing agents, except for experiments with the purpose of evaluating the heating rate.

The tests were divided into two groups: the first consisting of five experiments, defined to evaluate the influence of reducing agents on the decomposition of magnesium sulfate, and the second containing twelve

tests, used to analyze the impact of sulfate hydration and the heating equipment in the decomposition of sulfates.

For the first group, operating conditions were defined as a temperature range from 298 K to 1673 K, a mass of approximately 10 mg of the analyzed mixture with a stoichiometric ratio of 1:1. The stoichiometric was calculated according to the Boudouard´s equation at a temperature of 1200 K (CALO; PERKINS, 1987; LAHIJANI et al., 2015). These experiments had a heating rate of 10 K.min-1, commonly used in the literature (KOBERTZ; MÜLLER, 2014; MELLO et al., 2020; REGO et al., 2021; ZHENG et al., 2020).

In the second group, the experiments maintained the operating temperature range and the mass used in the previous experiments, however, they presented a variation in the heating rates. The twelve trials present in this group were divided into three subgroups of four trials, each using a magnesium sulfate with different hydration and the four heating rates that were evaluated. Therefore, the experiments were carried out as follows:

- Subgroup 1: Experiments using anhydrous magnesium sulfate and heating rates of 5, 10, 15, and 20 $K.min^{-1}$.
- Subgroup 2: Experiments using magnesium sulfate monohydrate and heating rates of 5, 10, 15, and 20 $K.min^{-1}$.
- Subgroup 3: Experiments using magnesium sulfate heptahydrate and heating rates of 5, 10, 15, and 20 $K.min^{-1}$.

All thermogravimetric tests were performed on the STA 449 F3 Jupiter® simultaneous thermal analyzer from Netzsch, from the Department of Chemical and Materials Engineering of the Pontifical Catholic University of Rio de Janeiro (DEQM/PUC-Rio).

3.4. Kinetics modeling

Each thermogravimetric experiment performed provided a dataset that describes the variation of the sample's mass as a function of

temperature and time. These data were used in kinetic modeling, to obtain the kinetic data of reaction order (n) and activation energy (Ea).

The kinetic modeling of the data from the thermogravimetric curves is presented by the mathematical model developed by Speyer (1994) and Vachuška and Vobořil (1971). The initial formula is represented by equation 4.

$$f = \frac{m-m_o}{m_f-m_o} \quad (4)$$

Where f is the weight fraction, m_o is the initial value of mass loss, m_f is the final value of mass loss, and m is the value of mass loss in a given time. a derivation of f with respect to time can be described by equation 5.

$$\frac{df}{dt} = k_o exp\left(\frac{-Ea}{RT}\right) m_o^{n-1}(1-f)^n \quad (5)$$

Where t is time, k_o is the pre-exponential factor, R is the universal gas constant, T is temperature, n is the apparent order of reaction, and Ea is the activation energy. Applying the natural logarithm on both sides and differentiating with respect to t we have the resulting equation equation 6.

$$\frac{\mathrm{d}}{\mathrm{dt}}\left(ln\frac{df}{dt}\right) = \frac{\frac{d^2f}{dt^2}}{\frac{df}{dt}} = \frac{-n\left(\frac{df}{dt}\right)}{1-f} + \frac{E_a}{RT^2}\frac{dT}{dt} \quad (6)$$

Considering that $\frac{dT}{dt}$ is the heating rate (∅) and that the temperature is a function of time, T = ($\emptyset t$+Tr), then we can obtain equation 7.

$$(\varphi t + T_r)^2 \frac{\frac{d^2f}{dt^2}}{\frac{df}{dt}} = -n\left[\frac{(\varphi t+T_r)^2\left(\frac{df}{dt}\right)}{1-f}\right] + \frac{E_a\varphi}{R} \quad (7)$$

In equation 7, Tr is de temperature obtained from TGA assays.

Where f, $\frac{df}{dt}$ e $\frac{d^2f}{dt^2}$ can be calculated from the thermogravimetric curve and its derivatives, as shown in figure Figure 1.

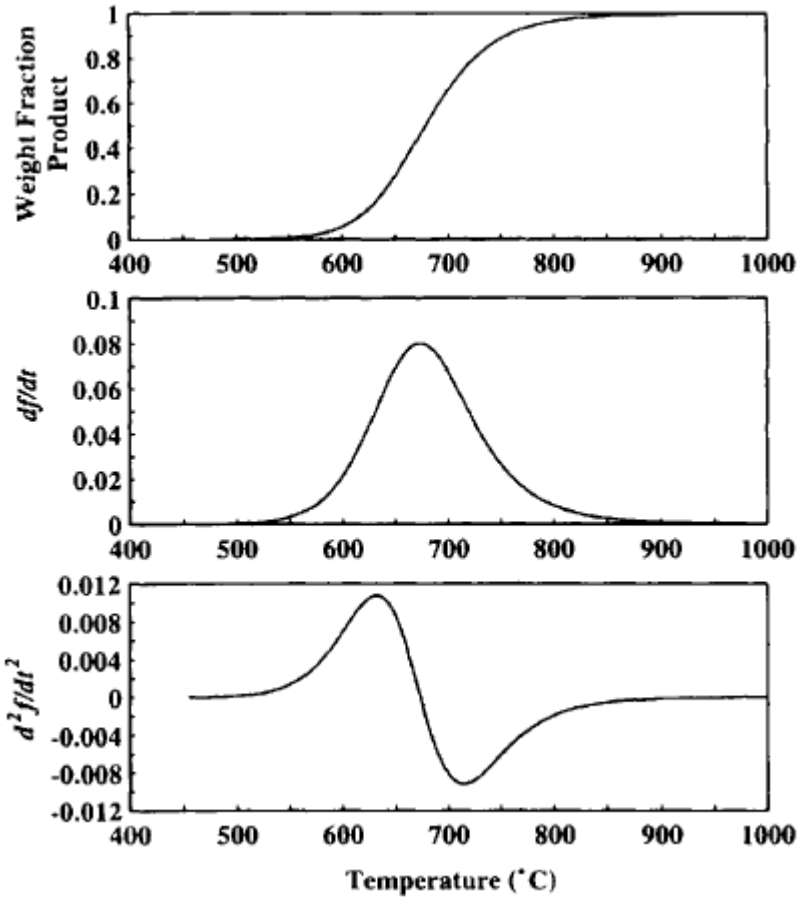

Figure 1 - Method of determination of f, $\frac{df}{dt}$ e $\frac{d^2f}{dt^2}$ (SPEYER, 1994).

To determine the derivatives, a sigmoidal function was used (equation 8), through a code in MATLAB R2021a (THE MATHWORKS INC, 2021). With the same code, the activation energy and the reaction order of each test were determined.

$$f(x) = \frac{1}{1+\exp(-a_1(t-a_2))} \quad (8)$$

4. A brief discussion of the contribution of scientific production

The analyzes and evaluations present in this work were carried out and presented in two different articles to deepen the pertinent discussions. In this topic, these procedures and analyzes were arranged uniquely to show the integrality of the subjects present in the articles.

After determining the intended evaluations of the work and the experimental procedures to be carried out, we started to carry out these procedures. To produce more accurate thermogravimetric experiments, thermodynamic studies were carried out with the reaction systems that would be used.

4.1. Thermodynamic appreciation

To make it possible to evaluate the points proposed in the objectives of this work, it was necessary to carry out experiments that addressed the reaction systems listed below. Among these systems, the last three cover the experiments presented in the first article, while the first two involve the experiments carried out in the second article.

- System 1 Mg-S-O: A system involving the decomposition of anhydrous magnesium sulfate.
- System 2 Mg-S-O-H: A system involving the decomposition of hydrated magnesium sulfates.
- System 3 Mg-S-O-C: A system involving the decomposition of anhydrous magnesium sulfate in the presence of reducing agents.
- System 4 Mg-S-O-C-H: A system involving the decomposition of hydrated magnesium sulfates in the presence of reducing agents.

Using the HSC Chemistry 10 program (ROINE, 2021), it was possible to construct the figures used to evaluate the behavior of the three reaction systems. These figures were used to determine the behavior of each system, the compounds formed in each situation, and to perform a graphic comparison between the reaction systems. These figures demonstrate the

distribution of the species formed as a function of temperatures, both for solid and gaseous phases. All simulations of the reaction systems used 1 mol of N_2 as the reaction atmosphere.

4.1.1. System 1: Mg-S-O

For the evaluation of the system referring to the thermal decomposition of anhydrous magnesium sulfate, figures 2 and 3 were constructed. In them, it is possible to identify that MgO is the only solid product and that it contains Mg at the end of decomposition. Another important aspect for analysis is the theoretical decomposition temperature range of anhydrous $MgSO_4$, it is possible to verify from figure 2 that the sulfate starts to decompose from 850 K and reaches complete decomposition around 1500 K.

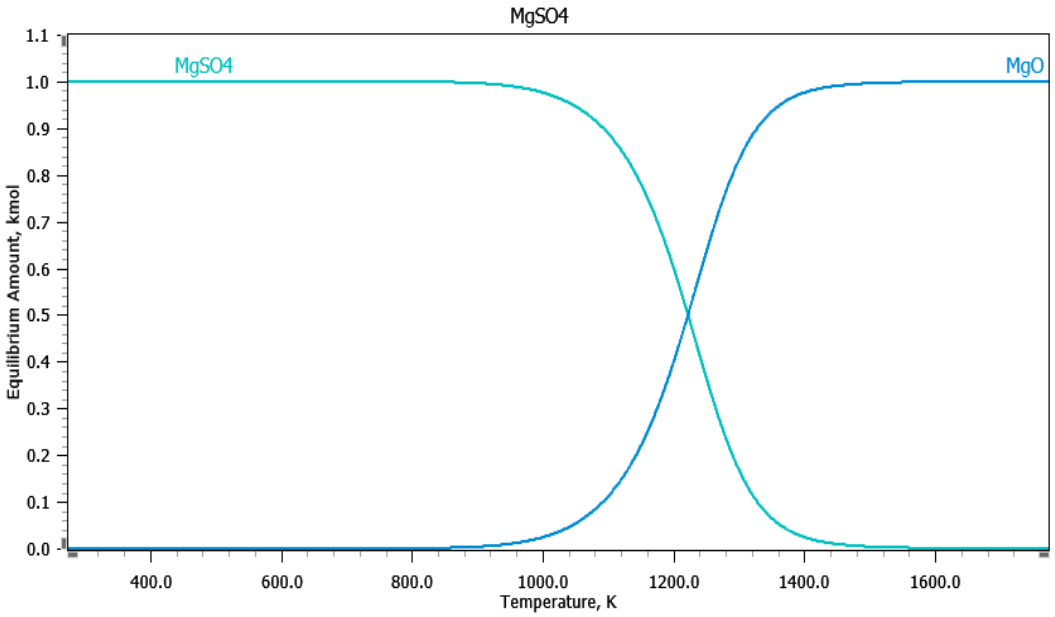

Figure 2- Species distribution diagram at equilibrium for the thermal decomposition of anhydrous $MgSO_4$ to the solid phase, constructed by the author using HSC Chemistry 10.

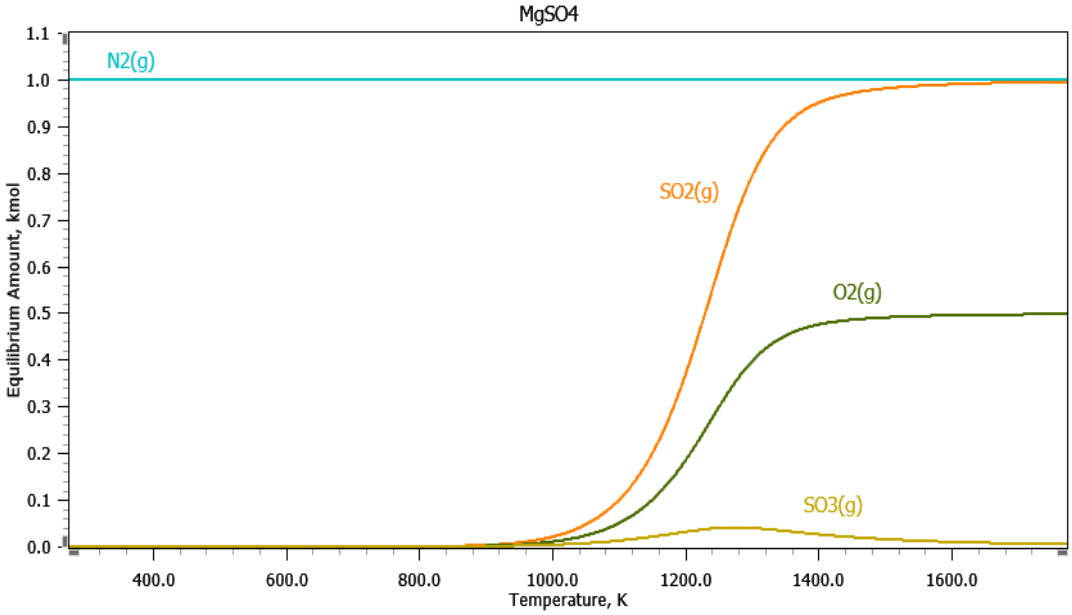

Figure 3- Species distribution diagram at equilibrium for the thermal decomposition of anhydrous $MgSO_4$ to the gas phase, built by the author using HSC Chemistry 10.

4.1.2. System 2: Mg-S-O-H

Figures 4 to 7 served as a basis for the analysis of the reaction system alluding to the thermal decomposition of hydrated sulfates. Figures 4 and 6, which represent the species present in the solid phases, indicate that before the start of decomposition of magnesium sulfate, dehydration steps take place. In both cases, sulfate decomposition only occurs after complete dehydration of the sulfate and presents MgO as the only magnesium-containing product. For sulfate monohydrate the decomposition starts at approximately 850 K and ends around 1430 K, for sulfate heptahydrate the decomposition occurs between 900 K and 1400 K. Observing figures 5 and 7, referring to the gaseous phases of the decompositions, it is possible to confirm that the concentration of H_2O reached the maximum values before the formation of compounds generated by the decomposition of $MgSO_4$, O_2, SO_3 and SO_2.

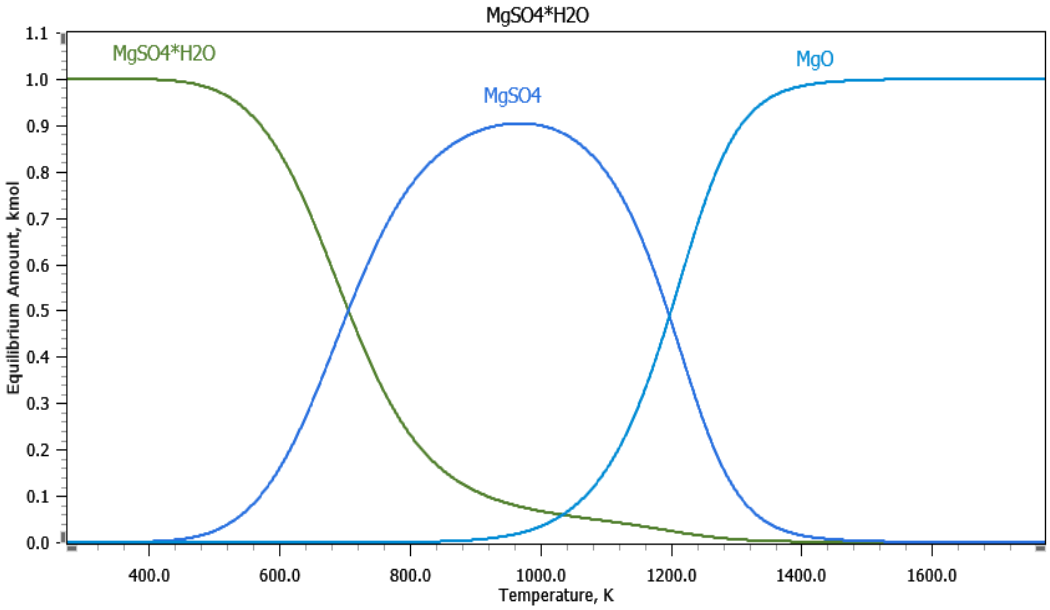

Figure 4- Species distribution diagram at equilibrium for the thermal decomposition of $MgSO_4$ monohydrate to the solid phase, constructed by the author using HSC Chemistry 10.

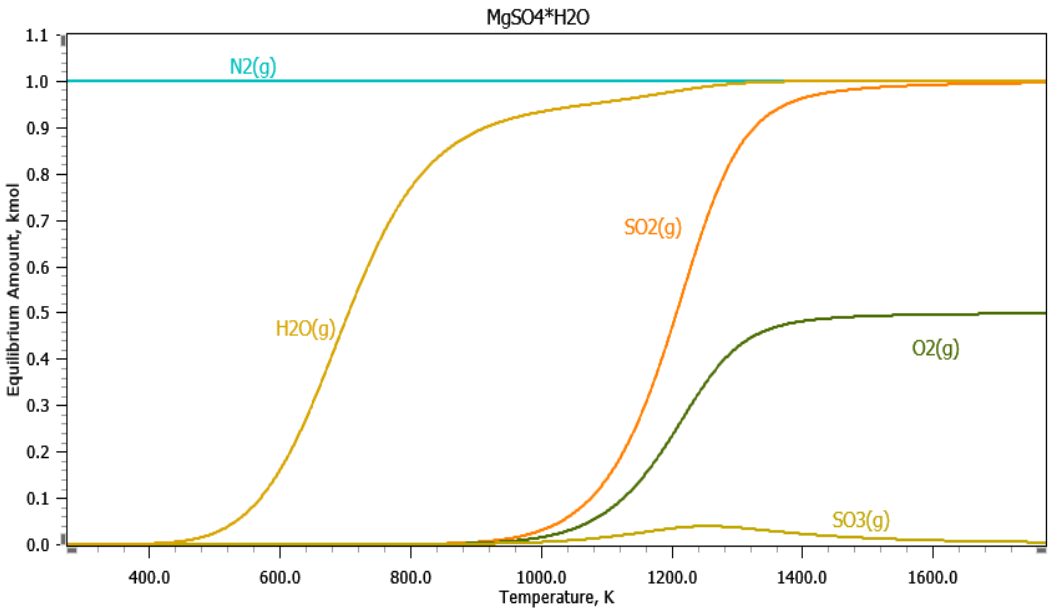

Figure 5- Species distribution diagram at equilibrium for the thermal decomposition of $MgSO_4$ monohydrate to the gas phase, constructed by the author using HSC Chemistry 10.

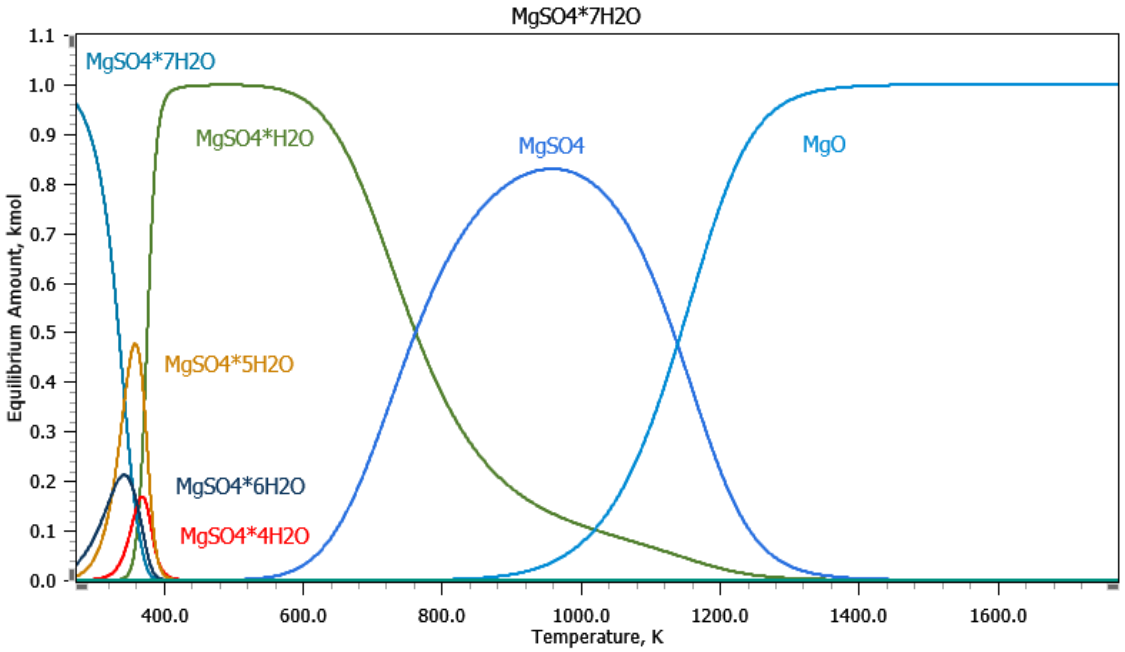

Figure 6- Species distribution diagram at equilibrium for the thermal decomposition of $MgSO_4$ heptahydrate to the solid phase, constructed by the author using HSC Chemistry 10.

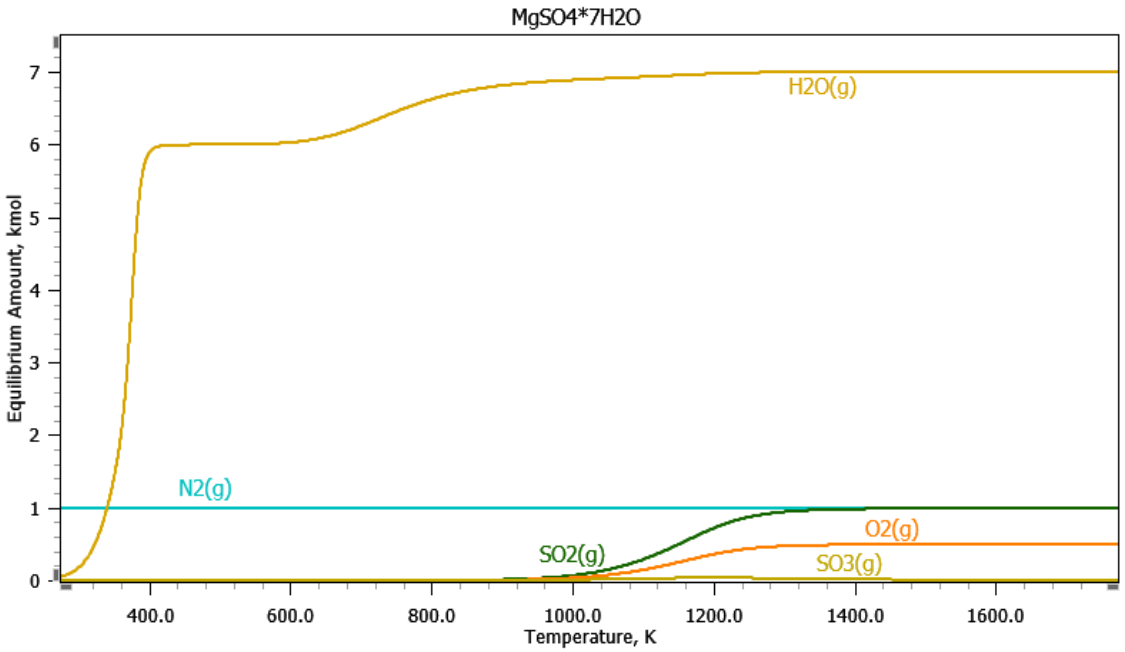

Figure 7- Species distribution diagram at equilibrium for the thermal decomposition of $MgSO_4$ heptahydrate to the gas phase, constructed by the author using the HSC Chemistry 10.

4.1.3. System 3: Mg-S-O-C

Figures 8 and 9 were used to evaluate the carbothermic decomposition of anhydrous magnesium sulfate. These figures indicate that the decomposition starts from 400 K and ends at 700 K, the decomposition has in MgO the only product containing Mg. The presence of carbon prevents the formation of O_2, instead, the formation of carbon oxides occurs. The determining factor for the formation of CO or CO_2 is temperature.

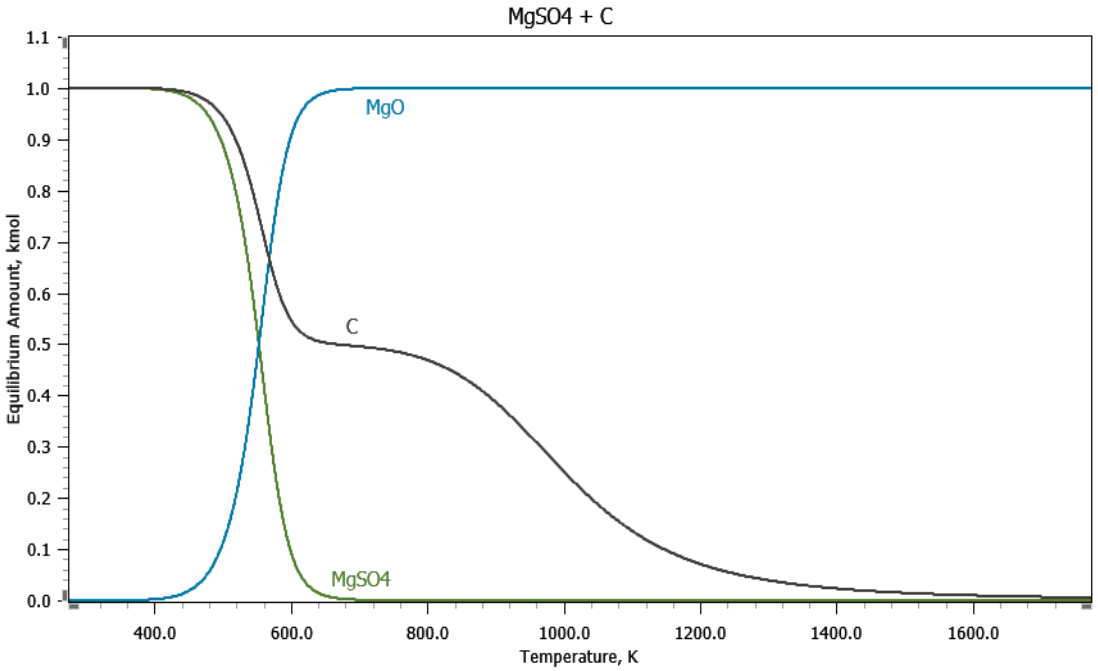

Figure 8- Species distribution diagram at equilibrium for the carbothermic decomposition of anhydrous $MgSO_4$ to the solid phase, constructed by the author using HSC Chemistry 10.

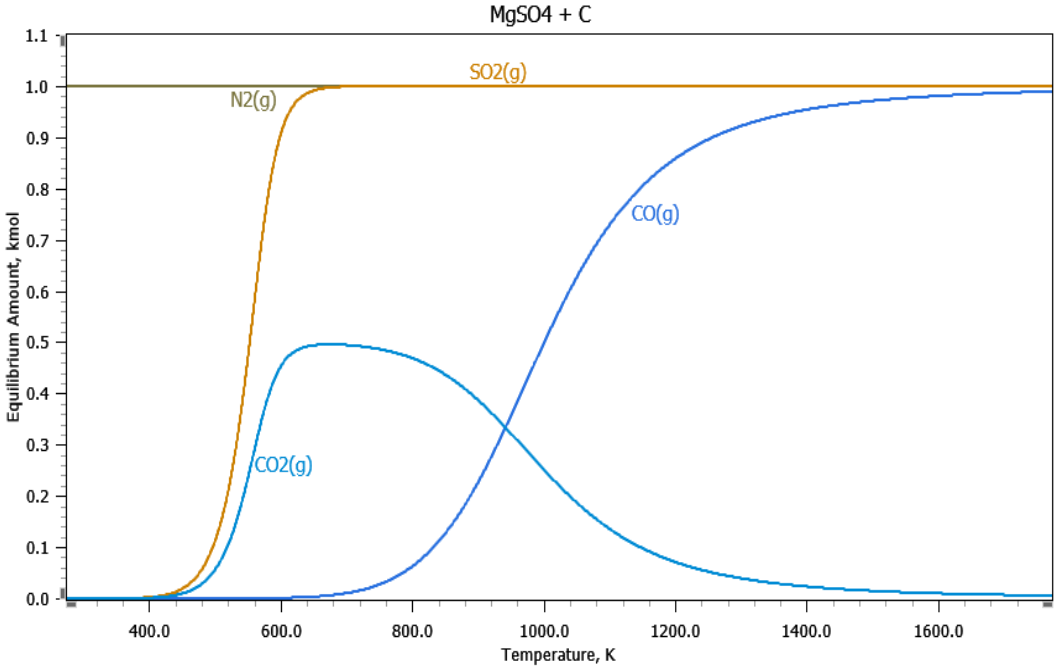

Figure 9- Species distribution diagram at equilibrium for the carbothermic decomposition of anhydrous $MgSO_4$ to the gas phase, constructed by the author using the HSC Chemistry 10.

4.1.4. System 4: Mg-S-O-C-H

The evaluation of the reaction system of the carbothermic decomposition of the hydrated sulfates was carried out from figures 10 to 13. The analysis of the solid phases, figures 10 and 12, shows that the sulfate decomposition begins before the end of dehydration for both sulfates. , it is also possible to observe that MgO is the only compound containing magnesium at the end of the decompositions. The decomposition of magnesium sulfate monohydrate occurs between 400 K and 700 K, whereas that of sulfate heptahydrate occurs in the range of 440 K to 680 K. The analysis of the gaseous phases allowed us to identify that, as in the previous reaction system, the formation of the two carbon oxides.

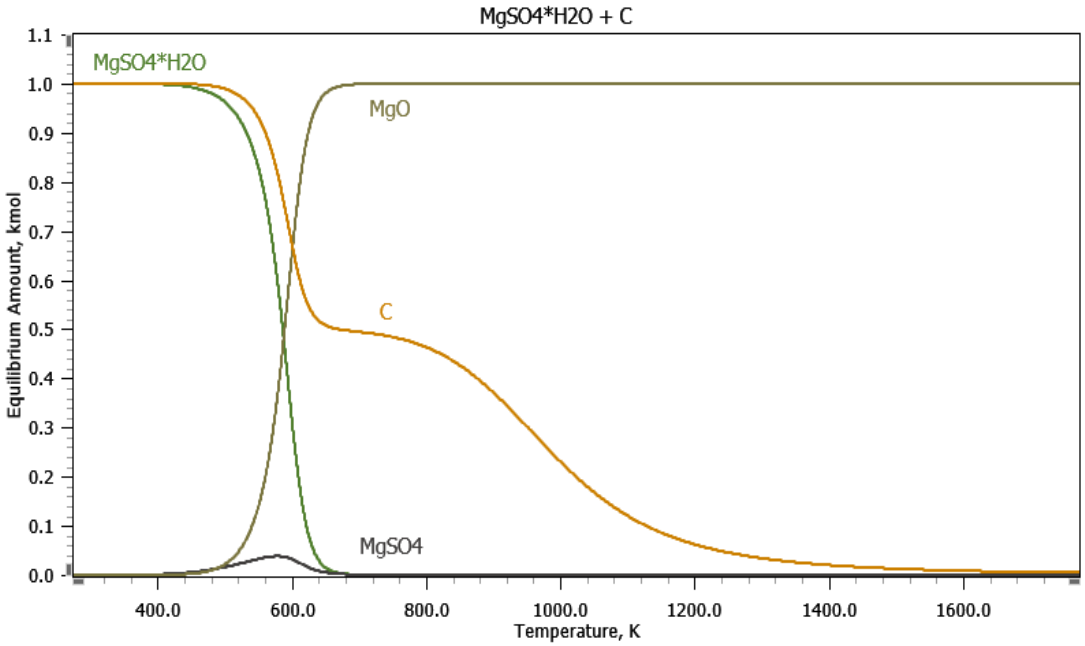

Figure 10- Species distribution diagram at equilibrium for the carbothermic decomposition of $MgSO_4$ monohydrate to the solid phase, constructed by the author using HSC Chemistry 10.

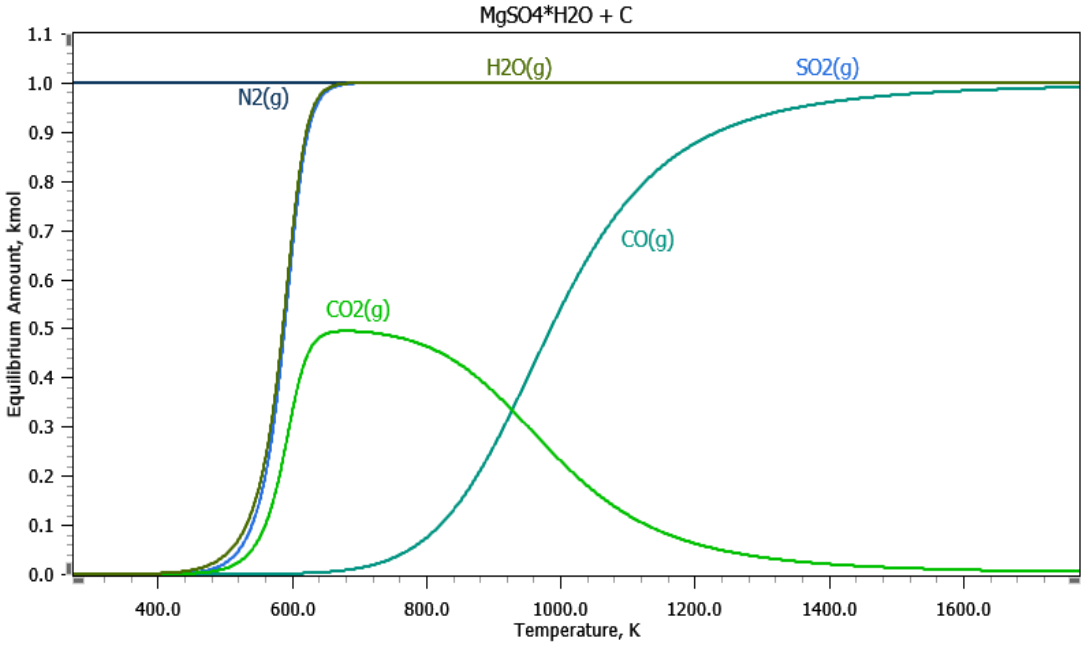

Figure 11- Species distribution diagram at equilibrium for the carbothermic decomposition of $MgSO_4$ monohydrate to the gas phase, constructed by the author using the HSC Chemistry 10.

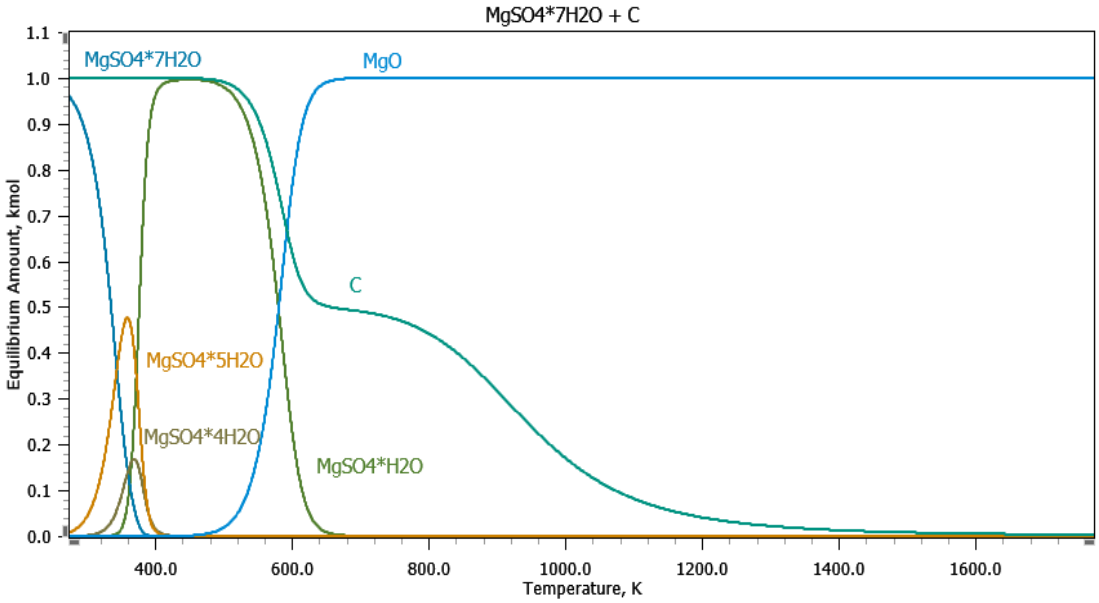

Figure 12- Species distribution diagram at equilibrium for the carbothermic decomposition of $MgSO_4$ heptahydrate to the solid phase, constructed by the author using HSC Chemistry 10.

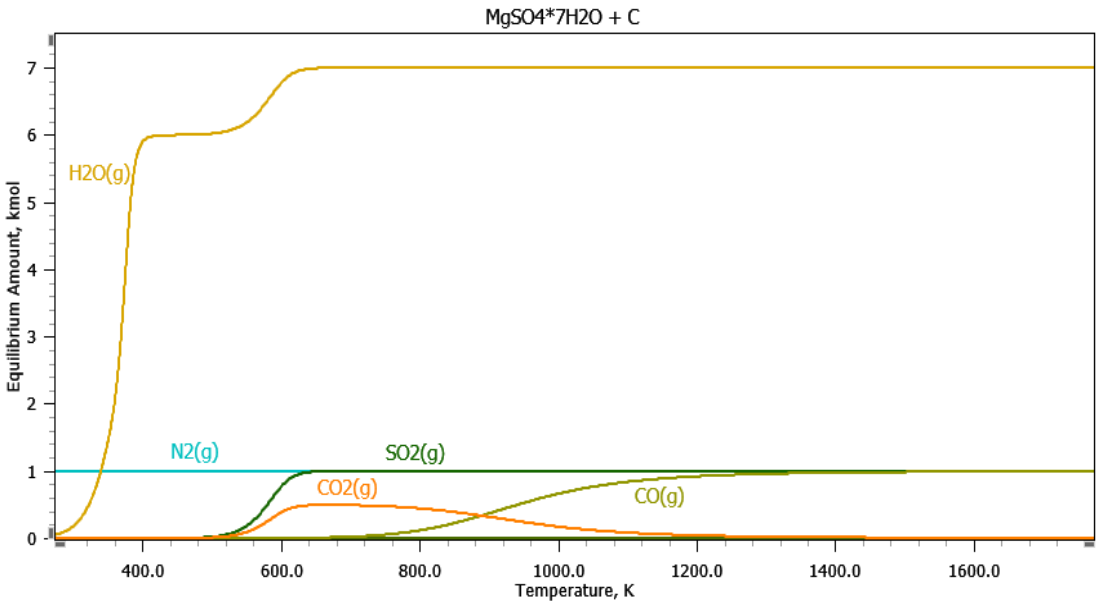

Figure 13- Species distribution diagram at equilibrium for the carbothermic decomposition of $MgSO_4$ heptahydrate to the gas phase, constructed by the author using the HSC Chemistry 10.

4.1.5. Boudouard's Equation

The study of the influence of temperature on the formation of carbon oxides in the carbothermic decomposition of sulfates is of great importance for the experiments since it is through it that it is possible to calculate the stoichiometric ratio of the sulfate + reducing agent mixture. Balanced

equations 9 and 10 describe the two possibilities of product formations for the decomposition of magnesium sulfate in the presence of carbon.

$$MgSO_4 + 1/2C \rightarrow MgO + 1/2CO_{2(g)} + SO_{2(g)} \quad (9)$$

$$MgSO_4 + C \rightarrow MgO + CO_{(g)} + SO_{2(g)} \quad (10)$$

Figures 9, 11, and 13 show the gaseous phases of the decomposition of sulfates in the presence of carbon, through which it is possible to identify a pattern of behavior between the formation of CO and CO_2. In the three figures, the decomposition of sulfates generates only CO_2 at the initial temperatures and CO from 600 K. According to equation 6, one mol of sulfate generates half a mol of CO_2, this value is, therefore, the value of the highest possible concentration of CO_2, in the three figures, this concentration is reached at the moment of the beginning of the formation of CO in the systems.

From this moment on, the CO_2 in the system starts to decrease while the CO increases, this behavior continues until approximately 1600 K, when the CO_2 goes to zero and the CO reaches 1. This behavior is described by the Boudouard equation (equation 11), through which it is possible to calculate the theoretical concentrations of CO_2 and CO according to the desired temperature. Although at approximately 900 K the concentration of CO is equal to the concentration of CO_2, this is not the equilibrium point between the compounds. Since for each mole of CO_2 converted, two moles of CO are generated, the equilibrium point between the two compounds is reached when the concentration of CO is twice the concentration of CO_2. This point is reached at 973 K, figure 14 presents the values of ΔG_o of equation 11 and confirms this balance since at 973 K ΔG_o of the equation is equal to zero.

$$C + CO_{2(g)} \rightarrow 2CO_{(g)} \quad (11)$$

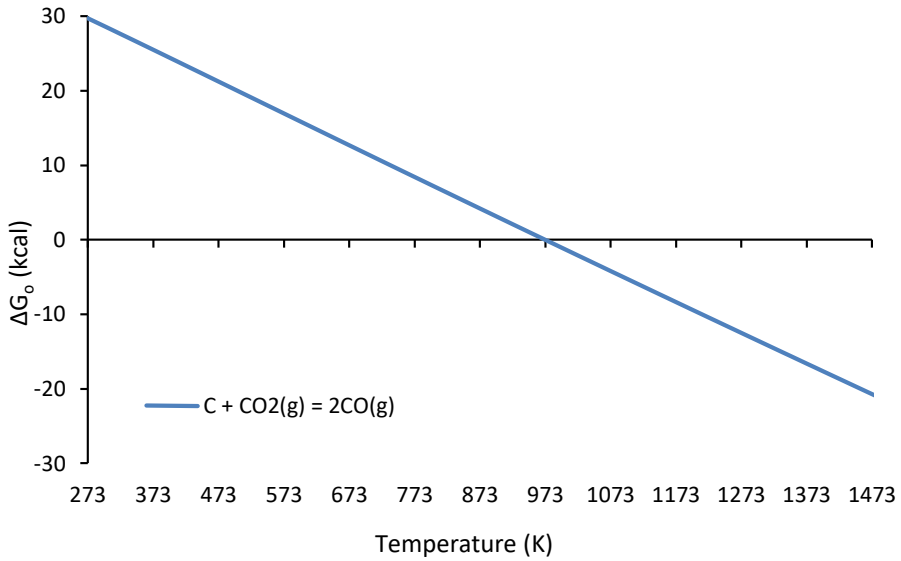

Figure 14- Values of ΔG_o of the Boudouard equation

4.2. Thermogravimetric analysis

The thermogravimetric analyzes present in this work were performed to allow a fluid analysis of the results. The results obtained by carrying out the first set of experiments are shown in figures 15 and 16. Through these figures, it was possible to observe a standard behavior in the five experiments. Both without the presence of reducing agents and with the presence of reducing agents, the curves present two distinct moments of mass loss. The first moment is related to the loss of mass from the dehydration of sulfates, the second moment is related to the loss of mass that occurs in the decomposition of sulfates. The five analyzed curves belong to reaction system 4 and although thermodynamic analysis has indicated that for this system the sulfate decomposition would occur before complete dehydration, these curves show the opposite.

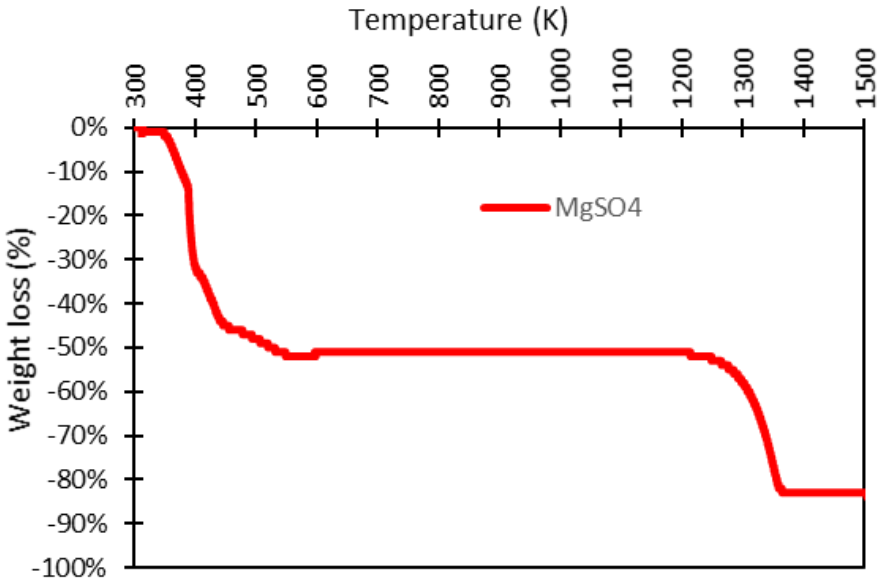

Figure 15- Thermogravimetric analysis of magnesium sulfate heptahydrate decomposition.

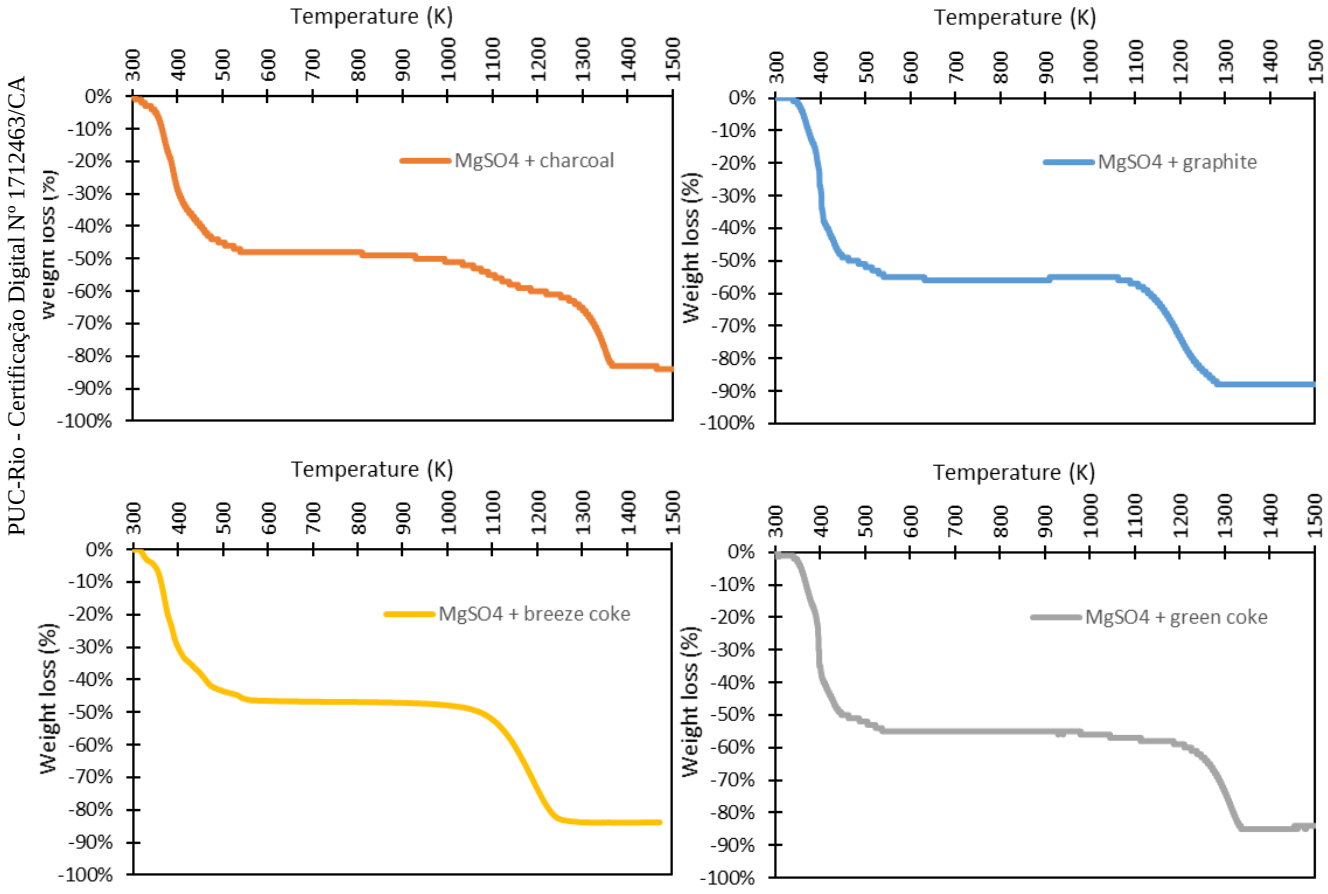

Figure 16- Thermogravimetric analysis of magnesium sulfate heptahydrate decomposition in the presence of reducing agents.

Even with this general pattern of behavior of the curves, some differences were observed during the comparison of the figures. Even though in all curves the dehydration processes of the sulfate molecules took

place before the decomposition processes, the intervals between these processes were different. In the pure sulfate curve, this interval was 665 K, while in the sulfate curves with reducing agents, these intervals were, on average, 130 K smaller.

This difference in results is due to the fact that in the presence of reducing agents, sulfate decomposition starts at lower temperatures, since the initial and final temperatures of dehydration have an average variation of values of +3%, while the initial temperature of decomposition presents an average variation of -7.5%.

The second set of thermogravimetric analyzes carried out allowed the analysis of the impact of the presence of water molecules on the sulfate structure and the heating rate for the sulfate decomposition. These curves are arranged in figures 17 to 19.

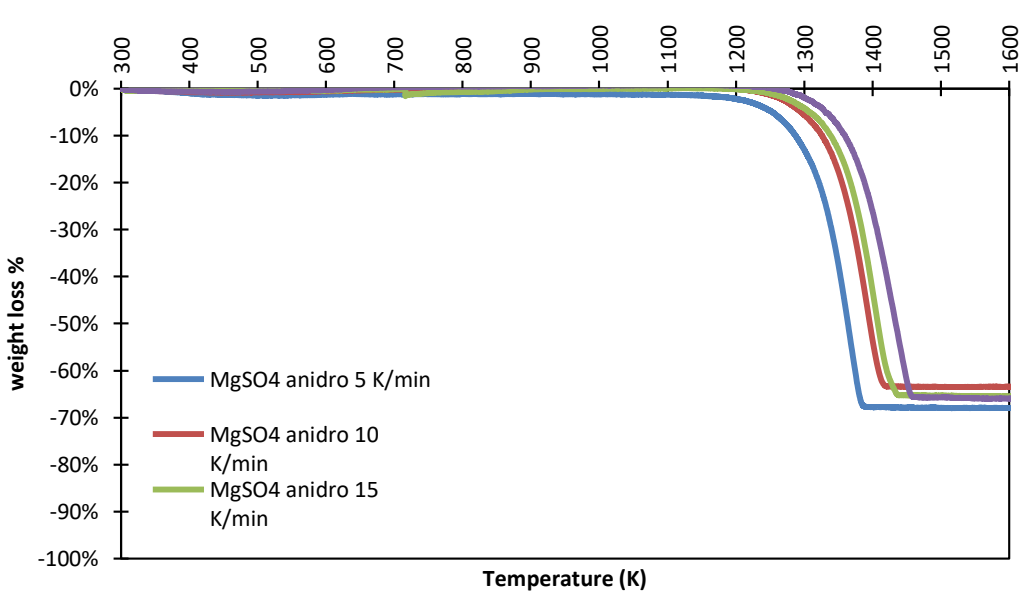

Figure 17- Thermogravimetric analysis of anhydrous magnesium sulfate.

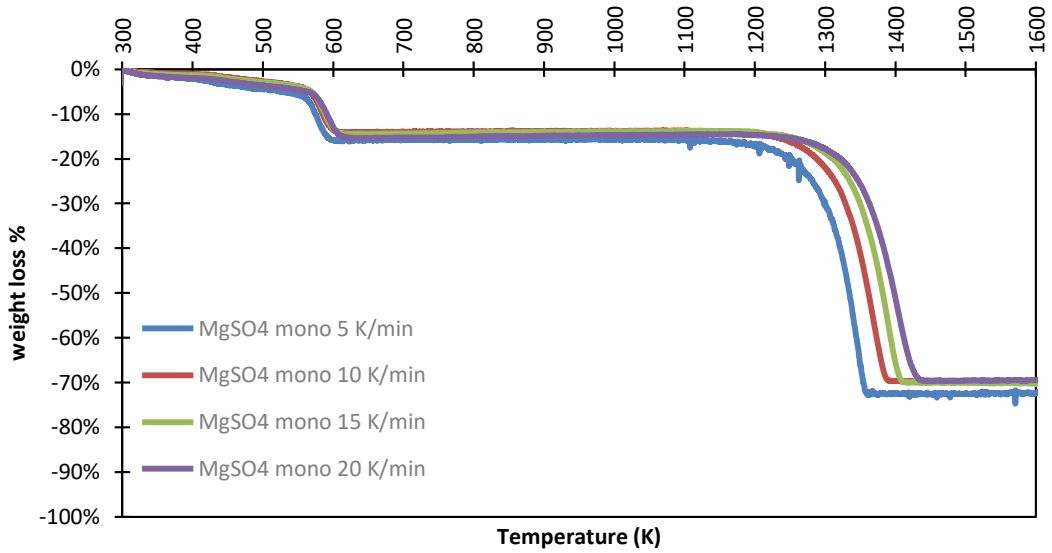

Figure 18- Thermogravimetric analysis of magnesium sulfate monohydrate.

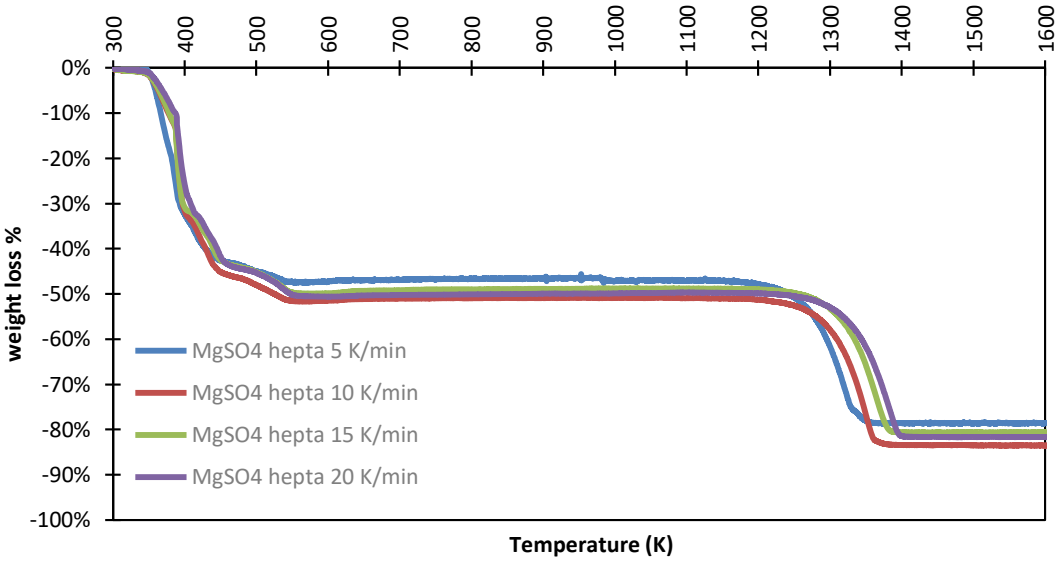

Figure 19- Thermogravimetric analysis of magnesium sulfate heptahydrate.

These figures present the thermogravimetric curves according to the three subgroups described in item 3.3. Through them, it is possible to evaluate the influence of the heating rate of the experiments on the dehydration and decomposition of sulfates. In figures 18 and 19 it is possible to observe the dehydration steps of the sulfates, the initial and final temperatures of dehydration do not present a pattern that makes it possible to identify an influence of the heating rates.

As for the decomposition of sulfates, the curves in the three figures present the same behavior, the curves relating to the experiments with lower

heating rates present the lowest values of initial and final temperatures of decomposition. In them, it is possible to identify that as the heating rates increase, the temperatures also increase. The values of the initial and final temperatures of the decompositions are presented in table 1 and help to complement this analysis. The values presented in table 1 indicate that for the decompositions of hydrated sulfates, the increase in the rate caused an equal percentage increase in the initial and final temperatures of the processes.

Table 1– Initial and final temperatures of magnesium sulfate decomposition.

Reagents	Rate ($K.min^{-1}$)	T_o (K)	Variation (%)	T_f (K)	Variation (%)
$MgSO_4$	5	916		1118	
$MgSO_4$	10	976	+ 7	1142	+ 2
$MgSO_4$	15	988	+ 8	1161	+ 4
$MgSO_4$	20	1000	+ 9	1185	+ 6
$MgSO_4*H_2O$	5	910		1083	
$MgSO_4*H_2O$	10	935	+ 3	1117	+ 3
$MgSO_4*H_2O$	15	952	+ 5	1136	+ 5
$MgSO_4*H_2O$	20	981	+ 8	1165	+ 8
$MgSO_4*7H_2O$	5	920		1072	
$MgSO_4*7H_2O$	10	941	+2	1092	+2
$MgSO_4*7H_2O$	15	961	+4	1115	+4
$MgSO_4*7H_2O$	20	976	+6	1131	+6

4.3. Kinetics modeling

The data that compose the thermogravimetric curves were processed by the mathematical model developed by Speyer (1994), this model was used in other studies present in the literature (KURBAN et al., 2022; MELLO et al., 2020; REGO et al., 2021). Through this model, it was possible to calculate the kinetic parameters necessary for the analyzes proposed in this work.

4.3.1. Model adjustment

To achieve the objectives of this work, the data evaluated by the model were the mass loss data referring to sulfate decomposition. The first aspect related to the mathematical model to be observed is the adjustment of the model to the data that was processed by it. The coefficient of determination (R^2) is the parameter that indicates the level of fit of the data

generated by the model to the experimental data. The R^2 values range from 0 to 1, the closer the R^2 value is to 1, the more accurate the mathematical model. Table 2 presents the obtained values of R^2 for each analyzed curve.

Table 2- Data of the coefficients of determination of the kinetic modeling of the analyzed intervals of the thermogravimetric curves.

Reaction system	R^2
$MgSO_4*7H_2O$ + charcoal	0.9987
$MgSO_4*7H_2O$ + green coke	0.9994
$MgSO_4*7H_2O$ + graphite	0.9996
$MgSO_4*7H_2O$ + breeze coke	0.9996
$MgSO_4$ anhydrous 5 $K.min^{-1}$	0.9998
$MgSO_4$ anhydrous 10 $K.min^{-1}$	0.9995
$MgSO_4$ anhydrous 15 $K.min^{-1}$	0.9994
$MgSO_4$ anhydrous 20 $K.min^{-1}$	0.9989
$MgSO_4$ monohydrate 5 $K.min^{-1}$	0.9998
$MgSO_4$ monohydrate 10 $K.min^{-1}$	0.9996
$MgSO_4$ monohydrate 15 $K.min^{-1}$	0.9994
$MgSO_4$ monohydrate 20 $K.min^{-1}$	0.9992
$MgSO_4$ heptahydrate 5 $K.min^{-1}$	0.9999
$MgSO_4$ heptahydrate 10 $K.min^{-1}$	0.9996
$MgSO_4$ heptahydrate 15 $K.min^{-1}$	0.9995
$MgSO_4$ heptahydrate 20 $K.min^{-1}$	0.9992

The values presented in table 2 indicated an excellent fit of the mathematical model since in all applications of the model the values obtained for R^2 were greater than 0.998. As expected, the experiments with the lowest heating rates were the ones that obtained the highest values of R^2, since these experiments generate a greater amount of data.

The figures 20 to 23, displays the results of the linear regressions obtained for the data from the thermogravimetric curves of the decompositions of all experiments. Through them, it was possible to observe that the experimental data and the model data were very close. This figures, confirm the values of the coefficients of determination (R^2) shown in table 2.

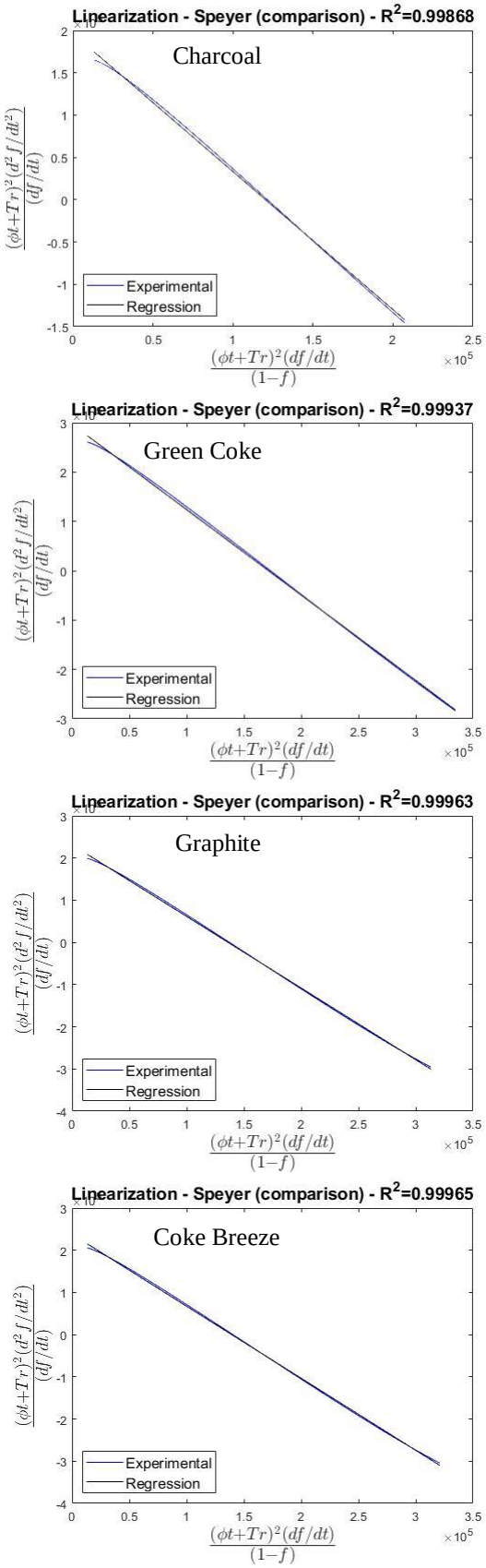

Figure 20 – Linear regression obtained for the decompositions of MgSO4*7H2O with reducing agent.

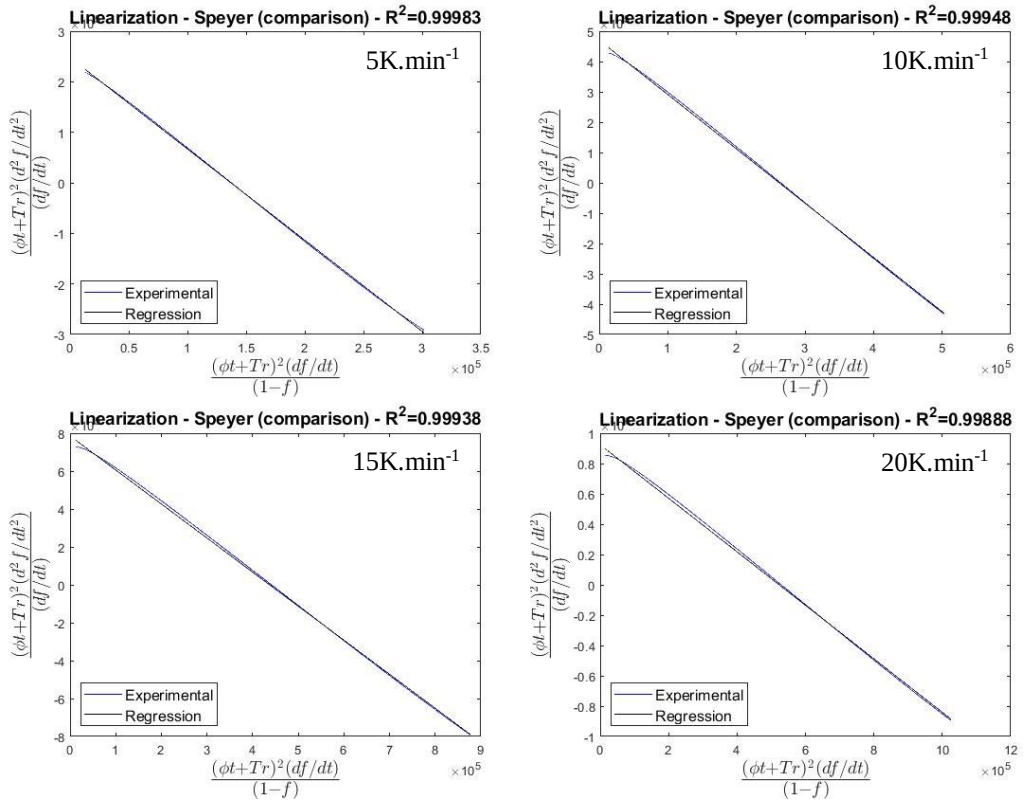

Figure 21 – Linear regression obtained for anhydrous $MgSO_4$ decompositions.

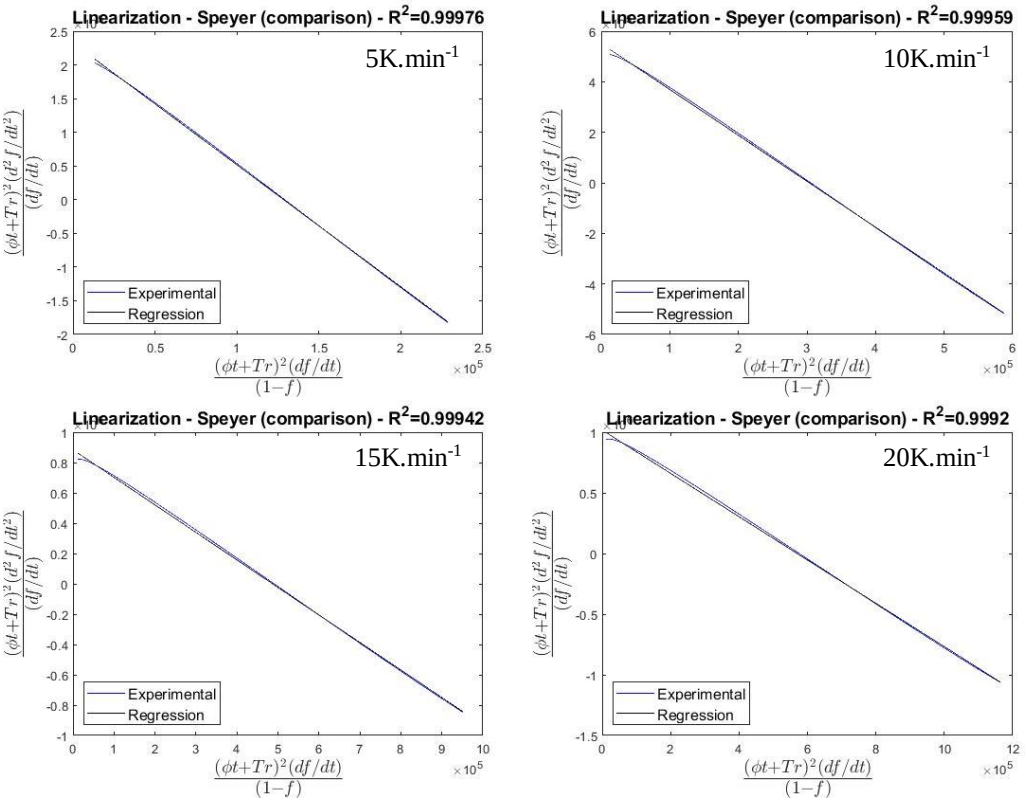

Figure 22 – Linear regression obtained for monohydrate $MgSO_4$ decompositions.

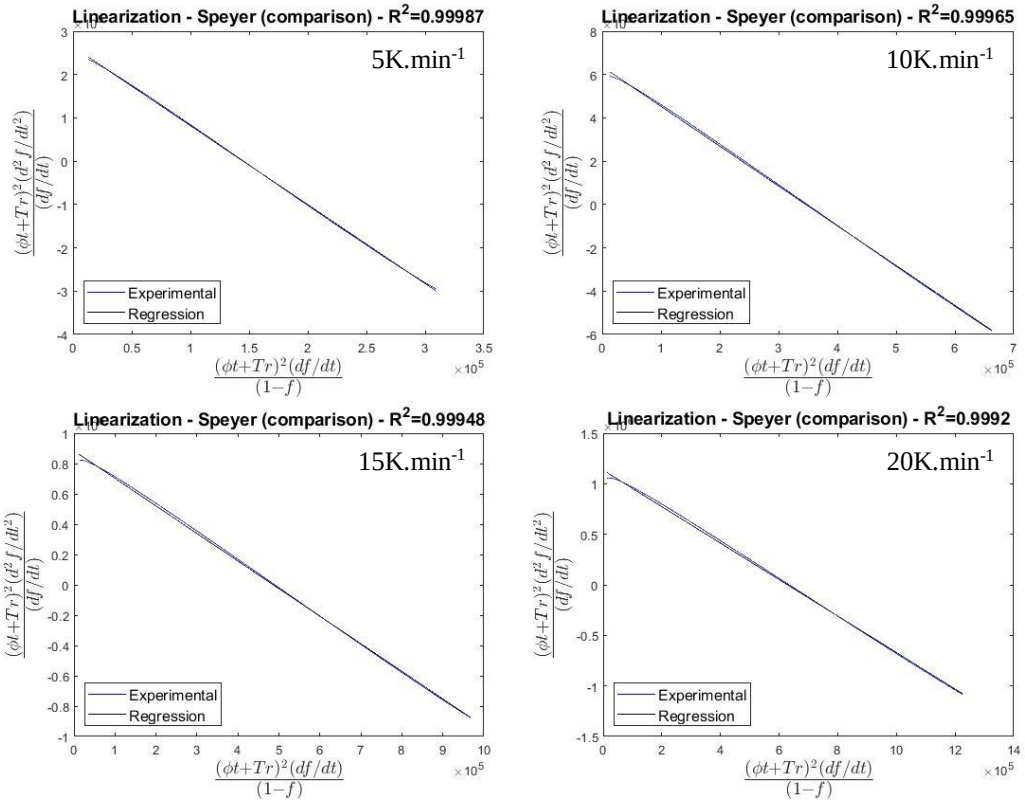

Figure 23 – Linear regression obtained for heptahydrate $MgSO_4$ decompositions.

4.3.2. Kinetic parameters

Once the values of the coefficients of determination confirmed that the model served to process the data of the thermogravimetric curves, the kinetic parameters obtained through it could be evaluated. The kinetic parameters were evaluated according to the groups of thermogravimetric curves defined by the methodology.

Table 3 presents the kinetic parameters obtained from tests involving reducing agents and a test with pure sulfate. The activation energy of the decomposition of pure magnesium sulfate heptahydrate was 422.731 $kJ.mol^{-1}$, the order of the decomposition reaction was 1.8, these data served as points of analysis for the other values. Decompositions with reducing agents obtained Ea values below the value found for pure sulfate, these values were up to 62% lower. The order values of the sulfate decomposition reactions followed the pattern presented by the activation energies and were lower than 1.8.

Table 3– Kinetic parameters of the kinetic modeling of $MgSO_4*7H_2O$ decompositions with and without reducing agents.

Reagents	n	E_a (kJ.mol^{-1})
$MgSO_4*7H_2O$ pure	1.809	422.731
$MgSO_4*7H_2O$ + green coke	1.783	340.391
$MgSO_4*7H_2O$ + graphite	1.708	196.120
$MgSO_4*7H_2O$ + breeze coke	1.698	191.100
$MgSO_4*7H_2O$ + charcoal	1.631	162.302

Table 4 shows the kinetic parameters obtained by modeling the curves from the decomposition of pure sulfates. Through these values, it was possible to evaluate the influence of the heating rate and the sulfate hydration in the decomposition process.

The values of the orders of the reactions found in the twelve experiments were close, with a variation of less than 3% between them. Despite the proximity between the values, the orders of the reactions showed a pattern, where the order of the reaction decreased with the increase of the heating rate. Activation energies did not show any pattern in relation to heating rates.

Table 4– Kinetic parameters of the kinetic modeling of pure $MgSO_4$ decompositions.

Reagent	n	E_a (kJ.mol^{-1})
$MgSO_4$ anhydrous 5 K.min^{-1}	1.807	386.46
$MgSO_4$ anhydrous 10 K.min^{-1}	1.799	412.60
$MgSO_4$ anhydrous 15 K.min^{-1}	1.796	430.92
$MgSO_4$ anhydrous 20 K.min^{-1}	1.773	398.05
$MgSO_4$ monohydrate 5 K.min^{-1}	1.811	387.14
$MgSO_4$ monohydrate 10 K.min^{-1}	1.797	397.07
$MgSO_4$ monohydrate 15 K.min^{-1}	1.792	416.57
$MgSO_4$ monohydrate 20 K.min^{-1}	1.786	417.24
$MgSO_4$ heptahydrate 5 K.min^{-1}	1.831	445.73
$MgSO_4$ heptahydrate 10 K.min^{-1}	1.809	422.73
$MgSO_4$ heptahydrate 15 K.min^{-1}	1.803	434.66
$MgSO_4$ heptahydrate 20 K.min^{-1}	1.791	422.42

Table 5 presents the averages of the kinetic parameters for the decomposition of each hydration degree. The reaction order values show a slight increase with increasing hydration degrees. The activation energies obtained for the decomposition of anhydrous and monohydrated sulfates had similar values, while that of the heptahydrate sulfate was 5% higher.

Table 5– Means of the kinetic parameters of the kinetic modeling of pure $MgSO_4$ decomposition.

Reagent	n	E_a ($kJ.mol^{-1}$)
$MgSO_4$ anhydrous	1.79	407.01
$MgSO_4$ monohydrate	1.80	404.51
$MgSO_4$ heptahydrate	1.81	431.39

5. Final remarks

According to Souza (2020), thermogravimetric tests generated thermogravimetric curves with expected behavior. All curves obtained from tests containing hydrated magnesium sulfate showed two intervals of mass loss. This behavior was expected since it was expected that at first, the sulfates would lose their hydration and only after decomposition. The only curves that do not show this behavior were those obtained by tests with anhydrous sulfate, which was to be expected since these sulfates do not have H_2O molecules to undergo the dehydration step.

After observing the graphic behavior of the curves, the values of the initial and final temperatures of the sulfate decomposition allowed an analysis of the influence of the evaluated factors on the thermodynamics of the systems. The first factor evaluated was the influence of reducing agents. Regarding the initial decomposition temperature, charcoal, coke breeze, and graphite obtained an initial temperature approximately 100 K lower than that of pure sulfate. The test with green coke did not show a representative reduction, remaining around 20 K. As for the final temperature of decomposition, breeze coke showed the best result, causing a reduction of approximately 110 K. Graphite showed a reduction of 65 K, while green coke and charcoal showed a variation of less than 15 K.

The next factor analyzed was the heating rate of the system. Although concerning the initial temperature of decomposition, the heating rates indicate a similar behavior for the three sulfates analyzed, with the initial temperatures increasing according to the heating rates. For the final decomposition temperatures, the systems do not show any pattern that indicates the influence of heating rates.

The third factor investigated was the influence of the sulfate hydration level on its decomposition. Regarding the initial temperature data, the values do not indicate an influence of hydration. For the final decomposition temperatures, although the increase in hydration is known with the decrease in these temperatures, this decrease is not significant.

The kinetic modeling used during this work to treat the data obtained in the thermogravimetric tests proved to be efficient to describe the behavior of the thermogravimetric curves of all experiments. Of the 16 tests carried out, in 14 the values of the coefficients of determination obtained were greater than 0.999, indicating that the mathematical model obtained data extremely close to the data obtained experimentally. Only in 2 cases were the R2 values lower than 0.999, even so, the values obtained in these cases were very close to the value, 0.9987 for the decomposition of $MgSO_4$ + charcoal and 0.9989 for the decomposition of anhydrous $MgSO_4$ with a rate of 20 $K.min^{-1}$.

The evaluation of the kinetic parameters confirmed some indications of the thermodynamic evaluation. When evaluating the influence of the reducing agents, the kinetic data indicated that the four contributed to the decrease in the activation energy of the decomposition of the sulfate heptahydrate. While the Ea of the pure sulfate decomposition was 422.731 $KJ.mol^{-1}$, the Ea of the decomposition in the presence of the four reducing agents obtained a decrease. This decrease being approximately 20% for green coke (340,391 $KJ.mol^{-1}$), 55% for breeze coke (196,120 $KJ.mol^{-1}$), and graphite (191,100 $KJ.mol^{-1}$), and 62% for charcoal (162,302 $KJ.mol^{-1}$).

Regarding the three different levels of hydration, the kinetic data indicated a behavior contrary to that expected by the thermodynamic data. While thermodynamic data indicated magnesium sulfate decomposition favored by increasing hydration degree, kinetic data indicated that sulfate monohydrate had the lowest activation energy (404,505 $KJ.mol^{-1}$), closely followed by anhydrous sulfate (407,009 $KJ.mol^{-1}$), while sulfate heptahydrate had the highest Ea value (433,333 $KJ.mol^{-1}$). Regarding the heating rate, again it was not possible to observe behavior that would indicate an influence on the system.

6. Suggestions for futures development

Throughout this work, the experimental tests and kinetic modeling contributed to the achievement of the objectives outlined at the beginning of the work. However, while these goals were achieved, new questions arose. These new questions serve as a basis for possible future work and are listed as new proposals:

- To analyze the reactivity of the products obtained, to evaluate the influence of the heating rates and the hydrations of the magnesium sulfate used in its decomposition.
- Carry out a characterization of the carbon sources used
- Carry out tests with mixtures of carbon sources.
- To analyze the reactivity of the products obtained in the presence of the reducing agents, to evaluate the influence of the reducing agents.
- Carry out a characterization of the products obtained in the thermogravimetric tests.
- Evaluate the use of other reaction atmospheres, such as O_2 and H_2.
- Perform the experiment with a magnesium sulfate from a precipitation with impurities.

7. References

ACHAR, B. N. N.; BRINDLEY, G. W.; SHARP, J. H. **Kinetics and mechanism of dehydroxylation processes. III Applications and limitations of Dynamic methods**. Proceedings of the International Clay Conference. **Anais**...Jerusalem: 1966

AGATZINI-LEONARDOU, S. et al. Hydrometallurgical process for the separation and recovery of nickel from sulphate heap leach liquor of nickeliferrous laterite ores. **Minerals Engineering**, v. 22, n. 14, p. 1181–1192, 2009.

AINA, V. et al. Magnesium- and strontium-co-substituted hydroxyapatite: the effects of doped-ions on the structure and chemico-physical properties. **Journal of Materials Science: Materials in Medicine**, v. 23, n. 12, p. 2867–2879, 2012.

AL-TABBAA, A. Reactive magnesia cement. In: **Eco-Efficient Concrete**. [s.l.] Elsevier, 2013. p. 523–543.

ALI, S. H. et al. Mineral supply for sustainable development requires resource governance. **Nature**, v. 543, n. 7645, p. 367–372, 2017.

ANM. **Anuário Mineral Brasileiro: principais substâncias metálicas 2020**. Brasília: [s.n.]. Disponível em: <www.anm.gov.br>. Acesso em: 29 dez. 2021.

APHANE, M. E.; VAN DER MERWE, E. M.; STRYDOM, C. A. Influence of hydration time on the hydration of MgO in water and in a magnesium acetate solution. **Journal of Thermal Analysis and Calorimetry**, v. 96, n. 3, p. 987–992, 2009.

ASENCIOS, Y. J. O.; ASSAF, E. M. Combination of dry reforming and partial oxidation of methane on NiO-MgO-ZrO2 catalyst: Effect of nickel content. **Fuel Processing Technology**, v. 106, p. 247–252, 2013.

ASENCIOS, Y. J. O.; NASCENTE, P. A. P.; ASSAF, E. M. Partial oxidation of methane on NiO-MgO-ZrO 2 catalysts. **Fuel**, v. 97, p. 630–

637, 2012.

AVRAMI, M. Granulation, Phase Change, and Microstructure Kinetics of Phase Change. **The Journal of Chemical Physics**, v. 9, n. December, p. 177–184, 1941.

BARBOSA, L. I.; GONZÁLEZ, J. A.; DEL CARMEN RUIZ, M. Extraction of lithium from β-spodumene using chlorination roasting with calcium chloride. **Thermochimica Acta**, v. 605, p. 63–67, 10 abr. 2015.

BARIN, I.; SCHULER, W. On the kinetics of the chlorination of titanium dioxide in the presence of solid carbon. **Metallurgical Transactions B**, v. 11, n. 2, p. 199–207, jun. 1980.

BARTLEY, J. K. et al. Simple method to synthesize high surface area magnesium oxide and its use as a heterogeneous base catalyst. **Applied Catalysis B: Environmental**, v. 128, p. 31–38, 2012.

BOOSTER, J. L.; SANDWIJK, A. VAN; REUTER, M. A. MAGNESIUM REMOVAL IN THE ELECTROLYTIC ZINC INDUSTRY. **Minerals Engineering**, v. 13, n. 5, p. 517–526, 2000.

BOYD, C. E. **Water Quality**. Third Edit ed. Cham: Springer International Publishing, 2020.

BRANCATO, V. et al. MgSO4·7H2O filled macro cellular foams: An innovative composite sorbent for thermo-chemical energy storage applications for solar buildings. **Solar Energy**, v. 173, n. February, p. 1278–1286, 2018.

BROCCHI, E. A.; MOURA, F. J. Chlorination methods applied to recover refractory metals from tin slags. **Minerals Engineering**, v. 21, n. 2, p. 150–156, jan. 2008.

BROWN, R. E. Magnesium recycling yesterday, today, and tomorrow. **The Minerals, Metals and Materials Society, Warrendale**, p. 1318–1329, 2000.

BROWNELL, W. E. Reactions Between Alkaline-Earth Sulfates and.

Journal of The American Ceramic Society, v. 46, n. 3, p. 125–128, 1951.

BURTON, M. **Oferta menor de magnésio da China ameaça empregos na Europa**. Disponível em: <https://www.bloomberglinea.com.br/2021/10/23/oferta-menor-de-magnesio-da-china-ameaca-empregos-na-europa/>. Acesso em: 8 dez. 2021.

CALDAS, T. D. P. **Análise de Trincas e Coating em Pelotas de Minério de Ferro por Processamento Digital de Imagens**. [s.l.] Pontifícia Universidade Católica do Rio de Janeiro, 2019.

CALO, J. M.; PERKINS, M. T. A heterogeneous surface model for the “steady-state” kinetics of the boudouard reaction. **Carbon**, v. 25, n. 3, p. 395–407, 1987.

CARABALLO, M. A. et al. Field multi-step limestone and MgO passive system to treat acid mine drainage with high metal concentrations. **Applied Geochemistry**, v. 24, n. 12, p. 2301–2311, 2009.

CARDOSO, J. H. **Decomposição redutora de MgSO4.7H2O na presença de H2(g) Dissertação**. [s.l.] Pontifícia Universidade Católica do Rio de Janeiro, 2018.

CHENG, C. Y. et al. Recovery of nickel and cobalt from laterite leach solutions using direct solvent extraction: Part 1 - Selection of a synergistic SX system. **Hydrometallurgy**, v. 104, n. 1, p. 45–52, 2010.

CHENG, C. Y. et al. Synergistic solvent extraction of nickel and cobalt: A review of recent developments. **Solvent Extraction and Ion Exchange**, v. 29, n. 5–6, p. 719–754, 2011.

CHIPERA, S. J.; VANIMAN, D. T. Experimental stability of magnesium sulfate hydrates that may be present on Mars. **Geochimica et Cosmochimica Acta**, v. 71, n. 1, p. 241–250, 2007.

CIPOLLINA, A. et al. Reactive crystallisation process for magnesium

recovery from concentrated brines. **Desalination and Water Treatment**, v. 55, p. 2377–2388, 2015.

COATS, A. W.; REDFERN, J. P. Kinetic Parameters from Thermogravimetric Data. **Nature**, v. 201, p. 68–69, 1964.

COSTA, R. H. **Recovery of magnesium sulfate from a zinc ore flotation tailing using hydrometallurgical route.** São Paulo: Universidade de São Paulo, 1 dez. 2020.

COURTIAL, M.; CABRILLAC, R.; DUVAL, R. Recycling of magnesium slags in construction block form. **Studies in Environmental Science**, v. 60, n. C, p. 599–604, 1994.

CURRY, K. C.; VAN OSS, H. G. 2017 Minerals Yearbook: Magnesium Compounds. **US Geological Survey, Washington DC**, n. March, 2020.

DA SILVA, A. M. V. **Estudos sobre a recuperação do titânio contido no rejeito da concentração de magnetita**. [s.l.] Pontifícia Universidade Católica do Rio de Janeiro , 2018.

DĄBROWSKI, A. et al. Selective removal of the heavy metal ions from waters and industrial wastewaters by ion-exchange method. **Chemosphere**, v. 56, n. 2, p. 91–106, 2004.

DALY, T. **China Oct magnesium exports rebound to 19-month high**. Disponível em: <https://www.reuters.com/markets/commodities/china-oct-magnesium-exports-rebound-19-month-high-2021-11-22/>. Acesso em: 10 dez. 2021.

DAMAYANTI, R.; KHAERUNISSA, H. COMPOSITION AND CHARACTERISTICS OF RED MUD: A CASE STUDY ON TAYAN BAUXITE RESIDUE FROM ALUMINA PROCESSING PLANT AT WEST KALIMANTAN. **INDONESIAN MINING JOURNAL**, v. 19, n. 3, p. 179–190, 2016.

DENISENKO, Y. G. et al. Thermal decomposition of europium sulfates Eu2(SO4)3·8H2O and EuSO4. **Journal of Solid State Chemistry**, v. 255,

n. August, p. 219–224, 2017.

DHARWADKAR, S. R.; CHANDRASEKHARAIAH, M. S.; KARKHANAVALA, M. D. Evaluation of kinetic parameters from thermogravimetric curves. **Thermochimica Acta**, v. 25, p. 372–375, 1978.

DING, K. et al. Thermochemical reduction of magnesium sulfate by natural gas: Insights from an experimental study. **Geochemical Journal**, v. 45, n. 2, p. 97–108, 2011.

DONG, H. et al. Synthesis of reactive MgO from reject brine via the addition of NH4OH. **Hydrometallurgy**, v. 169, p. 165–172, 2017.

DONG, H. et al. Investigation of the properties of MgO recovered from reject brine obtained from desalination plants. **Journal of Cleaner Production**, v. 196, p. 100–108, 20 set. 2018.

DOU, W. et al. Sulfate removal from wastewater using ettringite precipitation: Magnesium ion inhibition and process optimization. **Journal of Environmental Management**, v. 196, p. 518–526, 2017.

DUPONT, C.; CAMPAGNE, A.; CONSTANT, F. Efficacy and Safety of a Magnesium Sulfate-Rich Natural Mineral Water for Patients With Functional Constipation. **Clinical Gastroenterology and Hepatology**, v. 12, n. 8, p. 1280–1287, 2014.

EUROPEAN COMMISSION. **COMMITTEE AND THE COMMITTEE OF THE REGIONS Critical Raw Materials Resilience: Charting a Path towards greater Security and Sustainability. COM(2020) 474 final**. [s.l: s.n.]. Disponível em: <http://info.worldbank.org/governance/wgi/.>.

FAN, C. et al. Leaching behavior of metals from chlorinated limonitic nickel laterite. **International Journal of Mineral Processing**, v. 110–111, p. 117–120, jul. 2012.

FERNANDES, F. R. C. et al. **TENDÊNCIAS TECNOLÓGICAS BRASIL 2015 - Geociências e Tecnologia Mineral**. Rio de Janeiro, Brazil: CETEM - Centro de Tecnologia Mineral, 2007.

FREEMAN, E. S.; CARROLL, B. The Application of Thermoanalytical Techniques to Reaction Kinetics: The Thermogravimetric Evaluation of the Kinetics of the Decomposition of Calcium Oxalate Monohydrate. **The Journal of Physical Chemistry**, v. 62, n. 4, p. 394–397, 1958.

FREITAS, E. V. DE S. et al. Indução da fitoextração de chumbo por ácido cítrico em solo contaminado por baterias automotivas. **Revista Brasileira de Ciência do Solo**, v. 33, n. 2, p. 467–473, abr. 2009.

GALLAGHER, P. K.; JOHNSON, D. W.; SCHREY, F. Thermal Decomposition of Iron (II) Sulfates. **Journal of The American Ceramic Society**, v. 53, n. 12, p. 666–670, 1970.

GAO, F. et al. Recovery of magnesium from ferronickel slag to prepare hydrated magnesium sulfate by hydrometallurgy method. **Journal of Cleaner Production**, v. 303, p. 127049, 2021.

GARCES-GRANDA, A.; LAPIDUS, G. T.; RESTREPO-BAENA, O. J. The effect of calcination as pre treatment to enhance the nickel extraction from low-grade laterites. **Minerals Engineering**, v. 120, n. November 2017, p. 127–131, 2018.

GENCELI, F. E. et al. Crystallization and Characterization of a New Magnesium Sulfate Hydrate MgSO4·11H2O. **Crystal Growth & Design**, v. 7, n. 12, p. 2460–2466, 2007.

GRIGOROVA, D.; PAUNOVA, R. Thermodynamic and kinetic investigation of carbothermic reduction of electric arc furnace dust. **Metalurgija**, v. 61, n. 1, p. 189–192, 2022.

GUAN, Q. JUN et al. Recovery of cobalt and nickel in the presence of magnesium and calcium from sulfate solutions by Versatic 10 and mixtures of Versatic 10 and Cyanex 301. **Transactions of Nonferrous Metals Society of China (English Edition)**, v. 26, n. 3, p. 865–873, 2016.

HABASHI, F. **Handbook of Extractive Metallurgy - Vol. 2**. Weinheim - Chicester - New Youk - Toronto - Brisbane - Singapore: WILEY-VCH, 1997.

HAJBI, F. et al. Thermodynamic study of magnesium sulfate crystallization: application of Pitzer model and quinary diagrams. **Desalination and Water Treatment**, p. 12, 2015.

HAN, D. et al. A review on ignition mechanisms and characteristics of magnesium alloys. **Journal of Magnesium and Alloys**, v. 8, n. 2, p. 329–344, 2020.

HARVEY, R.; HANNAH, R.; VAUGHAN, J. Selective precipitation of mixed nickel-cobalt hydroxide. **Hydrometallurgy**, v. 105, n. 3–4, p. 222–228, 2011.

HIGHFIELD, J. et al. RSC Advances Activation of serpentine for CO2 mineralization by flux extraction of soluble magnesium salts using ammonium sulfate. **The Royal Society of Chemistry**, v. 2, p. 6535–6541, 2012.

HLABELA, P. S. et al. Thermal reduction of barium sulphate with carbon monoxide-A thermogravimetric study. **Thermochimica Acta**, v. 498, n. 1–2, p. 67–70, 2010.

HOTEIT, A. et al. Sulfate decomposition from circulating fluidized bed combustors bottom ash. **Chemical Engineering Science**, v. 62, n. 23, p. 6827–6835, 1 dez. 2007.

HUANG, P. et al. A sustainable process to utilize ferrous sulfate waste from titanium oxide industry by reductive decomposition reaction with pyrite. **Thermochimica Acta**, v. 620, p. 18–27, 2015.

HULBERT, S. F. Effect of processing parameters on the kinetics of decomposition of magnesium sulphate. **Materials Science and Engineering**, v. 2, n. 5, p. 262–268, 1968.

INEICH, T. et al. Utilization efficiency of lime consumption during magnesium sulfate precipitation. **Hydrometallurgy**, v. 173, n. September, p. 241–249, 2017.

IONASHIRO, M. **Princípios Básicos da Termogravimetria e Análise**

Térmica Diferencial/ Calorimetria Exploratória Diferencial. [s.l: s.n.].

JAVAID, A. et al. LITERATURE REVIEW ON MAGNESIUM RECYCLING. **Magnesium Technology**, p. 7–12, 2006.

JENA, B. C.; DRESLER, W.; REILLY, I. G. Extraction of titanium, vanadium and iron from titanomagnetite deposits at pipestone lake, Manitoba, Canada. **Minerals Engineering**, v. 8, n. 1–2, p. 159–168, jan. 1995.

JIANG, M. et al. Mechanism of sodium sulfate in promoting selective reduction of nickel laterite ore during reduction roasting process. **International Journal of Mineral Processing**, v. 123, p. 32–38, 2013.

JIAO, F. et al. Recovery of chromium and magnesium from spent magnesia-chrome refractories by acid leaching combined with alkali precipitation and evaporation. **Separation and Purification Technology**, v. 227, n. June, p. 115705, 2019.

JIN, F.; AL-TABBAA, A. Strength and hydration products of reactive MgO-silica pastes. **Cement and Concrete Composites**, v. 52, p. 27–33, 2014.

JOHNSON, D. W.; GALLAGHER, P. K. Kinetics of the Decomposition of Freeze-Dried Aluminum Sulfate and Ammonium Aluminum Sulfate. **Journal of the American Ceramic Society**, v. 54, n. 9, p. 461–465, 1971.

KANARI, N. et al. Thermal Behavior of Hydrated Iron Sulfate in Various Atmospheres. **Metals**, v. 8, n. 12, p. 1084, 2018.

KANARI, N.; GABALLAH, I. Chlorination and carbochlorination of magnesium oxide. **Metallurgical and Materials Transactions B**, v. 30, n. 3, p. 383–391, jun. 1999.

KARIDAKIS, T.; AGATZINI-LEONARDOU, S.; NEOU-SYNGOUNA, P. Removal of magnesium from nickel laterite leach liquors by chemical precipitation using calcium hydroxide and the potential use of the precipitate as a filler material. **Hydrometallurgy**, v. 76, n. 1–2, p. 105–

114, 2005.

KATO, H. et al. Decomposition of carbon dioxide to carbon by hydrogen-reduced Ni(II)-bearing ferrite. **Journal of Materials Science**, v. 29, n. 21, p. 5689–5692, 1994.

KAYA, S.; TOPKAYA, Y. A. High pressure acid leaching of a refractory lateritic nickel ore. **Minerals Engineering**, v. 24, n. 11, p. 1188–1197, 2011.

KHAIRUL, M. A.; ZANGANEH, J.; MOGHTADERI, B. The Composition, Recycling and Utilisation of Bayer Red Mud. **Conservation and Recycling**, v. 141, n. February, p. 483–498, 2019.

KHOO, J. Z.; HAQUE, N.; BHATTACHARYA, S. Process simulation and exergy analysis of two nickel laterite processing technologies. **International Journal of Mineral Processing**, v. 161, p. 83–93, 2017.

KIM, B. S. et al. A kinetic study of the carbothermic reduction of zinc oxide with various additives. **Materials Transactions**, v. 47, n. 9, p. 2421–2426, 2006.

KIM, J.; AZIMI, G. Resources, Conservation & Recycling Selective Precipitation of Titanium, Magnesium, and Aluminum from the Steelmaking Slag Leach Liquor. **Resources, Conservation & Recycling**, v. 180, n. January, p. 106177, 2022.

KOBERTZ, D.; MÜLLER, M. Experimental studies on NiSO4 by thermal analysis and calorimetry. **Calphad: Computer Coupling of Phase Diagrams and Thermochemistry**, v. 45, p. 55–61, 2014.

KONGOLO, K. et al. Cobalt and zinc recovery from copper sulphate solution by solvent extraction. **Minerals Engineering**, v. 16, n. 12, p. 1371–1374, 2003.

KOVACHEVA, P.; DJINGOVA, R. Ion-exchange method for separation and concentration of platinum and palladium for analysis of environmental samples by inductively coupled plasma atomic emission spectrometry.

Analytica Chimica Acta, v. 464, n. 1, p. 7–13, 2002.

KURBAN, G. V. T. et al. Thermodynamics and Kinetic Modeling of the ZnSO4·H2O Thermal Decomposition in the Presence of a Pd/Al2O3 Catalyst. **Energies**, v. 15, n. 2, p. 548, 2022.

KUUSIK, R.; SALKKONEN, P.; NIINISTÖ, L. Thermal decomposition of calcium sulphate in carbon monoxide. **Journal of Thermal Analysis**, v. 30, n. 1, p. 187–193, 1985.

L'VOV, B. V.; UGOLKOV, V. L. Kinetics of free-surface decomposition of magnesium and barium sulfates analyzed thermogravimetrically by the third-law method. **Thermochimica Acta**, v. 411, n. 1, p. 73–79, 2004.

LAHIJANI, P. et al. Conversion of the greenhouse gas CO2 to the fuel gas CO via the Boudouard reaction: A review. **Renewable and Sustainable Energy Reviews**, v. 41, p. 615–632, 2015.

LAUREIRO, Y. et al. Kinetic parameters for the thermal decomposition reactions of CrO3 in AIR. **Thermochimica Acta**, v. 143, n. C, p. 347–350, maio 1989.

LEE, E. K. et al. Magnesium oxide as an effective catalyst in catalytic wet oxidation of H2S to sulfur. **Reaction Kinetics and Catalysis Letters**, v. 82, n. 2, p. 241–246, 2004.

LEMOS, F.; ANGORA, M.; MASSON, I. Lixiviação sob pressão de minérios lateríticos. p. 131–136, 2007.

LENOIR, D.; SCHRAMM, K. W.; LALAH, J. O. Green Chemistry: Some important forerunners and current issues. **Sustainable Chemistry and Pharmacy**, v. 18, n. September, p. 100313, 2020.

LI, H. et al. Investigation on the recovery of gold and silver from cyanide tailings using chlorination roasting process. **Journal of Alloys and Compounds**, v. 763, p. 241–249, 30 set. 2018.

LI, J. et al. Preparation of boric acid from low-grade ascharite and recovery of magnesium sulfate. **Transactions of Nonferrous Metals**

Society of China (English Edition), v. 20, n. 6, p. 1161–1165, 2010.

LI, X. MING et al. Improvement of carbothermic reduction of nickel slag by addition of CaCO3. **Transactions of Nonferrous Metals Society of China (English Edition)**, v. 29, n. 12, p. 2658–2666, 2019a.

LI, Z. et al. Efficient and Sustainable Removal of Magnesium from Brines for Lithium/Magnesium Separation Using Binary Extractants. **ACS Sustainable Chemistry and Engineering**, v. 7, p. 19225–19234, 2019b.

LIU, X. W. et al. Recovery of valuable metals from a low-grade nickel ore using an ammonium sulfate roasting-leaching process. **International Journal of Minerals, Metallurgy and Materials**, v. 19, n. 5, p. 377–383, 2012.

LIU, Y. et al. Magnesium ammonium phosphate formation , recovery and its application as valuable resources: a review. **Journal of Chemical Technology & Biotechnology**, v. 88, n. May, p. 181–189, 2013.

LIU, Y.; NAIDU, R. **Hidden values in bauxite residue (red mud): Recovery of metalsWaste Management**, 2014.

LÜDKE, M. C. **A ROTA METALÚRGICA DO SILÍCIO: DA EXTRAÇÃO DO QUARTZO À OBTENÇÃO DO SILÍCIO DE GRAU FOTOVOLTAICO**. [s.l.] UNIVERSIDADE FEDERAL DE SANTA CATARINA, 2018.

LUO, A. A.; SACHDEV, A. K. **Applications of magnesium alloys in automotive engineering**. [s.l.] Woodhead Publishing Limited, 2012.

LV, X. et al. Non-isothermal kinetics study on carbothermic reduction of nickel laterite ore. **Powder Technology**, v. 340, p. 495–501, 2018.

MA, X. et al. One-step synthesis of basic magnesium sulfate whiskers by atmospheric pressure reflux. **Particuology**, v. 24, p. 191–196, 2016.

MACCARTHY, J. et al. Atmospheric acid leaching mechanisms and kinetics and rheological studies of a low grade saprolitic nickel laterite ore. **Hydrometallurgy**, v. 160, p. 26–37, 2016.

MACINGOVA, E.; LUPTAKOVA, A. Recovery of metals from acid mine drainage. **Chemical Engineering Transactions**, v. 28, n. 3, p. 109–114, 2012.

MAHMUD, N. et al. Magnesium recovery from desalination reject brine as pretreatment for membraneless electrolysis. **Desalination**, v. 525, n. August 2021, p. 115489, 2022.

MANN, R. A.; BAVOR, H. J. Phosphorus removal in constructed wetlands using gravel and industrial waste substrata. **Water Science and Technology**, v. 27, n. 1, p. 107–113, 1993.

MARCHI, J. et al. Influence of Mg-substitution on the physicochemical properties of calcium phosphate powders. **Materials Research Bulletin**, v. 42, n. 6, p. 1040–1050, 2007.

MCDONALD, R. G.; WHITTINGTON, B. I. Atmospheric acid leaching of nickel laterites review. Part II. Chloride and bio-technologies. **Hydrometallurgy**, v. 91, n. 1–4, p. 56–69, 2008.

MEHRA, D.; MAHAPATRA, M. M.; HARSHA, S. P. Processing of RZ5-10wt%TiC in-situ magnesium matrix composite. **Journal of Magnesium and Alloys**, v. 6, n. 1, p. 100–105, 2018.

MELLO, N. M. et al. Effect of an alumina supported palladium catalyst on the magnesium sulfate decomposition kinetics. **Materials Research**, v. 23, n. 6, 2020.

MENG, L. et al. Recovery of Ni, Co, Mn, and Mg from nickel laterite ores using alkaline oxidation and hydrochloric acid leaching. **Separation and Purification Technology**, v. 143, p. 80–87, 2015.

MME. **Boletim do Setor Mineral 2020**. Brasília, DF: [s.n.].

MO, L.; DENG, M.; TANG, M. Effects of calcination condition on expansion property of MgO-type expansive agent used in cement-based materials. **Cement and Concrete Research**, v. 40, n. 3, p. 437–446, 2010.

MONTEIRO, F. Z. R. **Estudo da decomposição térmica da fibra do**

coco verde na presença de um catalisador nano estruturado. [s.l.] Pontifícia Universidade Católica do Rio de Janeiro, 2017.

MOODLEY, S. et al. **Chlorination of titania feedstocks**. TMS Annual Meeting. **Anais**...Hoboken, NJ, USA: John Wiley & Sons, Inc., 15 maio 2012Disponível em: <https://onlinelibrary.wiley.com/doi/10.1002/9781118364987.ch12>

MORCALI, M. H.; KHAJAVI, L. T.; DREISINGER, D. B. Extraction of nickel and cobalt from nickeliferous limonitic laterite ore using borax containing slags. **International Journal of Mineral Processing**, v. 167, p. 27–34, 2017.

MOUSSAVI, G.; MAHMOUDI, M. Removal of azo and anthraquinone reactive dyes from industrial wastewaters using MgO nanoparticles. **Journal of Hazardous Materials**, v. 168, n. 2–3, p. 806–812, 2009.

NARAYAN, R.; TABATABAIE-RAISSI, A.; ANTAL JR, M. J. A Study of Zinc Sulfate Decomposition at Low Heating Rates. **Industrial & Engineering Chemistry Research**, v. 27, n. 6, p. 1050–1058, 1988.

NETZSCH. **Simultaneous Thermal Analyzer – STA 449 F3 Jupiter®**, 2022.

NKOSI, S. et al. **A comparative study of vanadium recovery from titaniferous magnetite using salt, sulphate, and soda ash roast-leach processes**. The Southern African Institute of Mining and Metallurgy. **Anais**...Pretoria: 2017Disponível em: <http://www.mintek.co.za/Pyromet/Files/2017Nkosi.pdf>. Acesso em: 7 fev. 2019

NURUNNABI, M. et al. Additive effect of noble metals on NiO-MgO solid solution in oxidative steam reforming of methane under atmospheric and pressurized conditions. **Applied Catalysis A: General**, v. 299, n. 1–2, p. 145–156, 2006.

OBERLE, B. et al. **Global Resources Outlook 2019: Natural Resources for the Future We Want.Global Resources Outlook 2019**. Nairobi,

Kenya: UN, 16 set. 2020. Disponível em: <https://www.un-ilibrary.org/content/books/9789280737417>.

OKHRIMENKO, L. et al. Thermodynamic study of MgSO4 – H2O system dehydration at low pressure in view of heat storage. **Thermochimica Acta**, v. 656, n. August, p. 135–143, 2017.

OKHRIMENKO, L. et al. New kinetic model of the dehydration reaction of magnesium sulfate hexahydrate: Application for heat storage. **Thermochimica Acta**, v. 687, n. July 2019, p. 178569, 2020.

OKUMURA, S. et al. Recovery of CaO by Reductive Decomposition of Spent Gypsum in a CO-CO 2-N2 Atmosphere. **Industrial and Engineering Chemistry Research**, v. 42, n. 24, p. 6046–6052, 2003.

OSLANEC, P.; IŽDINSKÝ, K.; SIMANČÍK, F. Possibilities of magnesium recycling. **Material Science and Technology**, v. 4, p. 83–88, 2008.

OSTROFFT, A. G.; SANDERSON, R. T. THERMAL STABILITY OF SOME METAL Department of Chemistry , State University of Iowa , Iowa City Abstract--The thermal decomposition of eleven (If) sulphates has been studied by a combination of thermogravimetric and differential thermal anlaysis . The re. **Journal of Inorganic and Nuclear Chemistry**, v. 9, p. 45–50, 1959.

OXLEY, A.; BARCZA, N. Hydro-pyro integration in the processing of nickel laterites. **Minerals Engineering**, v. 54, p. 2–13, 2013.

ÖZDEMIR, M.; ÇAKIR, D.; KIPÇAK, Í. Magnesium recovery from magnesite tailings by acid leaching and production of magnesium chloride hexahydrate from leaching solution by evaporation. **The International Journal of Mineral Processing**, v. 93, p. 209–212, 2009.

OZGA, P.; RIESENKAMPF, W. Effect of zinc sulphide concentrate composition and roasting temperature on magnesium distribution in zinc calcine. **Canadian Metallurgical Quarterly**, v. 35, n. 3, p. 235–244, 1996.

PAN, F.; YANG, M.; CHEN, X. A Review on Casting Magnesium Alloys:

Modification of Commercial Alloys and Development of New Alloys. **Journal of Materials Science & Technology**, v. 32, n. 12, p. 1211–1221, 2016.

PAUL, S. A.; CHAVAN, S. K.; KHAMBE, S. D. Studies on characterization of textile industrial waste water in Solapur city. **International Journal of Chemical Sciences**, v. 10, n. 2, p. 635–642, 2012.

PAULIK, J.; PAULIK, F.; ARNOLD, M. Dehydration of magnesium sulphate heptahydrate investigated by quasi isothermal-quasi isobaric TG. **Thermochimica Acta**, v. 50, n. 1–3, p. 105–110, 1981.

PICKLES, C. A. Thermodynamic analysis of the selective chlorination of electric arc furnace dust. **Journal of Hazardous Materials**, v. 166, n. 2–3, p. 1030–1042, 30 jul. 2009.

PILARSKA, A. A.; KLAPISZEWSKI, Ł.; JESIONOWSKI, T. Recent development in the synthesis, modification and application of Mg(OH)2 and MgO: A review. **Powder Technology**, v. 319, p. 373–407, 2017.

PLEWA, J.; STEINDOR, J. Kinetics of reduction of magnesium sulfate by carbon oxide. **Journal of Thermal Analysis**, v. 32, n. 6, p. 1809–1820, 9 nov. 1987.

POMIRO, F. J. et al. Study of the Reaction Stages and Kinetics of the Europium Oxide Carbochlorination. **Metallurgical and Materials Transactions B: Process Metallurgy and Materials Processing Science**, v. 46, n. 1, p. 304–315, 2014.

RAM, A. **China's magnesium supply for rest of 2021 to lag demand: sources**. Disponível em: <https://www.spglobal.com/platts/en/market-insights/latest-news/metals/110321-chinas-magnesium-supply-for-rest-of-2021-to-lag-demand-sources>. Acesso em: 10 dez. 2021.

RAMALINGOM, S.; PODDER, J.; NARAYANA KALKURA, S. Crystallization and characterization of orthorhombic β-MgSO4·7H2O. **Crystal Research and Technology**, v. 36, n. 12, p. 1357–1364, 2001.

REGO, A. S. C. et al. KAl(SO4)2 thermal decomposition kinetics modeling through graphical and PSO methods. **Journal of Materials Research and Technology**, v. 14, n. 3, p. 1975–1984, set. 2021.

RIVA, L. et al. A study of densified biochar as carbon source in the silicon and ferrosilicon production. **Energy**, v. 181, p. 985–996, 15 ago. 2019.

ROCHE, E. G.; PRASAD, J. **Magnesium Oxide Recovery**USA, 2009.

RODE, H.; HLAVACEK, V. Detailed kinetics of titanium nitride synthesis. **AIChE Journal**, v. 41, n. 2, p. 377–388, fev. 1995.

RODRIGUES, R. **Modelagem Cinética e de Equilíbrio Combinadas para Simulação de Processos de Gaseificação**. [s.l.] UNIVERSIDADE FEDERAL DO RIO GRANDE DO SUL, 2015.

ROINE, A. O. **HSC Chemistry 10**Pori, Finland, 2021.

ROSITA, W. et al. Recovery of rare earth elements and Yttrium from Indonesia coal fly ash using sulphuric acid leaching. **AIP Conference Proceedings**, v. 2223, n. April, 2020.

SABATIER, M. et al. Influence of the consumption pattern of magnesium from magnesium-rich mineral water on magnesium bioavailability. **British Journal of Nutrition**, v. 106, n. 3, p. 331–334, 2011.

SAHOO, R. N.; NAIK, P. K.; DAS, S. C. Leaching of manganese from low-grade manganese ore using oxalic acid as reductant in sulphuric acid solution. **Hydrometallurgy**, v. 62, n. 3, p. 157–163, 2001.

SAKAKIBARA, M. et al. Kinetic Analysis of Thermogravimetric Data. **Nippon Kagaku Kaishi**, v. 1989, n. 10, p. 1729–1732, 1989.

SANCHEZ, M. E. et al. Thermogravimetric kinetic analysis of the combustion of biowastes. **Renewable Energy journal**, v. 34, p. 1622–1627, 2009.

SANTOS, F. et al. Behavior of Zn and Fe Content in Electric Arc Furnace Dust as Submitted to Chlorination Methods. **Metallurgical and Materials**

Transactions B, v. 46, n. 4, p. 1729–1741, 21 ago. 2015.

SCHEIDEMA, M. **The reaction mechanism and operating window for the decomposition of hydrated magnesium sulfate under reducing conditions**. Helsinki: School of Chemical Technology, 2015.

SCHEIDEMA, M. N.; TASKINEN, P. Decomposition thermodynamics of magnesium sulfate. **Industrial and Engineering Chemistry Research**, v. 50, n. 16, p. 9550–9556, 2011.

SCHEIDEMA, M.; TASKINEN, P.; METSÄRINTA, M. L. Reductive decomposition of magnesium sulfate. **Proceedings - European Metallurgical Conference, EMC 2011**, v. 3, n. January, p. 1021–1032, 2011.

SETIAWAN, A. et al. Kinetics and Mechanisms of Carbothermic Reduction of Weathered Ilmenite Using Palm Kernel Shell Biomass. **Journal of Sustainable Metallurgy**, 2021.

SILVA, A. M.; LIMA, R. M. F.; LEÃO, V. A. Mine water treatment with limestone for sulfate removal. **Journal of Hazardous Materials**, v. 221–222, p. 45–55, 2012.

SILVA, L. R. DA. Magnesita. In: **Sumário Brasileiro Mineral 2018**. [s.l: s.n.]. p. 3.

SIRIWARDANE, R. V. et al. Decomposition of the sulfates of copper, iron (II), iron (III), nickel, and zinc: XPS, SEM, DRIFTS, XRD, and TGA study. **Applied Surface Science**, v. 152, n. 3, p. 219–236, 1999.

SOTO-DÍAZ, O. et al. Metal sulfate decomposition using green Pd-based catalysts supported on ΓAl2O3 and SiC: A common step in sulfur-family thermochemical cycles. **International Journal of Hydrogen Energy**, v. 4, p. 12309–12314, 2019.

SOUZA, A. D. et al. Kinetics of sulphuric acid leaching of a zinc silicate calcine. **Hydrometallurgy**, v. 89, n. 3–4, p. 337–345, 2007.

SOUZA, B. et al. MgSO4 carbothermic reductive decomposition to

produce a highly reactive MgO powder. **Journal of Materials Research and Technology**, p. 9, 16 jan. 2020.

SOUZA, R. et al. Potassium alum thermal decomposition study under non-reductive and reductive conditions. **Journal of Materials Research and Technology**, v. 8, n. 1, p. 745–751, 2019.

SPEYER, R. **Thermal Analysis of Materials**. 1st Editio ed. Boca Raton: CRC Press, 1994.

STOPIC, S.; FRIEDRICH, B. Hydrometallurgical processing of nickel lateritic ores. **Vojnotehnicki glasnik**, v. 64, n. 4, p. 1033–1047, 2016.

STOPIC, S.; FRIEDRICH, B.; FUCHS, R. Sulphuric acid leaching of the Serbian nickel lateritic ore. **Erzmetall: Journal for Exploration, Mining and Metallurgy**, v. 56, n. 4, p. 204–209, 2003.

SUK, N. I.; KOTELNIKOV, A. R.; KOVALSKII, A. M. Iron-magnesium minerals from differentiated rocks of Lovozersky alkaline massif. **Geochemistry, Mineralogy and Petrology.**, v. 47, p. 97–107, 2009.

TAIT, S. et al. Removal of sulfate from high-strength wastewater by crystallisation. **Water Research**, v. 43, n. 3, p. 762–772, 2009.

TANG, X. et al. Prospect of recovering phosphorus in magnesium slag-packed wetland filter. **Environmental Science and Pollution Research**, v. 24, p. 22808–22815, 2017.

THE ECONOMIST. **Why it matters that magnesium is in short supply**. Disponível em: <https://www.economist.com/the-economist-explains/2021/11/15/why-it-matters-that-magnesium-is-in-short-supply>. Acesso em: 8 dez. 2021.

THE MATHWORKS INC. **MATLAB R2021a**, 2021.

THE WORLD BANK. **The Growing Role of Minerals and Metals for a Low Carbon Future**. [s.l.] World Bank, Washington, DC, 2017.

TOLONEN, E. T.; RÄMÖ, J.; LASSI, U. The effect of magnesium on partial

sulphate removal from mine water as gypsum. **Journal of Environmental Management**, v. 159, p. 143–146, 2015.

TOMAZ, M. A.; ANDRADE, F. V.; CANDIDO, A. D. O. Ph , Cálcio E Magnésio Influenciados Pelo Uso De Resíduos Industriais Utilizados Como Corretivos , Em Lavoura De Café Conilon Ph , Calcium and Magnesium Influenced By the Use of Industrial Waste Used As Correctives in Conilon Coffee Plantation. 2011.

U.S. GEOLOGICAL SURVEY. **Mineral Commodity Summaries 2021**. [s.l: s.n.].

UN DEPARTMENT OF ECONOMICS AND SOCIAL AFFAIRS. **World Population Prospects - Population Division - United Nations**. Disponível em: <https://population.un.org/wpp2019/>. Acesso em: 1 dez. 2021.

UNITED NATIONS. **United Nations Conference on the Human Environment**. Water Research. **Anais**...Stockholm: United Nations, 1973Disponível em: <https://linkinghub.elsevier.com/retrieve/pii/0043135473900778>

UNITED NATIONS. **World Population Prospects 2019: Highlights**. New York: [s.n.]. Disponível em: <http://www.ncbi.nlm.nih.gov/pubmed/12283219>.

UNLUER, C.; AL-TABBAA, A. Impact of hydrated magnesium carbonate additives on the carbonation of reactive MgO cements. **Cement and Concrete Research**, v. 54, p. 87–97, 2013.

UNLUER, C.; AL-TABBAA, A. Enhancing the carbonation of MgO cement porous blocks through improved curing conditions. **Cement and Concrete Research**, v. 59, p. 55–65, 2014.

UROSEVIC, D. M. et al. Recovery of copper from copper slag and copper slag flotation tailings by oxidative leaching. **Physicochemical Problems of Mineral Processing**, v. 51, n. 1, p. 73–82, 2015.

VACHUŠKA, J.; VOBOŘIL, M. Kinetic data computation from non-isothermal thermogravimetric curves of non-uniform heating rate. **Thermochimica Acta**, v. 2, n. 5, p. 379–392, 1971.

VEDABOURISWARAN, G.; ARAVINDAN, S. Development and characterization studies on magnesium alloy (RZ 5) surface metal matrix composites through friction stir processing. **Journal of Magnesium and Alloys**, v. 6, n. 2, p. 145–163, 2018.

WANDERLEY, K. B. **Recuperação de magnésio do licor de lixiviação de minério limonítico por cristalização.** São Paulo: Universidade de São Paulo, 24 maio 2018.

WANDERLEY, K. B. et al. Kinetic and thermodynamic study of magnesium obtaining as sulfate monohydrate from nickel laterite leach waste by crystallization. **Journal of Cleaner Production**, v. 272, 2020.

WANG, F. et al. Three-year performance of in-situ mass stabilised contaminated site soils using MgO-bearing binders. **Journal of Hazardous Materials**, v. 318, p. 302–307, 2016a.

WANG, Q. et al. Selective chlorination of CaO from titania slag by CO+Cl2 mixtures in fluidized bed. **Thermochimica Acta**, v. 640, p. 66–73, 2016b.

WANG, Y. et al. Kinetic study on preparation of substoichiometric titanium oxide via carbothermal process. **Journal of Thermal Analysis and Calorimetry**, v. 122, n. 2, p. 635–644, 2015.

WANG, Y.; AKAISHI, M.; YAMAOKA, S. Diamond formation from graphite in the presence of anhydrous and hydrous magnesium sulfate at high pressures and high temperatures. **Diamond and Related Materials**, v. 8, n. 1, p. 73–77, 1999.

WEBMINERAL. **www.webmineral.com**. Disponível em: <www.webmineral.com>. Acesso em: 6 abr. 2022.

WHITTINGTON, B. I. Characterization of scales obtained during continuous nickel latérite pilot-plant leaching. **Metallurgical and Materials**

Transactions B: Process Metallurgy and Materials Processing Science, v. 31, n. 6, p. 1175–1186, 2000.

WHITTINGTON, B. I.; MUIR, D. Pressure Acid Leaching of Nickel Laterites: A Review. **Mineral Processing and Extractive Metallurgy Review: An International Journal**, v. 21, n. 6, p. 527–599, out. 2000.

XIA, X. et al. Recovery of CaO from CaSO4 via CO reduction decomposition under different atmospheres. **Journal of Environmental Management**, v. 301, n. June 2021, p. 113855, 2022.

XIAO, J. et al. Extraction of Nickel from Garnierite Laterite Ore Using Roasting and Magnetic Separation with Calcium Chloride and Iron Concentrate. **Minerals**, v. 10, n. 4, p. 352, 15 abr. 2020.

XUE-YI, G. U. O. et al. Leaching behavior of metals from limonitic laterite ore by high pressure acid leaching. **Transactions of Nonferrous Metals Society of China**, v. 21, n. 1, p. 191–195, 2010.

YAM, B. J. Y. et al. Recycling of magnesium waste into magnesium hydroxide aerogels. **Journal of Environmental Chemical Engineering**, v. 8, n. 5, p. 104101, out. 2020.

YANFEI, X. et al. Recovery of rare earths from weathered crust elution-deposited rare earth ore without ammonia-nitrogen pollution: I. leaching with magnesium sulfate. **Hydrometallurgy**, v. 153, p. 58–65, 2015.

YANG, J. et al. Recovery of Magnesium from Ferronickel Slag to Prepare Magnesium Oxide by Sulfuric Acid Leaching. **Minerals**, v. 11, n. 12, p. 1375, 6 dez. 2021.

YANG, Z. et al. Catalytic partial oxidation of coke oven gas to syngas in an oxygen permeation membrane reactor combined with NiO/MgO catalyst. **Renewable Energy**, v. 35, n. 12, p. 6239–6247, 2010.

YAROSHEVSKY, A. A. Abundances of Chemical Elements in the Earth's Crust. **Geochemistry International**, v. 44, n. 1, p. 48–55, 2006.

YÖRÜKOĞLU, A.; OBUT, A.; GIRGIN, I. Effect of thiourea on sulphuric

acid leaching of bastnaesite. **Hydrometallurgy**, v. 68, n. 1–3, p. 195–202, 2003.

ZHAI, X. et al. Intensification of sulphation and pressure acid leaching of nickel laterite by microwave radiation. **Hydrometallurgy**, v. 99, n. 3–4, p. 189–193, 2009.

ZHANG, B. et al. Remediation of the vanadium slag processing residue and recovery of the valuable elements. **Process Safety and Environmental Protection**, v. 128, p. 362–371, 1 ago. 2019.

ZHANG, W.; ZHU, Z.; CHENG, C. Y. A literature review of titanium metallurgical processes. **Hydrometallurgy**, v. 108, n. 3–4, p. 177–188, jul. 2011.

ZHANG, X. et al. Density functional theory study on the mechanism of calcium sulfate reductive decomposition by carbon monoxide. **Industrial and Engineering Chemistry Research**, v. 51, n. 18, p. 6563–6570, 2012.

ZHANG, X. et al. Density functional theory study on the mechanism of calcium sulfate reductive decomposition by methane. **Fuel**, v. 110, p. 204–211, 2013.

ZHAO, Q. et al. Recovery of calcium and magnesium bearing phases from iron– and steelmaking slag for CO2 sequestration. **Process Safety and Environmental Protection**, v. 135, p. 81–90, 2020.

ZHENG, G. et al. Study on kinetics of the pyrolysis process of aluminum sulfate. **Phosphorus, Sulfur and Silicon and the Related Elements**, v. 195, n. 4, p. 285–292, 2020.

ZHU, F. L. et al. Behavior of titanium dioxide in alumina carbothermic reduction-chlorination process in vacuum. **Transactions of Nonferrous Metals Society of China (English Edition)**, v. 21, n. 8, p. 1855–1859, ago. 2011.

ZHU, T. et al. Innovative Vacuum Distillation for Magnesium Recycling. In: **Essential Readings in Magnesium Technology**. Cham: Springer

International Publishing, 2016. p. 157–162.

8. Attachments

8.1. Attachment 1

Kinetic analysis of carbothermic decomposition of $MgSO_4$ with different carbon sources.

Bruno Souza [a],Nathalli Mello[a], Artur Rego [a], Rodrigo Souza[a], Eduardo Brocchi [a].

[a] Pontifícia Universidade Católica do Rio de Janeiro (PUC-Rio), Departamento de Engenharia Química e de Materiais (DEQM), Rio de Janeiro, RJ, Brasil

Abstract

The decomposition of $MgSO_4$ at high temperatures generates a MgO with low reactivity, so it is interesting to add reducing agents to reduce this temperature. In this work, the effects of using four different reducing agents on magnesium sulfate decomposition were evaluated, namely: charcoal, green coke, breeze coke, and graphite. Despite being a widely used and known reaction, there are not much kinetic data referring to it in the literature. Thermogravimetric experiments of sulfate decomposition were carried out with each of the four reducing agents, in addition to one with the pure sulfate which served as a reference point. These experiments demonstrated that three of the four reducing agents were able to reduce the decomposition temperature. After these experiments, the data went through a kinetic modeling process to calculate the desired kinetic data. The modeling proved to be effective, obtaining R^2 values greater than 0.99 for the tests. Kinetic data of the reactions with the reducing agents indicated a decrease in activation energy values of up to 62% compared to decomposition without the reducing agents. The activation energy of sulfate decomposition without reducing agents was 422,731 $kJ.mol^{-1}$ while with green coke, graphite, breeze coke, and charcoal the values were respectively 340,391 $kJ.mol^{-1}$, 196,120 $kJ.mol^{-1}$, 191,100 $kJ.mol^{-1}$, and 162,302 $kJ.mol^{-1}$.

Keywords: Carbothermal decomposition kinetics, magnesium sulfate,

reducing agents.

1. Introduction

Mg^{+2} and SO_4^{-2} ions are commonly found in various industrial tailings, such as mine drainage water and flue gas desulfurization water, tailings from leaching processes, and landfills (DOU et al., 2017; TAIT et al., 2009; TOLONEN; RÄMÖ; LASSI, 2015). These ions can be synthesized as magnesium sulfate allowing the waste from one process to be used in other processes (MA et al., 2016).

Magnesium sulfate can be used in several areas of industry, being applied in agriculture, in the manufacture of rubber, paper, and cellulose, in pharmaceutical products, and others (CURRY; VAN OSS, 2020). Another way of using sulfate is as a reagent for the formation of other compounds, such as magnesium oxide (SOUZA et al., 2020).

Among magnesium compounds, the most consumed is its oxide, it can be used as a soil pH regulator, as a dye trap in industrial waste, as an antibacterial agent, in cement applications and the treatment of acid mine waste, and among others (ASENCIOS; ASSAF, 2013; CARABALLO et al., 2009; JIN; AL-TABBAA, 2014; LEE et al., 2004; MOUSSAVI; MAHMOUDI, 2009; PILARSKA; KLAPISZEWSKI; JESIONOWSKI, 2017; TOMAZ; ANDRADE; CANDIDO, 2011; UNLUER; AL-TABBAA, 2013, 2014; WANG et al., 2016a). Among its many uses, its use as a pH-regulating agent appears as a possible way to recycle magnesium from waste processes with acidic leaching. (FREITAS et al., 2009; MO; DENG; TANG, 2010; SCHEIDEMA; TASKINEN, 2011).

However, for magnesium oxide (MgO) to be used for this function, it must have some specific characteristics, such as high surfaces areas and porosity. These two characteristics are essential for the oxide to have adequate reactivity for this use (MO; DENG; TANG, 2010). The oxides formed from the thermal decomposition of MgSO4 at temperatures above 1273 K do not present these characteristics, and it is necessary to reduce this decomposition temperature (JIN; AL-TABBAA, 2014; SCHEIDEMA;

TASKINEN, 2011; UNLUER; AL-TABBAA, 2013).

It is then necessary to search for how to carry out this decrease in the decomposition temperature. Hoteit et al. (2007), highlight as conditions for this reduction to occur, an atmosphere with low concentrations of oxygen and the presence of reducing agents. In the literature, it is possible to find several studies applying some type of reducing agent in their experiment, whether gaseous or solid (BARIN; SCHULER, 1980; KANARI; GABALLAH, 1999; SCHEIDEMA; TASKINEN, 2011; ZHANG et al., 2012; ZHU et al., 2011). Over the years, several reducing agents have been tested for sulfate decompositions, from simple agents such as carbon, hydrogen, and carbon monoxide (KUUSIK; SALKKONEN; NIINISTÖ, 1985; SCHEIDEMA; TASKINEN, 2011), to more complex agents such as catalysts (MELLO et al., 2020; SOTO-DÍAZ et al., 2019), through metallic agents such as sulfides and pure metals (HUANG et al., 2015).

Among the agents, carbon has been widely studied and used in various processes. It has the great advantage of being able to be used through numerous different compounds CO, CH4, CaCO3 (KIM et al., 2006; XIA et al., 2022; ZHANG et al., 2013), in addition to solid elemental carbon compounds (LV et al., 2018; MORCALI; KHAJAVI; DREISINGER, 2017; RIVA et al., 2019; SOUZA et al., 2020).

Therefore, this work aimed to evaluate the effects of using four different carbon sources on magnesium sulfate decomposition, namely: charcoal, green coke, breeze coke, and graphite. This evaluation was performed using thermogravimetric data obtained experimentally and kinetic data obtained through kinetic modeling. Magnesium sulfate heptahydrate was chosen for this study since the anhydrous form of the sulfate, which would be the best to be used, does not occur naturally (SCHEIDEMA; TASKINEN, 2011).

2. Carbothermic decomposition kinetics of magnesium sulphate

To carry out a precise kinetic analysis, a understanding of the mechanism of the carbothermic decomposition of $MgSO_4$ is essential. As

the sulfate used in the experiments is a hydrated sulfate, studies show that the dehydration of the sulfate occurs before its decomposition (equation 1) (OKHRIMENKO et al., 2017, 2020; PAULIK; PAULIK; ARNOLD, 1981; SOUZA et al., 2020; ZHENG et al., 2020).

After dehydration, the anhydrous sulfate reacts with the reducing agent to form magnesium oxide. This reaction occurs by forming, in addition to the oxide, sulfur dioxide, and carbon oxide, the latter being either carbon monoxide or carbon dioxide, depending on the operating conditions (equations 2 and 3).

$$MgSO_4.7H_2O \rightarrow MgSO_4 + 7H_2O_{(g)} \quad (1)$$

$$MgSO_4 + C \rightarrow MgO + SO_{2(g)} + CO_{2(g)} \quad (2)$$

$$MgSO_4 + 2C \rightarrow MgO + SO_{2(g)} + 2CO_{(g)} \quad (3)$$

There are few studies in the literature that address the decomposition of magnesium sulfate and present kinetic data. The values found for the activation energy of this decomposition are close and vary from 311.7 ± 12,5 $kJ.mol^{-1}$ (HULBERT, 1968), passing through 335.7 ± 1.7 $kJ.mol^{-1}$ (L'VOV; UGOLKOV, 2004) up to 368.2 $kJ.mol^{-1}$ (MELLO et al., 2020). When it comes to the decomposition of $MgSO_4$ in the presence of a reducing agent, no data were found that could serve as a basis for comparison.

Even expanding the search for kinetic data of other processes that use reducing agents, few works present kinetic data for these processes. And even these works do not present kinetic data without the presence of the reducing agents used, making it difficult to compare the efficiency of these reducing agents (GRIGOROVA; PAUNOVA, 2022; LI et al., 2019a; LV et al., 2018; SETIAWAN et al., 2021; WANG et al., 2015).

3. Materials and methods

3.1. Chemicals

For this work, four different carbon sources were used, namely: ground charcoal (Glades Distribuidora), green coke, breeze coke fines, and

graphite. The magnesium sulfate used in the experiments was >99% heptahydrate from Merck. The tests were carried out in an inert atmosphere, using Linde's 99.9% Nitrogen gas.

3.2. Thermodynamics assessment

Thermodynamic analysis was performed using the HSC Chemistry 10 program (ROINE, 2021). Analyzes of the equilibrium compositions of the Mg-S-O-C system were carried out, considering the possible species formed both in the gas phase and in the solid phase. With it, it was possible to determine the products obtained in this system and its behavior.

3.3. Thermogravimetric analyses

After the thermodynamic assessment, thermogravimetric tests were performed on the Netzsch STA 449 F3 Jupiter® simultaneous thermal analyzer. These involved the reactions of magnesium sulfate heptahydrate with the four different carbon sources employed. The tests followed the following conditions:

• Temperature ranges from 298 K to 1673 K.

• Heating rate of 10 $K.min^{-1}$.

• 1:1 stoichiometric ratio, based on CO and CO_2 concentrations at 1200 K.

• Mass close to 10 mg of the mixture.

3.4. Kinetics modeling

The kinetic modeling of the data resulting from the thermogravimetric curves is presented by the mathematical model developed by Speyer (1994) and Vachuška and Vobořil (1971), through equation 4.

$$(\varphi t + T_r)^2 \frac{\frac{d^2f}{dt^2}}{\frac{df}{dt}} = -n\left[\frac{(\varphi t+T_r)^2\left(\frac{df}{dt}\right)}{1-f}\right] + \frac{E_a\varphi}{R} \quad (4)$$

Were f, $\frac{df}{dt}$ e $\frac{d^2f}{dt^2}$ can be calculated from the thermogravimetric curve and its derivatives, as shown in Figure 1.

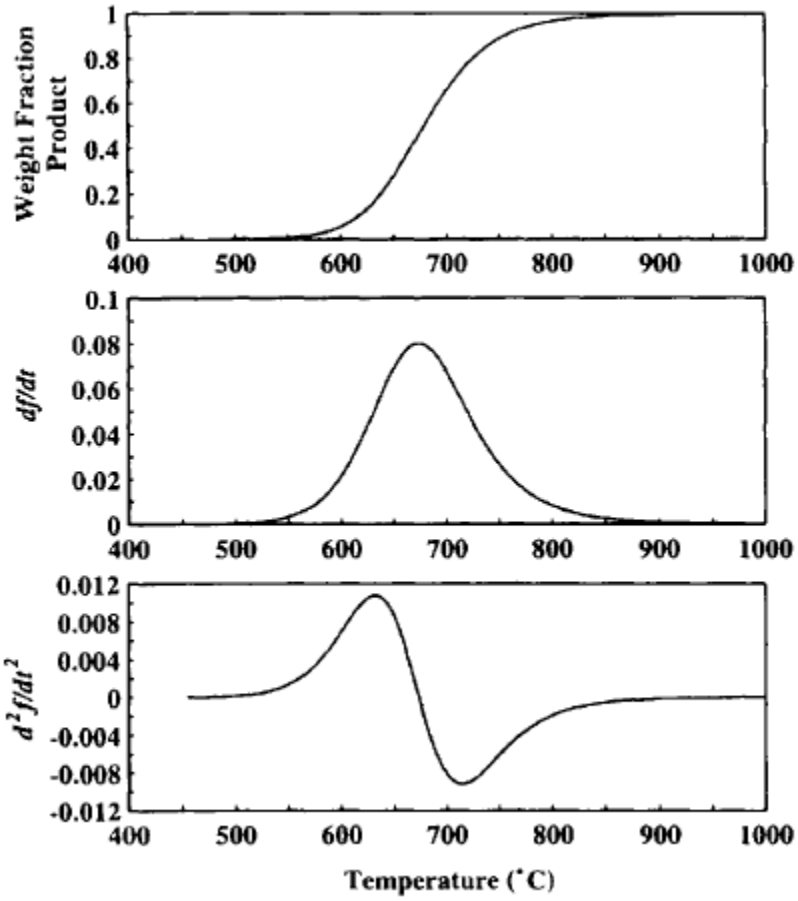

Figure 1 - Method of determination of f, $\frac{df}{dt}$ e $\frac{d^2f}{dt^2}$ (SPEYER, 1994).

To determine the derivatives, a sigmoidal function was used (equation 5), through a code in MATLAB R2021a (THE MATHWORKS INC, 2021). With the same code, the activation energy (Ea) and the order of reaction of each test were determined.

$$f(x) = \frac{1}{1+\exp(-a_1(t-a_2))} \quad (5)$$

4. Results and discussion

4.1. Thermodynamics assessment

Thermodynamic analysis was performed to compare the reaction system of the thermal decomposition of $MgSO_4*7H_2O$ in the presence of the reducing agent and without the presence of it. Through this analysis, it was possible to identify the compounds formed along with the temperature variation and the ranges where these compounds can be formed. The

analysis used for the construction of figures 2 and 3 were the equilibrium species distribution.

The distribution of species was analyzed separately for the analyzed phases, the solid and the gas. Figure 2 shows the distribution of solid species present in the decomposition of $MgSO_4*7H_2O$ without the presence (a) and with the presence of the reducing agent (b). From figure 2, it is possible to observe that the sulfate goes through two processes, dehydration, and decomposition. Without the presence of the reducing agent (a) the dehydration step takes place through different steps, dehydrating the sulfate equally before entering the next dehydration step. The sulfate changes from heptahydrate to pentahydrate, then to monohydrate, and finally to anhydrous, this dehydration occurs around 750 K. Only after the sulfate is completely dehydrated does it begin to decompose, from 900 K onwards. of decomposition, around 1180 K, MgO is the only compound containing magnesium in the system.

In the presence of the reducing agent (b), dehydration occurs more chaotically, with the simultaneous occurrence of more than one hydrated species of the sulfate, the sulfate coexists in heptahydrate, pentahydrate, tetrahydrate, and monohydrate forms between 350 and 400 K. Furthermore, the complete dehydration of the sulfate does not occur before its decomposition begins, from approximately 450 K the monohydrate sulfate (the only hydrated form of the sulfate from 420 K) begins to decompose and form magnesium oxide. From 700 K onwards, MgO becomes the only magnesium compound in the system.

By comparing the two parts, it is possible to determine that the presence of the reducing agent indicates a decrease in the initial and final decomposition temperature of, respectively, 300 K and 480 K. In addition to this decrease, the presence of the reducing agent makes the reaction system more chaotic, causing dehydration not to occur gradually and reducing the distance between dehydration and decomposition.

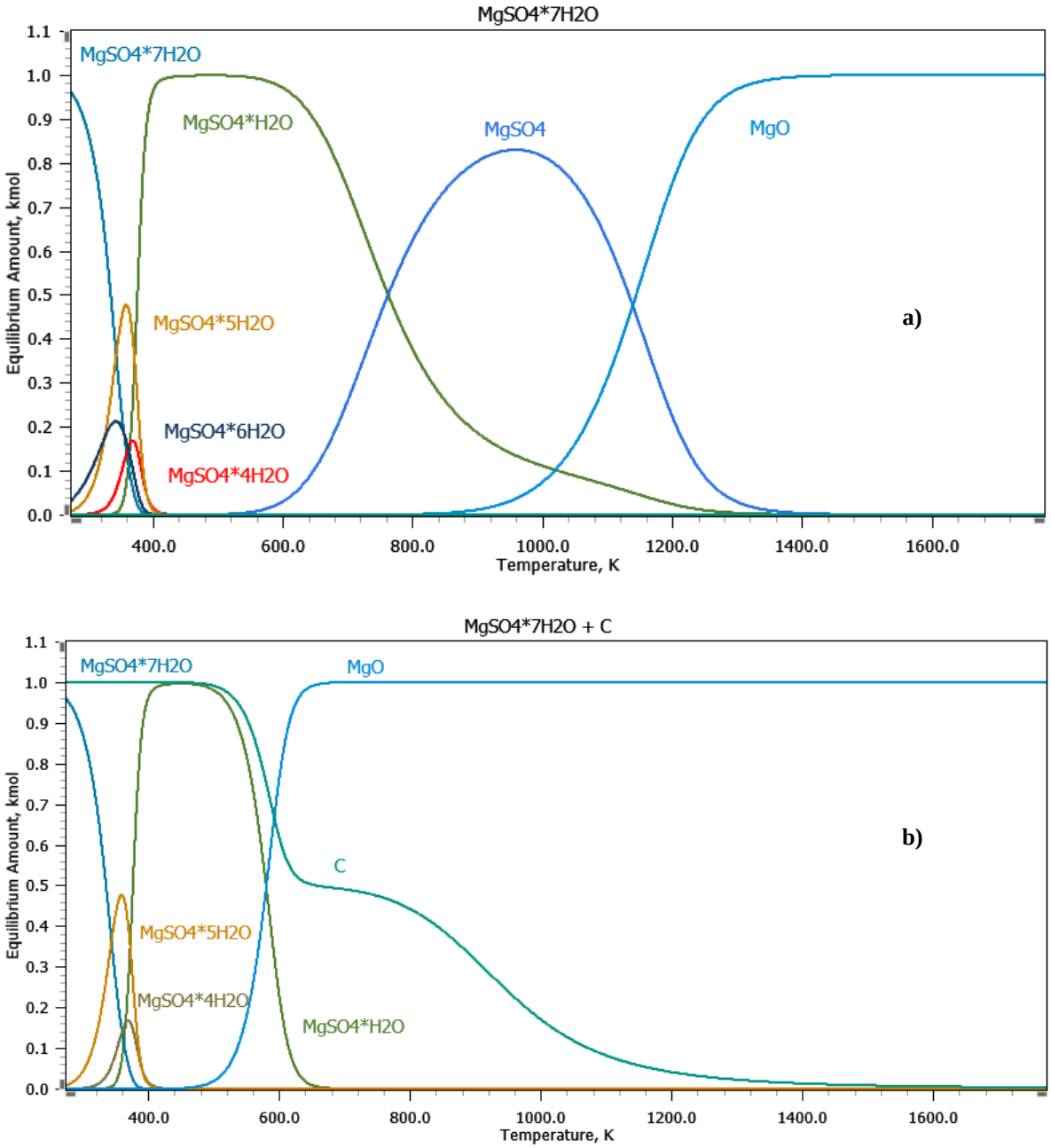

Figure 2 - Equilibrium species distribution diagram for the solid phase for the thermal decomposition of $MgSO_4$ heptahydrate, constructed by the author using HSC Chemistry 10, being a) without the reducing agent b) with the reducing agent.

Figure 3 shows the distribution of gaseous species present in the decomposition of $MgSO_4*7H_2O$ without the presence (a) and with the presence of the reducing agent (b). Looking at the formation of water molecules in the system a and b, it is possible to observe that the behavior analyzed in the dehydration of sulfate, in figure 2, is confirmed by the patterns presented. Without the presence of the reducing agent, the formation of water molecules is practically represented by isotherms and

the formation of all molecules occurs before the appearance of any compound formed by the sulfate decomposition. In the presence of the reducing agent, the water molecules are formed over a shorter interval and the formation of other compounds occurs before the formation of all the water molecules.

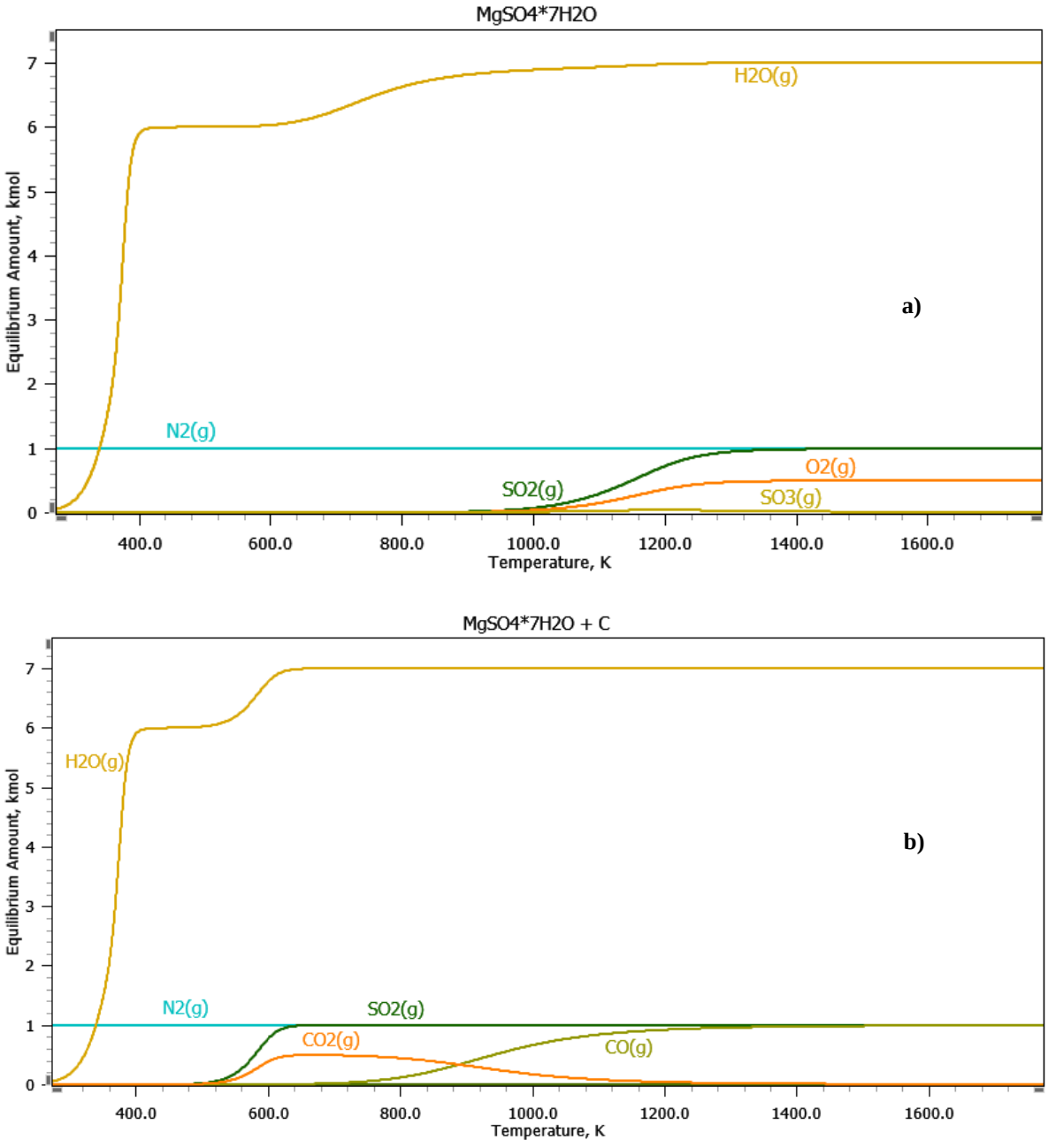

Figure 3 - Equilibrium species distribution diagram for the gas phase for the thermal decomposition of $MgSO_4$ heptahydrate, constructed by the author using HSC Chemistry 10, being a) without the reducing agent b) with the reducing agent.

An important part of the analysis of the behavior of the magnesium sulfate decomposition reaction system is the investigation of the products formed and how they can influence the rest of the process. According to Hoteit *et al.* (2007) atmospheres with low oxygen concentration favor decomposition, looking at the products of the two systems, the presence of carbon removes oxygen from the reaction atmosphere of the sulfate decomposition. Another factor caused by the presence of carbon is the formation of carbon oxides among the decomposition products.

The behavior of the formation of these oxides is of great importance since, according to the oxide formed, the stoichiometric ratio of carbon necessary for decomposition changes, according to equations 2 and 3. According to figure 3, the formation of CO_2 and CO vary according to the temperature of the system, CO_2 is formed between 520 K and 1500 K, while CO is formed from 640 K. It is possible to observe that around 640 K, before the formation of CO, the CO_2 concentration is at its highest value. From the beginning of the formation of CO, the concentration of CO_2 starts to drop until practically zero at 1500 K, at this temperature the CO reaches its maximum concentration and becomes the only carbon-containing compound in the system. The turning point in the concentrations of CO_2 and CO appears in the figure at 900 K. This behavior agrees with the Boudouard equation (equation 6).

$$C + CO_{2(g)} \rightarrow 2CO_{(g)} \quad (6)$$

Figure 4 presents the ΔG_o values of the Boudouard equation. Through the analysis of this figure, it is possible to identify that for temperatures below 973 K the values of ΔG_o are positive, which demonstrates a favoring of the formation of CO. While for temperatures above 973 K these values are negative, indicating that the equation is favored by the formation of products and with it the CO_2. These data were used for the stoichiometric calculations used for the reagent mixtures.

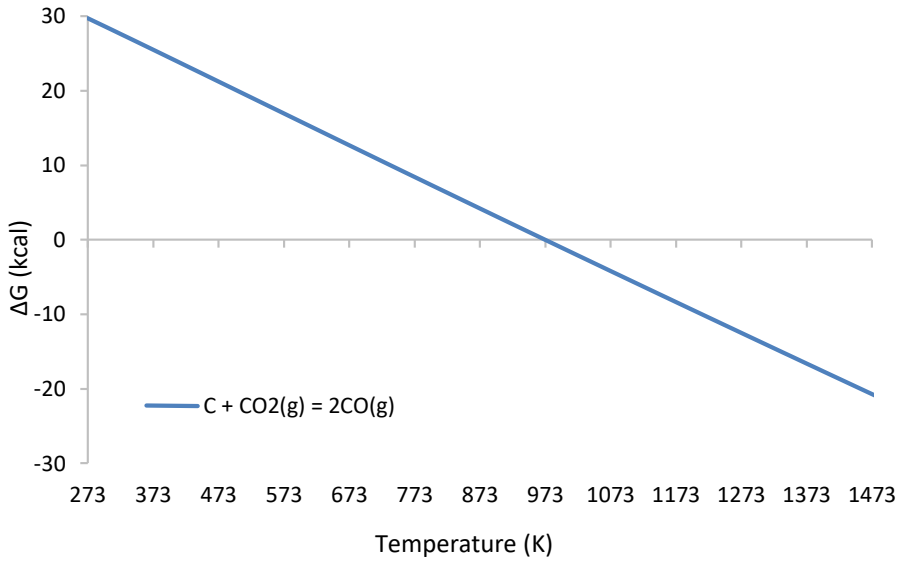

Figure 4 – ΔG_o values of the Boudouard equation.

4.2. Thermogravimetric analyses

For this work, five thermogravimetric analyzes were performed, the first using pure magnesium sulfate heptahydrate and the other four using $MgSO_4*7H_2O$ in the presence of one of the four reducing agents. All tests containing some of the reducing agents used a 1:1 stoichiometric ratio based on the concentrations of CO_2 and CO to 1200 K, using a reducing agent per sulfate ratio of 0.0480.

From each thermogravimetric analysis, it was possible to build a graph with the data obtained, these graphs were gathered and arranged through figures 5 and 6. Figure 5 shows the thermogravimetric analysis of the decomposition of pure magnesium sulfate heptahydrate, the values in this analysis were used as reference points for judgments about the influence of reducing agents in this decomposition. From figure 5 it is possible to identify two moments of mass loss in the system. The first loss of mass is related to sulfate dehydration and the second is related to its decomposition. For pure sulfate, dehydration occurs between 310 K and 550 K, whereas the decomposition process occurs between 1210 K and 1370 K, the interval between the two steps was 665 K. The total mass loss was 83%, which indicates complete decomposition of the sulfate.

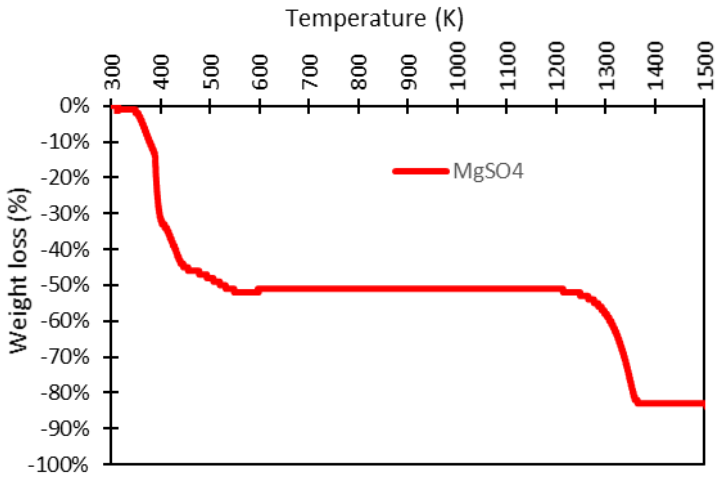

Figure 5 - Thermogravimetric analysis of the magnesium sulfate decomposition

Figure 6 shows the curves from thermogravimetric analyzes of $MgSO_4*7H_2O$ decompositions in the presence of reducing agents. Each curve refers to the system containing one of the reducing agents, according to the legends on them.

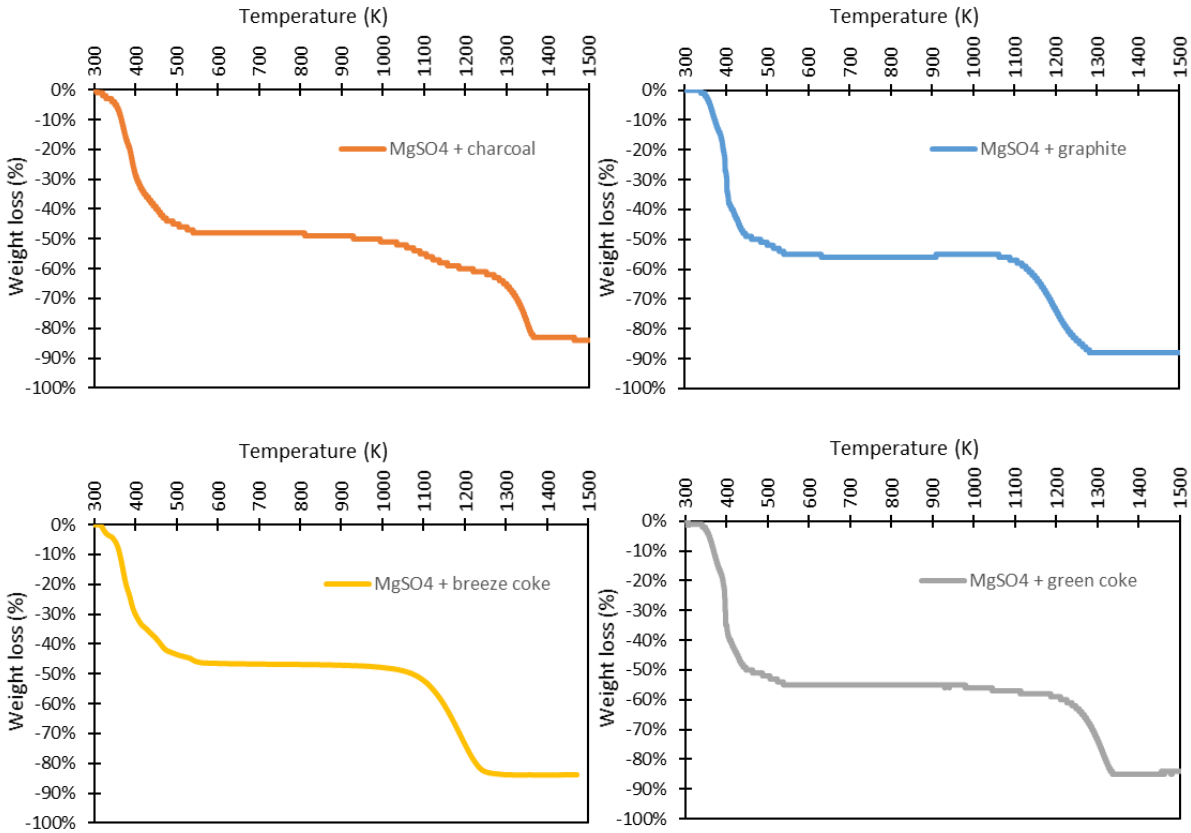

Figure 6 - Thermogravimetric analysis of the magnesium sulfate decomposition with reducing agents.

Through the analysis of figure 6, it was possible to identify the behavior of magnesium sulfate decomposition in the presence of each of the reducing agents. From the curves, it can be seen that in all experiments the decompositions reached a stable endpoint where the mass loss was the maximum reached, all final mass losses were higher than the 83% recorded by the decomposition of pure sulfate, indicating complete decompositions of sulfate in all tests.

Another aspect observed was that the stages of dehydration and decomposition occurred differently in all tests, a fact that, according to thermodynamic assessment, would not happen. In this aspect, the presence of reducing agents did not change the behavior of the reaction system. While in the experiment without the reducing agents these two phases occurred with a difference of 665 K, in the presence of the reducing agents these intervals were 632, 536, 518, and 460 K, respectively in the presence of green coke, graphite, charcoal, and breeze coke.

Analyzing these steps individually, in the dehydration step, contrary to what was indicated by thermodynamics, the curves referring to the tests with the reducing agents resulted in initial and final points close to those found in the curve without the presence of the agents. Three of the reducing agents (charcoal, green coke, graphite) obtained temperatures very close to those of the decomposition of pure sulfate, with dehydration occurring in an interval of approximately 230 K. For these tests, the initial (320 K ± 15 K) and final temperatures (550 K ± 10 K) of dehydration were also close to those of pure sulfate. In the other test (coke breeze), the final dehydration temperature was slightly higher than the others (602 K) which resulted in a greater dehydration interval, 285 K.

Regarding the decomposition step, the pure sulfate curve has an initial temperature of 1214 K and a final temperature of 1365 K, with a range of 151 K. Thermodynamics indicates that with the presence of reducing agents, the initial decomposition temperature tends to decrease, a fact that is confirmed when analyzing figure 6. Three of the four thermogravimetric curves referring to the tests containing some of the reducing agents, present

an initial decomposition temperature lower than 1100 K. Only the curve of the sulfate + green coke mixture presents an initial decomposition temperature close to the test temperature without reducing agent, with an initial temperature of 1195 K.

As with the initial decomposition temperature, the final decomposition temperatures of the tests with breeze coke, and graphite were lower than those of the test without reducing agent, being respectively 1255 K, and 1300 K. The experiments containing coke green and charcoal had a final decomposition temperature of 1352 K and 1365 K, respectively.

Among the three reducing agents that showed good thermodynamic results, charcoal was the one with the lowest value for the initial decomposition temperature, 1057 K. This value represented a decrease of more than 10% compared of the experiment with pure sulfate. On the other hand, the presence of green coke did not significantly influence the sulfate decomposition, obtaining temperatures only 15 K lower.

4.3. Kinetics modeling

4.3.1. Model adjustment

As the objective of this work was to evaluate the influence of reducing agents on magnesium sulfate decomposition, the mathematical model was used to data from thermogravimetric curves in the second interval of mass loss of each curve, since these are the sections referring to the decompositions of the sulfate. The application of the mathematical model served to determine the kinetic parameters needed for further analysis.

The initial analysis of the data obtained by the mathematical model was related to the data of the coefficients of determination (R^2), these data are important to indicate the level of adjustment of the modeling in the thermogravimetric curves. The values of R^2 are between 0 and 1, and the closer to 1 the more efficient the models. The R^2 data obtained were presented in table 1.

Table 1 - Data from the coefficients of determination of the kinetic modeling of the analyzed intervals of the TGA curves of $MgSO_4$ heptahydrate with and without the presence of a carbon source.

Reagents	R^2
$MgSO_4*7H_2O$	0.99965
$MgSO_4*7H_2O$ + charcoal	0.99947
$MgSO_4*7H_2O$ + green coke	0.99937
$MgSO_4*7H_2O$ + graphite	0.99963
$MgSO_4*7H_2O$ + coke breeze	0.99965

The values presented in table 1 indicate that for all analyzed curves, the modeling used was efficient since all R^2 values were greater than 0.99. This indicates that the mathematical model correctly describes the behavior of the thermogravimetric curve. Although the R^2 values indicate an excellent fit of the model to the experimental points, graphical visualization of this adjustment is essential to confirm this adjustment. These graphical representations were presented through figures 7 and 8.

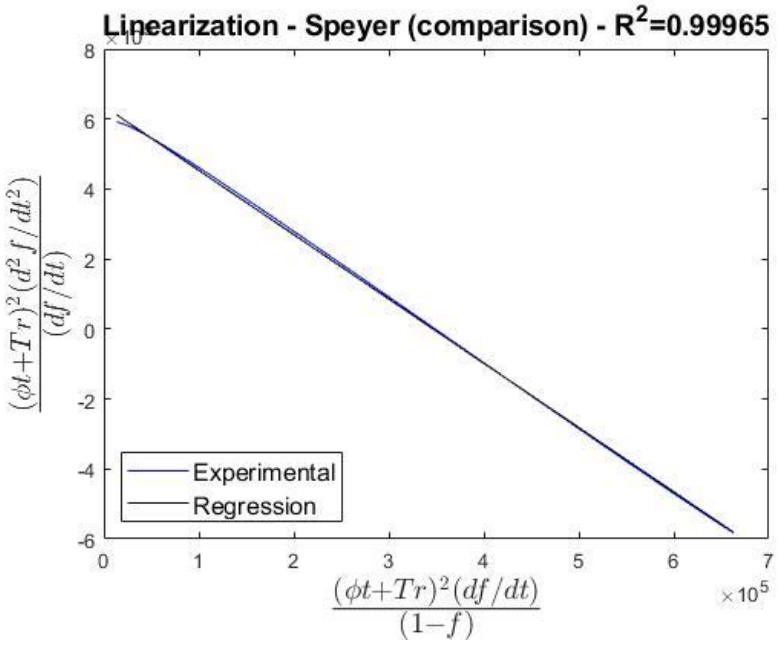

Figure 7 – Linear regression obtained for the decompositions of $MgSO_4*7H_2O$ without reducing agent.

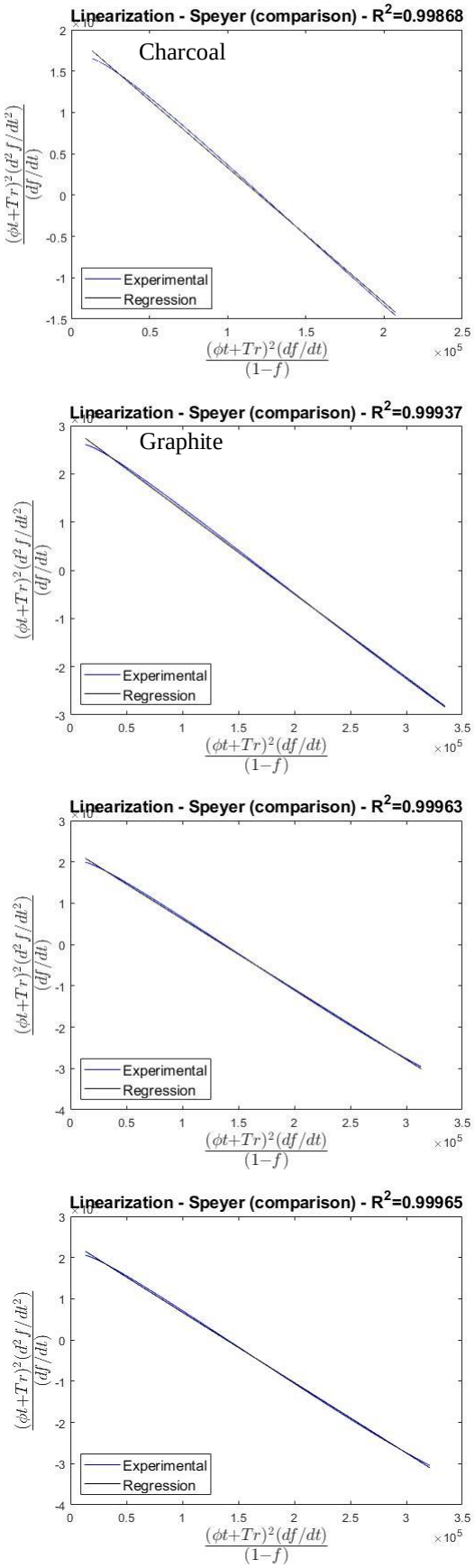

Figure 8 – Linear regression obtained for the decompositions of MgSO4*7H2O with reducing agent.

4.3.2. Kinetic parameters

Once the R^2 values and the linear regression graphs confirmed the efficiency of the mathematical model, the other data obtained through the modeling were analyzed. The kinetic model calculated the values of the activation energies (Ea) and the order of reaction (n) of the decompositions. These data were displayed in table 2.

Table 2 - Kinetic data from the kinetic modeling of TGA curves of $MgSO_4$ heptahydrate with and without the reducing agent.

Reagents	n	E_a (kJ.mol^{-1})
$MgSO_4*7H_2O$ pure	1.809	422.731
$MgSO_4*7H_2O$ + green coke	1.783	340.391
$MgSO_4*7H_2O$ + graphite	1.708	196.120
$MgSO_4*7H_2O$ + coke breeze	1.698	191.100
$MgSO_4*7H_2O$ + charcoal	1.631	162.302

The first data analyzed were the kinetic data preventing the thermogravimetric curve of the decomposition of pure magnesium sulfate and served as references for the evaluation of reducing agents. The activation energy found was 422,761 kJ.mol^{-1} and the order of reaction was 1,809. The other data in table 2 come from the sulfate decomposition curves mixed with one of the reducing agents.

These data served to analyze how the presence of reducing agents helped in decreasing the temperature ranges for decomposition. From thermodynamic data, green coke was the reducing agent that had the worst performance, reducing decomposition temperatures by approximately 15 K. Analyzing the kinetic data obtained in the green coke experiment, it is possible to identify the reason for this poor performance, the energy of calculated activation was 340.391 kJ.mol^{-1}, a decrease of less than 20% compared to the Ea of pure sulfate. The value for the order of reaction found was the closest to pure sulfate, 1.783.

The Ea of the other decomposition curves had valued at least 55% lower than the Ea of pure sulfate. Although the three reducing agents (charcoal, breeze coke, and graphite) reduced the initial sulfate decomposition temperatures to similar values, the Ea of the charcoal test was 20% lower than the others. The values of the orders of the reactions followed the behavior of the Ea values, with the values for the experiments with breeze coke and graphite being very close and the values for the charcoal test below the others.

5. Final remarks

The experiments carried out throughout this work made it possible to analyze the thermodynamic and kinetic effects of the presence of charcoal, green coke, breeze coke, and graphite on the thermal decomposition of magnesium sulfate heptahydrate. As expected after thermodynamic assessment, the presence of charcoal, coke breeze, and graphite resulted in a great decrease in the initial temperatures of sulfate decomposition, approximately 10%. However, the presence of green coke did not result in a significant decrease, only 2%.

The kinetic modeling was coherent with all observed systems, presenting R^2 values greater than 0.99 for all experiments. The values of n obtained through the modeling indicate that magnesium sulfate decompositions in the presence of reducing agents occur in a shorter time since the orders of reactions in the four experiments are smaller than the order of the reaction in the experiment without any reducing agent. However, for the experiment with green coke, this decrease was not satisfactory.

This behavior can be confirmed when the activation energy values are analyzed since in the presence of graphite, breeze coke, and charcoal the Ea values show a large decrease compared to the value obtained for decomposition without the reducing agents, this decrease was at least 55%. In the case of green coke, this decrease was less than 20%.

6. Acknowledgments

The authors are grateful to Coordination for the Improvement of Higher Education Personnel (CAPES) for their financial support throughout the research.

7. References

ACHAR, B. N. N.; BRINDLEY, G. W.; SHARP, J. H. **Kinetics and mechanism of dehydroxylation processes. III Applications and limitations of Dynamic methods**. Proceedings of the International Clay Conference. **Anais**...Jerusalem: 1966

AGATZINI-LEONARDOU, S. et al. Hydrometallurgical process for the separation and recovery of nickel from sulphate heap leach liquor of nickeliferrous laterite ores. **Minerals Engineering**, v. 22, n. 14, p. 1181–1192, 2009.

AINA, V. et al. Magnesium- and strontium-co-substituted hydroxyapatite: the effects of doped-ions on the structure and chemico-physical properties. **Journal of Materials Science: Materials in Medicine**, v. 23, n. 12, p. 2867–2879, 2012.

AL-TABBAA, A. Reactive magnesia cement. In: **Eco-Efficient Concrete**. [s.l.] Elsevier, 2013. p. 523–543.

ALI, S. H. et al. Mineral supply for sustainable development requires resource governance. **Nature**, v. 543, n. 7645, p. 367–372, 2017.

ANM. **Anuário Mineral Brasileiro: principais substâncias metálicas 2020**. Brasília: [s.n.]. Disponível em: <www.anm.gov.br>. Acesso em: 29 dez. 2021.

APHANE, M. E.; VAN DER MERWE, E. M.; STRYDOM, C. A. Influence of hydration time on the hydration of MgO in water and in a magnesium acetate solution. **Journal of Thermal Analysis and Calorimetry**, v. 96, n. 3, p. 987–992, 2009.

ASENCIOS, Y. J. O.; ASSAF, E. M. Combination of dry reforming and partial oxidation of methane on NiO-MgO-ZrO2 catalyst: Effect of nickel content. **Fuel Processing Technology**, v. 106, p. 247–252, 2013.

ASENCIOS, Y. J. O.; NASCENTE, P. A. P.; ASSAF, E. M. Partial oxidation of methane on NiO-MgO-ZrO 2 catalysts. **Fuel**, v. 97, p. 630–637, 2012.

AVRAMI, M. Granulation, Phase Change, and Microstructure Kinetics of Phase Change. **The Journal of Chemical Physics**, v. 9, n. December, p. 177–184, 1941.

BARBOSA, L. I.; GONZÁLEZ, J. A.; DEL CARMEN RUIZ, M. Extraction of lithium from β-spodumene using chlorination roasting with calcium chloride. **Thermochimica Acta**, v. 605, p. 63–67, 10 abr. 2015.

BARIN, I.; SCHULER, W. On the kinetics of the chlorination of titanium dioxide in the presence of solid carbon. **Metallurgical Transactions B**, v. 11, n. 2, p. 199–207, jun. 1980.

BARTLEY, J. K. et al. Simple method to synthesize high surface area magnesium oxide and its use as a heterogeneous base catalyst. **Applied Catalysis B: Environmental**, v. 128, p. 31–38, 2012.

BOOSTER, J. L.; SANDWIJK, A. VAN; REUTER, M. A. MAGNESIUM REMOVAL IN THE ELECTROLYTIC ZINC INDUSTRY. **Minerals Engineering**, v. 13, n. 5, p. 517–526, 2000.

BOYD, C. E. **Water Quality**. Third Edit ed. Cham: Springer International Publishing, 2020.

BRANCATO, V. et al. MgSO4·7H2O filled macro cellular foams: An innovative composite sorbent for thermo-chemical energy storage applications for solar buildings. **Solar Energy**, v. 173, n. February, p. 1278–1286, 2018.

BROCCHI, E. A.; MOURA, F. J. Chlorination methods applied to recover

refractory metals from tin slags. **Minerals Engineering**, v. 21, n. 2, p. 150–156, jan. 2008.

BROWN, R. E. Magnesium recycling yesterday, today, and tomorrow. **The Minerals, Metals and Materials Society, Warrendale**, p. 1318–1329, 2000.

BROWNELL, W. E. Reactions Between Alkaline-Earth Sulfates and. **Journal of The American Ceramic Society**, v. 46, n. 3, p. 125–128, 1951.

BURTON, M. **Oferta menor de magnésio da China ameaça empregos na Europa**. Disponível em: <https://www.bloomberglinea.com.br/2021/10/23/oferta-menor-de-magnesio-da-china-ameaca-empregos-na-europa/>. Acesso em: 8 dez. 2021.

CALDAS, T. D. P. **Análise de Trincas e Coating em Pelotas de Minério de Ferro por Processamento Digital de Imagens**. [s.l.] Pontifícia Universidade Católica do Rio de Janeiro, 2019.

CALO, J. M.; PERKINS, M. T. A heterogeneous surface model for the “steady-state” kinetics of the boudouard reaction. **Carbon**, v. 25, n. 3, p. 395–407, 1987.

CARABALLO, M. A. et al. Field multi-step limestone and MgO passive system to treat acid mine drainage with high metal concentrations. **Applied Geochemistry**, v. 24, n. 12, p. 2301–2311, 2009.

CARDOSO, J. H. **Decomposição redutora de MgSO4.7H2O na presença de H2(g) Dissertação**. [s.l.] Pontifícia Universidade Católica do Rio de Janeiro, 2018.

CHENG, C. Y. et al. Recovery of nickel and cobalt from laterite leach solutions using direct solvent extraction: Part 1 - Selection of a synergistic SX system. **Hydrometallurgy**, v. 104, n. 1, p. 45–52, 2010.

CHENG, C. Y. et al. Synergistic solvent extraction of nickel and cobalt: A review of recent developments. **Solvent Extraction and Ion Exchange**, v. 29, n. 5–6, p. 719–754, 2011.

CHIPERA, S. J.; VANIMAN, D. T. Experimental stability of magnesium sulfate hydrates that may be present on Mars. **Geochimica et Cosmochimica Acta**, v. 71, n. 1, p. 241–250, 2007.

CIPOLLINA, A. et al. Reactive crystallisation process for magnesium recovery from concentrated brines. **Desalination and Water Treatment**, v. 55, p. 2377–2388, 2015.

COATS, A. W.; REDFERN, J. P. Kinetic Parameters from Thermogravimetric Data. **Nature**, v. 201, p. 68–69, 1964.

COSTA, R. H. **Recovery of magnesium sulfate from a zinc ore flotation tailing using hydrometallurgical route.** São Paulo: Universidade de São Paulo, 1 dez. 2020.

COURTIAL, M.; CABRILLAC, R.; DUVAL, R. Recycling of magnesium slags in construction block form. **Studies in Environmental Science**, v. 60, n. C, p. 599–604, 1994.

CURRY, K. C.; VAN OSS, H. G. 2017 Minerals Yearbook: Magnesium Compounds. **US Geological Survey, Washington DC**, n. March, 2020.

DA SILVA, A. M. V. **Estudos sobre a recuperação do titânio contido no rejeito da concentração de magnetita**. [s.l.] Pontifícia Universidade Católica do Rio de Janeiro , 2018.

DĄBROWSKI, A. et al. Selective removal of the heavy metal ions from waters and industrial wastewaters by ion-exchange method. **Chemosphere**, v. 56, n. 2, p. 91–106, 2004.

DALY, T. **China Oct magnesium exports rebound to 19-month high**. Disponível em: <https://www.reuters.com/markets/commodities/china-oct-magnesium-exports-rebound-19-month-high-2021-11-22/>. Acesso em: 10

dez. 2021.

DAMAYANTI, R.; KHAERUNISSA, H. COMPOSITION AND CHARACTERISTICS OF RED MUD: A CASE STUDY ON TAYAN BAUXITE RESIDUE FROM ALUMINA PROCESSING PLANT AT WEST KALIMANTAN. **INDONESIAN MINING JOURNAL**, v. 19, n. 3, p. 179–190, 2016.

DENISENKO, Y. G. et al. Thermal decomposition of europium sulfates Eu2(SO4)3·8H2O and EuSO4. **Journal of Solid State Chemistry**, v. 255, n. August, p. 219–224, 2017.

DHARWADKAR, S. R.; CHANDRASEKHARAIAH, M. S.; KARKHANAVALA, M. D. Evaluation of kinetic parameters from thermogravimetric curves. **Thermochimica Acta**, v. 25, p. 372–375, 1978.

DING, K. et al. Thermochemical reduction of magnesium sulfate by natural gas: Insights from an experimental study. **Geochemical Journal**, v. 45, n. 2, p. 97–108, 2011.

DONG, H. et al. Synthesis of reactive MgO from reject brine via the addition of NH4OH. **Hydrometallurgy**, v. 169, p. 165–172, 2017.

DONG, H. et al. Investigation of the properties of MgO recovered from reject brine obtained from desalination plants. **Journal of Cleaner Production**, v. 196, p. 100–108, 20 set. 2018.

DOU, W. et al. Sulfate removal from wastewater using ettringite precipitation: Magnesium ion inhibition and process optimization. **Journal of Environmental Management**, v. 196, p. 518–526, 2017.

DUPONT, C.; CAMPAGNE, A.; CONSTANT, F. Efficacy and Safety of a Magnesium Sulfate-Rich Natural Mineral Water for Patients With Functional Constipation. **Clinical Gastroenterology and Hepatology**, v. 12, n. 8, p. 1280–1287, 2014.

EUROPEAN COMMISSION. **COMMITTEE AND THE COMMITTEE OF**

THE REGIONS Critical Raw Materials Resilience: Charting a Path towards greater Security and Sustainability. COM(2020) 474 final. [s.l: s.n.]. Disponível em: <http://info.worldbank.org/governance/wgi/.>.

FAN, C. et al. Leaching behavior of metals from chlorinated limonitic nickel laterite. **International Journal of Mineral Processing**, v. 110–111, p. 117–120, jul. 2012.

FERNANDES, F. R. C. et al. **TENDÊNCIAS TECNOLÓGICAS BRASIL 2015 - Geociências e Tecnologia Mineral**. Rio de Janeiro, Brazil: CETEM - Centro de Tecnologia Mineral, 2007.

FREEMAN, E. S.; CARROLL, B. The Application of Thermoanalytical Techniques to Reaction Kinetics: The Thermogravimetric Evaluation of the Kinetics of the Decomposition of Calcium Oxalate Monohydrate. **The Journal of Physical Chemistry**, v. 62, n. 4, p. 394–397, 1958.

FREITAS, E. V. DE S. et al. Indução da fitoextração de chumbo por ácido cítrico em solo contaminado por baterias automotivas. **Revista Brasileira de Ciência do Solo**, v. 33, n. 2, p. 467–473, abr. 2009.

GALLAGHER, P. K.; JOHNSON, D. W.; SCHREY, F. Thermal Decomposition of Iron (II) Sulfates. **Journal of The American Ceramic Society**, v. 53, n. 12, p. 666–670, 1970.

GAO, F. et al. Recovery of magnesium from ferronickel slag to prepare hydrated magnesium sulfate by hydrometallurgy method. **Journal of Cleaner Production**, v. 303, p. 127049, 2021.

GARCES-GRANDA, A.; LAPIDUS, G. T.; RESTREPO-BAENA, O. J. The effect of calcination as pre treatment to enhance the nickel extraction from low-grade laterites. **Minerals Engineering**, v. 120, n. November 2017, p. 127–131, 2018.

GENCELI, F. E. et al. Crystallization and Characterization of a New Magnesium Sulfate Hydrate MgSO4·11H2O. **Crystal Growth & Design**, v. 7, n. 12, p. 2460–2466, 2007.

GRIGOROVA, D.; PAUNOVA, R. Thermodynamic and kinetic investigation of carbothermic reduction of electric arc furnace dust. **Metalurgija**, v. 61, n. 1, p. 189–192, 2022.

GUAN, Q. JUN et al. Recovery of cobalt and nickel in the presence of magnesium and calcium from sulfate solutions by Versatic 10 and mixtures of Versatic 10 and Cyanex 301. **Transactions of Nonferrous Metals Society of China (English Edition)**, v. 26, n. 3, p. 865–873, 2016.

HABASHI, F. **Handbook of Extractive Metallurgy - Vol. 2**. Weinheim - Chicester - New Youk - Toronto - Brisbane - Singapore: WILEY-VCH, 1997.

HAJBI, F. et al. Thermodynamic study of magnesium sulfate crystallization: application of Pitzer model and quinary diagrams. **Desalination and Water Treatment**, p. 12, 2015.

HAN, D. et al. A review on ignition mechanisms and characteristics of magnesium alloys. **Journal of Magnesium and Alloys**, v. 8, n. 2, p. 329–344, 2020.

HARVEY, R.; HANNAH, R.; VAUGHAN, J. Selective precipitation of mixed nickel-cobalt hydroxide. **Hydrometallurgy**, v. 105, n. 3–4, p. 222–228, 2011.

HIGHFIELD, J. et al. RSC Advances Activation of serpentine for CO2 mineralization by flux extraction of soluble magnesium salts using ammonium sulfate. **The Royal Society of Chemistry**, v. 2, p. 6535–6541, 2012.

HLABELA, P. S. et al. Thermal reduction of barium sulphate with carbon monoxide-A thermogravimetric study. **Thermochimica Acta**, v. 498, n. 1–2, p. 67–70, 2010.

HOTEIT, A. et al. Sulfate decomposition from circulating fluidized bed combustors bottom ash. **Chemical Engineering Science**, v. 62, n. 23, p. 6827–6835, 1 dez. 2007.

HUANG, P. et al. A sustainable process to utilize ferrous sulfate waste from titanium oxide industry by reductive decomposition reaction with pyrite. **Thermochimica Acta**, v. 620, p. 18–27, 2015.

HULBERT, S. F. Effect of processing parameters on the kinetics of decomposition of magnesium sulphate. **Materials Science and Engineering**, v. 2, n. 5, p. 262–268, 1968.

INEICH, T. et al. Utilization efficiency of lime consumption during magnesium sulfate precipitation. **Hydrometallurgy**, v. 173, n. September, p. 241–249, 2017.

IONASHIRO, M. **Princípios Básicos da Termogravimetria e Análise Térmica Diferencial/ Calorimetria Exploratória Diferencial**. [s.l: s.n.].

JAVAID, A. et al. LITERATURE REVIEW ON MAGNESIUM RECYCLING. **Magnesium Technology**, p. 7–12, 2006.

JENA, B. C.; DRESLER, W.; REILLY, I. G. Extraction of titanium, vanadium and iron from titanomagnetite deposits at pipestone lake, Manitoba, Canada. **Minerals Engineering**, v. 8, n. 1–2, p. 159–168, jan. 1995.

JIANG, M. et al. Mechanism of sodium sulfate in promoting selective reduction of nickel laterite ore during reduction roasting process. **International Journal of Mineral Processing**, v. 123, p. 32–38, 2013.

JIAO, F. et al. Recovery of chromium and magnesium from spent magnesia-chrome refractories by acid leaching combined with alkali precipitation and evaporation. **Separation and Purification Technology**, v. 227, n. June, p. 115705, 2019.

JIN, F.; AL-TABBAA, A. Strength and hydration products of reactive MgO-silica pastes. **Cement and Concrete Composites**, v. 52, p. 27–33, 2014.

JOHNSON, D. W.; GALLAGHER, P. K. Kinetics of the Decomposition of Freeze-Dried Aluminum Sulfate and Ammonium Aluminum Sulfate.

Journal of the American Ceramic Society, v. 54, n. 9, p. 461–465, 1971.

KANARI, N. et al. Thermal Behavior of Hydrated Iron Sulfate in Various Atmospheres. **Metals**, v. 8, n. 12, p. 1084, 2018.

KANARI, N.; GABALLAH, I. Chlorination and carbochlorination of magnesium oxide. **Metallurgical and Materials Transactions B**, v. 30, n. 3, p. 383–391, jun. 1999.

KARIDAKIS, T.; AGATZINI-LEONARDOU, S.; NEOU-SYNGOUNA, P. Removal of magnesium from nickel laterite leach liquors by chemical precipitation using calcium hydroxide and the potential use of the precipitate as a filler material. **Hydrometallurgy**, v. 76, n. 1–2, p. 105–114, 2005.

KATO, H. et al. Decomposition of carbon dioxide to carbon by hydrogen-reduced Ni(II)-bearing ferrite. **Journal of Materials Science**, v. 29, n. 21, p. 5689–5692, 1994.

KAYA, S.; TOPKAYA, Y. A. High pressure acid leaching of a refractory lateritic nickel ore. **Minerals Engineering**, v. 24, n. 11, p. 1188–1197, 2011.

KHAIRUL, M. A.; ZANGANEH, J.; MOGHTADERI, B. The Composition, Recycling and Utilisation of Bayer Red Mud. **Conservation and Recycling**, v. 141, n. February, p. 483–498, 2019.

KHOO, J. Z.; HAQUE, N.; BHATTACHARYA, S. Process simulation and exergy analysis of two nickel laterite processing technologies. **International Journal of Mineral Processing**, v. 161, p. 83–93, 2017.

KIM, B. S. et al. A kinetic study of the carbothermic reduction of zinc oxide with various additives. **Materials Transactions**, v. 47, n. 9, p. 2421–2426, 2006.

KIM, J.; AZIMI, G. Resources, Conservation & Recycling Selective

Precipitation of Titanium, Magnesium, and Aluminum from the Steelmaking Slag Leach Liquor. **Resources, Conservation & Recycling**, v. 180, n. January, p. 106177, 2022.

KOBERTZ, D.; MÜLLER, M. Experimental studies on NiSO4 by thermal analysis and calorimetry. **Calphad: Computer Coupling of Phase Diagrams and Thermochemistry**, v. 45, p. 55–61, 2014.

KONGOLO, K. et al. Cobalt and zinc recovery from copper sulphate solution by solvent extraction. **Minerals Engineering**, v. 16, n. 12, p. 1371–1374, 2003.

KOVACHEVA, P.; DJINGOVA, R. Ion-exchange method for separation and concentration of platinum and palladium for analysis of environmental samples by inductively coupled plasma atomic emission spectrometry. **Analytica Chimica Acta**, v. 464, n. 1, p. 7–13, 2002.

KURBAN, G. V. T. et al. Thermodynamics and Kinetic Modeling of the ZnSO4·H2O Thermal Decomposition in the Presence of a Pd/Al2O3 Catalyst. **Energies**, v. 15, n. 2, p. 548, 2022.

KUUSIK, R.; SALKKONEN, P.; NIINISTÖ, L. Thermal decomposition of calcium sulphate in carbon monoxide. **Journal of Thermal Analysis**, v. 30, n. 1, p. 187–193, 1985.

L'VOV, B. V.; UGOLKOV, V. L. Kinetics of free-surface decomposition of magnesium and barium sulfates analyzed thermogravimetrically by the third-law method. **Thermochimica Acta**, v. 411, n. 1, p. 73–79, 2004.

LAHIJANI, P. et al. Conversion of the greenhouse gas CO2 to the fuel gas CO via the Boudouard reaction: A review. **Renewable and Sustainable Energy Reviews**, v. 41, p. 615–632, 2015.

LAUREIRO, Y. et al. Kinetic parameters for the thermal decomposition reactions of CrO3 in AIR. **Thermochimica Acta**, v. 143, n. C, p. 347–350, maio 1989.

LEE, E. K. et al. Magnesium oxide as an effective catalyst in catalytic wet oxidation of H2S to sulfur. **Reaction Kinetics and Catalysis Letters**, v. 82, n. 2, p. 241–246, 2004.

LEMOS, F.; ANGORA, M.; MASSON, I. Lixiviação sob pressão de minérios lateríticos. p. 131–136, 2007.

LENOIR, D.; SCHRAMM, K. W.; LALAH, J. O. Green Chemistry: Some important forerunners and current issues. **Sustainable Chemistry and Pharmacy**, v. 18, n. September, p. 100313, 2020.

LI, H. et al. Investigation on the recovery of gold and silver from cyanide tailings using chlorination roasting process. **Journal of Alloys and Compounds**, v. 763, p. 241–249, 30 set. 2018.

LI, J. et al. Preparation of boric acid from low-grade ascharite and recovery of magnesium sulfate. **Transactions of Nonferrous Metals Society of China (English Edition)**, v. 20, n. 6, p. 1161–1165, 2010.

LI, X. MING et al. Improvement of carbothermic reduction of nickel slag by addition of CaCO3. **Transactions of Nonferrous Metals Society of China (English Edition)**, v. 29, n. 12, p. 2658–2666, 2019a.

LI, Z. et al. Efficient and Sustainable Removal of Magnesium from Brines for Lithium/Magnesium Separation Using Binary Extractants. **ACS Sustainable Chemistry and Engineering**, v. 7, p. 19225–19234, 2019b.

LIU, X. W. et al. Recovery of valuable metals from a low-grade nickel ore using an ammonium sulfate roasting-leaching process. **International Journal of Minerals, Metallurgy and Materials**, v. 19, n. 5, p. 377–383, 2012.

LIU, Y. et al. Magnesium ammonium phosphate formation , recovery and its application as valuable resources: a review. **Journal of Chemical Technology & Biotechnology**, v. 88, n. May, p. 181–189, 2013.

LIU, Y.; NAIDU, R. **Hidden values in bauxite residue (red mud):**

Recovery of metalsWaste Management, 2014.

LÜDKE, M. C. **A ROTA METALÚRGICA DO SILÍCIO: DA EXTRAÇÃO DO QUARTZO À OBTENÇÃO DO SILÍCIO DE GRAU FOTOVOLTAICO**. [s.l.] UNIVERSIDADE FEDERAL DE SANTA CATARINA, 2018.

LUO, A. A.; SACHDEV, A. K. **Applications of magnesium alloys in automotive engineering**. [s.l.] Woodhead Publishing Limited, 2012.

LV, X. et al. Non-isothermal kinetics study on carbothermic reduction of nickel laterite ore. **Powder Technology**, v. 340, p. 495–501, 2018.

MA, X. et al. One-step synthesis of basic magnesium sulfate whiskers by atmospheric pressure reflux. **Particuology**, v. 24, p. 191–196, 2016.

MACCARTHY, J. et al. Atmospheric acid leaching mechanisms and kinetics and rheological studies of a low grade saprolitic nickel laterite ore. **Hydrometallurgy**, v. 160, p. 26–37, 2016.

MACINGOVA, E.; LUPTAKOVA, A. Recovery of metals from acid mine drainage. **Chemical Engineering Transactions**, v. 28, n. 3, p. 109–114, 2012.

MAHMUD, N. et al. Magnesium recovery from desalination reject brine as pretreatment for membraneless electrolysis. **Desalination**, v. 525, n. August 2021, p. 115489, 2022.

MANN, R. A.; BAVOR, H. J. Phosphorus removal in constructed wetlands using gravel and industrial waste substrata. **Water Science and Technology**, v. 27, n. 1, p. 107–113, 1993.

MARCHI, J. et al. Influence of Mg-substitution on the physicochemical properties of calcium phosphate powders. **Materials Research Bulletin**, v. 42, n. 6, p. 1040–1050, 2007.

MCDONALD, R. G.; WHITTINGTON, B. I. Atmospheric acid leaching of nickel laterites review. Part II. Chloride and bio-technologies. **Hydrometallurgy**, v. 91, n. 1–4, p. 56–69, 2008.

MEHRA, D.; MAHAPATRA, M. M.; HARSHA, S. P. Processing of RZ5-10wt%TiC in-situ magnesium matrix composite. **Journal of Magnesium and Alloys**, v. 6, n. 1, p. 100–105, 2018.

MELLO, N. M. et al. Effect of an alumina supported palladium catalyst on the magnesium sulfate decomposition kinetics. **Materials Research**, v. 23, n. 6, 2020.

MENG, L. et al. Recovery of Ni, Co, Mn, and Mg from nickel laterite ores using alkaline oxidation and hydrochloric acid leaching. **Separation and Purification Technology**, v. 143, p. 80–87, 2015.

MME. **Boletim do Setor Mineral 2020**. Brasília, DF: [s.n.].

MO, L.; DENG, M.; TANG, M. Effects of calcination condition on expansion property of MgO-type expansive agent used in cement-based materials. **Cement and Concrete Research**, v. 40, n. 3, p. 437–446, 2010.

MONTEIRO, F. Z. R. **Estudo da decomposição térmica da fibra do coco verde na presença de um catalisador nano estruturado**. [s.l.] Pontifícia Universidade Católica do Rio de Janeiro, 2017.

MOODLEY, S. et al. **Chlorination of titania feedstocks**. TMS Annual Meeting. **Anais**...Hoboken, NJ, USA: John Wiley & Sons, Inc., 15 maio 2012Disponível em: <https://onlinelibrary.wiley.com/doi/10.1002/9781118364987.ch12>

MORCALI, M. H.; KHAJAVI, L. T.; DREISINGER, D. B. Extraction of nickel and cobalt from nickeliferous limonitic laterite ore using borax containing slags. **International Journal of Mineral Processing**, v. 167, p. 27–34, 2017.

MOUSSAVI, G.; MAHMOUDI, M. Removal of azo and anthraquinone reactive dyes from industrial wastewaters using MgO nanoparticles. **Journal of Hazardous Materials**, v. 168, n. 2–3, p. 806–812, 2009.

NARAYAN, R.; TABATABAIE-RAISSI, A.; ANTAL JR, M. J. A Study of

Zinc Sulfate Decomposition at Low Heating Rates. **Industrial & Engineering Chemistry Research**, v. 27, n. 6, p. 1050–1058, 1988.

NETZSCH. **Simultaneous Thermal Analyzer – STA 449 F3 Jupiter®**, 2022.

NKOSI, S. et al. **A comparative study of vanadium recovery from titaniferous magnetite using salt, sulphate, and soda ash roast-leach processes**. The Southern African Institute of Mining and Metallurgy. **Anais**...Pretoria: 2017Disponível em: <http://www.mintek.co.za/Pyromet/Files/2017Nkosi.pdf>. Acesso em: 7 fev. 2019

NURUNNABI, M. et al. Additive effect of noble metals on NiO-MgO solid solution in oxidative steam reforming of methane under atmospheric and pressurized conditions. **Applied Catalysis A: General**, v. 299, n. 1–2, p. 145–156, 2006.

OBERLE, B. et al. **Global Resources Outlook 2019: Natural Resources for the Future We Want.Global Resources Outlook 2019**. Nairobi, Kenya: UN, 16 set. 2020. Disponível em: <https://www.un-ilibrary.org/content/books/9789280737417>.

OKHRIMENKO, L. et al. Thermodynamic study of MgSO4 – H2O system dehydration at low pressure in view of heat storage. **Thermochimica Acta**, v. 656, n. August, p. 135–143, 2017.

OKHRIMENKO, L. et al. New kinetic model of the dehydration reaction of magnesium sulfate hexahydrate: Application for heat storage. **Thermochimica Acta**, v. 687, n. July 2019, p. 178569, 2020.

OKUMURA, S. et al. Recovery of CaO by Reductive Decomposition of Spent Gypsum in a CO-CO 2-N2 Atmosphere. **Industrial and Engineering Chemistry Research**, v. 42, n. 24, p. 6046–6052, 2003.

OSLANEC, P.; IŽDINSKÝ, K.; SIMANČÍK, F. Possibilities of magnesium recycling. **Material Science and Technology**, v. 4, p. 83–88, 2008.

OSTROFFT, A. G.; SANDERSON, R. T. THERMAL STABILITY OF SOME METAL Department of Chemistry , State University of Iowa , Iowa City Abstract--The thermal decomposition of eleven (If) sulphates has been studied by a combination of thermogravimetric and differential thermal anlaysis . The re. **Journal of Inorganic and Nuclear Chemistry**, v. 9, p. 45–50, 1959.

OXLEY, A.; BARCZA, N. Hydro-pyro integration in the processing of nickel laterites. **Minerals Engineering**, v. 54, p. 2–13, 2013.

ÖZDEMIR, M.; ÇAKIR, D.; KIPÇAK, Í. Magnesium recovery from magnesite tailings by acid leaching and production of magnesium chloride hexahydrate from leaching solution by evaporation. **The International Journal of Mineral Processing**, v. 93, p. 209–212, 2009.

OZGA, P.; RIESENKAMPF, W. Effect of zinc sulphide concentrate composition and roasting temperature on magnesium distribution in zinc calcine. **Canadian Metallurgical Quarterly**, v. 35, n. 3, p. 235–244, 1996.

PAN, F.; YANG, M.; CHEN, X. A Review on Casting Magnesium Alloys: Modification of Commercial Alloys and Development of New Alloys. **Journal of Materials Science & Technology**, v. 32, n. 12, p. 1211–1221, 2016.

PAUL, S. A.; CHAVAN, S. K.; KHAMBE, S. D. Studies on characterization of textile industrial waste water in Solapur city. **International Journal of Chemical Sciences**, v. 10, n. 2, p. 635–642, 2012.

PAULIK, J.; PAULIK, F.; ARNOLD, M. Dehydration of magnesium sulphate heptahydrate investigated by quasi isothermal-quasi isobaric TG. **Thermochimica Acta**, v. 50, n. 1–3, p. 105–110, 1981.

PICKLES, C. A. Thermodynamic analysis of the selective chlorination of electric arc furnace dust. **Journal of Hazardous Materials**, v. 166, n. 2–3, p. 1030–1042, 30 jul. 2009.

PILARSKA, A. A.; KLAPISZEWSKI, Ł.; JESIONOWSKI, T. Recent

development in the synthesis, modification and application of Mg(OH)2 and MgO: A review. **Powder Technology**, v. 319, p. 373–407, 2017.

PLEWA, J.; STEINDOR, J. Kinetics of reduction of magnesium sulfate by carbon oxide. **Journal of Thermal Analysis**, v. 32, n. 6, p. 1809–1820, 9 nov. 1987.

POMIRO, F. J. et al. Study of the Reaction Stages and Kinetics of the Europium Oxide Carbochlorination. **Metallurgical and Materials Transactions B: Process Metallurgy and Materials Processing Science**, v. 46, n. 1, p. 304–315, 2014.

RAM, A. **China's magnesium supply for rest of 2021 to lag demand: sources**. Disponível em: <https://www.spglobal.com/platts/en/market-insights/latest-news/metals/110321-chinas-magnesium-supply-for-rest-of-2021-to-lag-demand-sources>. Acesso em: 10 dez. 2021.

RAMALINGOM, S.; PODDER, J.; NARAYANA KALKURA, S. Crystallization and characterization of orthorhombic β-MgSO4·7H2O. **Crystal Research and Technology**, v. 36, n. 12, p. 1357–1364, 2001.

REGO, A. S. C. et al. KAl(SO4)2 thermal decomposition kinetics modeling through graphical and PSO methods. **Journal of Materials Research and Technology**, v. 14, n. 3, p. 1975–1984, set. 2021.

RIVA, L. et al. A study of densified biochar as carbon source in the silicon and ferrosilicon production. **Energy**, v. 181, p. 985–996, 15 ago. 2019.

ROCHE, E. G.; PRASAD, J. **Magnesium Oxide Recovery**USA, 2009.

RODE, H.; HLAVACEK, V. Detailed kinetics of titanium nitride synthesis. **AIChE Journal**, v. 41, n. 2, p. 377–388, fev. 1995.

RODRIGUES, R. **Modelagem Cinética e de Equilíbrio Combinadas para Simulação de Processos de Gaseificação**. [s.l.] UNIVERSIDADE FEDERAL DO RIO GRANDE DO SUL, 2015.

ROINE, A. O. **HSC Chemistry 10**Pori, Finland, 2021.

ROSITA, W. et al. Recovery of rare earth elements and Yttrium from Indonesia coal fly ash using sulphuric acid leaching. **AIP Conference Proceedings**, v. 2223, n. April, 2020.

SABATIER, M. et al. Influence of the consumption pattern of magnesium from magnesium-rich mineral water on magnesium bioavailability. **British Journal of Nutrition**, v. 106, n. 3, p. 331–334, 2011.

SAHOO, R. N.; NAIK, P. K.; DAS, S. C. Leaching of manganese from low-grade manganese ore using oxalic acid as reductant in sulphuric acid solution. **Hydrometallurgy**, v. 62, n. 3, p. 157–163, 2001.

SAKAKIBARA, M. et al. Kinetic Analysis of Thermogravimetric Data. **Nippon Kagaku Kaishi**, v. 1989, n. 10, p. 1729–1732, 1989.

SANCHEZ, M. E. et al. Thermogravimetric kinetic analysis of the combustion of biowastes. **Renewable Energy journal**, v. 34, p. 1622–1627, 2009.

SANTOS, F. et al. Behavior of Zn and Fe Content in Electric Arc Furnace Dust as Submitted to Chlorination Methods. **Metallurgical and Materials Transactions B**, v. 46, n. 4, p. 1729–1741, 21 ago. 2015.

SCHEIDEMA, M. **The reaction mechanism and operating window for the decomposition of hydrated magnesium sulfate under reducing conditions**. Helsinki: School of Chemical Technology, 2015.

SCHEIDEMA, M. N.; TASKINEN, P. Decomposition thermodynamics of magnesium sulfate. **Industrial and Engineering Chemistry Research**, v. 50, n. 16, p. 9550–9556, 2011.

SCHEIDEMA, M.; TASKINEN, P.; METSÄRINTA, M. L. Reductive decomposition of magnesium sulfate. **Proceedings - European Metallurgical Conference, EMC 2011**, v. 3, n. January, p. 1021–1032, 2011.

SETIAWAN, A. et al. Kinetics and Mechanisms of Carbothermic Reduction

of Weathered Ilmenite Using Palm Kernel Shell Biomass. **Journal of Sustainable Metallurgy**, 2021.

SILVA, A. M.; LIMA, R. M. F.; LEÃO, V. A. Mine water treatment with limestone for sulfate removal. **Journal of Hazardous Materials**, v. 221–222, p. 45–55, 2012.

SILVA, L. R. DA. Magnesita. In: **Sumário Brasileiro Mineral 2018**. [s.l: s.n.]. p. 3.

SIRIWARDANE, R. V. et al. Decomposition of the sulfates of copper, iron (II), iron (III), nickel, and zinc: XPS, SEM, DRIFTS, XRD, and TGA study. **Applied Surface Science**, v. 152, n. 3, p. 219–236, 1999.

SOTO-DÍAZ, O. et al. Metal sulfate decomposition using green Pd-based catalysts supported on ΓAl2O3 and SiC: A common step in sulfur-family thermochemical cycles. **International Journal of Hydrogen Energy**, v. 4, p. 12309–12314, 2019.

SOUZA, A. D. et al. Kinetics of sulphuric acid leaching of a zinc silicate calcine. **Hydrometallurgy**, v. 89, n. 3–4, p. 337–345, 2007.

SOUZA, B. et al. MgSO4 carbothermic reductive decomposition to produce a highly reactive MgO powder. **Journal of Materials Research and Technology**, p. 9, 16 jan. 2020.

SOUZA, R. et al. Potassium alum thermal decomposition study under non-reductive and reductive conditions. **Journal of Materials Research and Technology**, v. 8, n. 1, p. 745–751, 2019.

SPEYER, R. **Thermal Analysis of Materials**. 1st Editio ed. Boca Raton: CRC Press, 1994.

STOPIC, S.; FRIEDRICH, B. Hydrometallurgical processing of nickel lateritic ores. **Vojnotehnicki glasnik**, v. 64, n. 4, p. 1033–1047, 2016.

STOPIC, S.; FRIEDRICH, B.; FUCHS, R. Sulphuric acid leaching of the Serbian nickel lateritic ore. **Erzmetall: Journal for Exploration, Mining**

and Metallurgy, v. 56, n. 4, p. 204–209, 2003.

SUK, N. I.; KOTELNIKOV, A. R.; KOVALSKII, A. M. Iron-magnesium minerals from differentiated rocks of Lovozersky alkaline massif. **Geochemistry, Mineralogy and Petrology.**, v. 47, p. 97–107, 2009.

TAIT, S. et al. Removal of sulfate from high-strength wastewater by crystallisation. **Water Research**, v. 43, n. 3, p. 762–772, 2009.

TANG, X. et al. Prospect of recovering phosphorus in magnesium slag-packed wetland filter. **Environmental Science and Pollution Research**, v. 24, p. 22808–22815, 2017.

THE ECONOMIST. **Why it matters that magnesium is in short supply**. Disponível em: <https://www.economist.com/the-economist-explains/2021/11/15/why-it-matters-that-magnesium-is-in-short-supply>. Acesso em: 8 dez. 2021.

THE MATHWORKS INC. **MATLAB R2021a**, 2021.

THE WORLD BANK. **The Growing Role of Minerals and Metals for a Low Carbon Future**. [s.l.] World Bank, Washington, DC, 2017.

TOLONEN, E. T.; RÄMÖ, J.; LASSI, U. The effect of magnesium on partial sulphate removal from mine water as gypsum. **Journal of Environmental Management**, v. 159, p. 143–146, 2015.

TOMAZ, M. A.; ANDRADE, F. V.; CANDIDO, A. D. O. Ph , Cálcio E Magnésio Influenciados Pelo Uso De Resíduos Industriais Utilizados Como Corretivos , Em Lavoura De Café Conilon Ph , Calcium and Magnesium Influenced By the Use of Industrial Waste Used As Correctives in Conilon Coffee Plantation. 2011.

U.S. GEOLOGICAL SURVEY. **Mineral Commodity Summaries 2021**. [s.l: s.n.].

UN DEPARTMENT OF ECONOMICS AND SOCIAL AFFAIRS. **World Population Prospects - Population Division - United Nations**.

Disponível em: <https://population.un.org/wpp2019/>. Acesso em: 1 dez. 2021.

UNITED NATIONS. **United Nations Conference on the Human Environment**. Water Research. **Anais**...Stockholm: United Nations, 1973Disponível em: <https://linkinghub.elsevier.com/retrieve/pii/0043135473900778>

UNITED NATIONS. **World Population Prospects 2019: Highlights**. New York: [s.n.]. Disponível em: <http://www.ncbi.nlm.nih.gov/pubmed/12283219>.

UNLUER, C.; AL-TABBAA, A. Impact of hydrated magnesium carbonate additives on the carbonation of reactive MgO cements. **Cement and Concrete Research**, v. 54, p. 87–97, 2013.

UNLUER, C.; AL-TABBAA, A. Enhancing the carbonation of MgO cement porous blocks through improved curing conditions. **Cement and Concrete Research**, v. 59, p. 55–65, 2014.

UROSEVIC, D. M. et al. Recovery of copper from copper slag and copper slag flotation tailings by oxidative leaching. **Physicochemical Problems of Mineral Processing**, v. 51, n. 1, p. 73–82, 2015.

VACHUŠKA, J.; VOBOŘIL, M. Kinetic data computation from non-isothermal thermogravimetric curves of non-uniform heating rate. **Thermochimica Acta**, v. 2, n. 5, p. 379–392, 1971.

VEDABOURISWARAN, G.; ARAVINDAN, S. Development and characterization studies on magnesium alloy (RZ 5) surface metal matrix composites through friction stir processing. **Journal of Magnesium and Alloys**, v. 6, n. 2, p. 145–163, 2018.

WANDERLEY, K. B. **Recuperação de magnésio do licor de lixiviação de minério limonítico por cristalização.** São Paulo: Universidade de São Paulo, 24 maio 2018.

WANDERLEY, K. B. et al. Kinetic and thermodynamic study of magnesium obtaining as sulfate monohydrate from nickel laterite leach waste by crystallization. **Journal of Cleaner Production**, v. 272, 2020.

WANG, F. et al. Three-year performance of in-situ mass stabilised contaminated site soils using MgO-bearing binders. **Journal of Hazardous Materials**, v. 318, p. 302–307, 2016a.

WANG, Q. et al. Selective chlorination of CaO from titania slag by CO+Cl2 mixtures in fluidized bed. **Thermochimica Acta**, v. 640, p. 66–73, 2016b.

WANG, Y. et al. Kinetic study on preparation of substoichiometric titanium oxide via carbothermal process. **Journal of Thermal Analysis and Calorimetry**, v. 122, n. 2, p. 635–644, 2015.

WANG, Y.; AKAISHI, M.; YAMAOKA, S. Diamond formation from graphite in the presence of anhydrous and hydrous magnesium sulfate at high pressures and high temperatures. **Diamond and Related Materials**, v. 8, n. 1, p. 73–77, 1999.

WEBMINERAL. **www.webmineral.com**. Disponível em: <www.webmineral.com>. Acesso em: 6 abr. 2022.

WHITTINGTON, B. I. Characterization of scales obtained during continuous nickel latérite pilot-plant leaching. **Metallurgical and Materials Transactions B: Process Metallurgy and Materials Processing Science**, v. 31, n. 6, p. 1175–1186, 2000.

WHITTINGTON, B. I.; MUIR, D. Pressure Acid Leaching of Nickel Laterites: A Review. **Mineral Processing and Extractive Metallurgy Review: An International Journal**, v. 21, n. 6, p. 527–599, out. 2000.

XIA, X. et al. Recovery of CaO from CaSO4 via CO reduction decomposition under different atmospheres. **Journal of Environmental Management**, v. 301, n. June 2021, p. 113855, 2022.

XIAO, J. et al. Extraction of Nickel from Garnierite Laterite Ore Using

Roasting and Magnetic Separation with Calcium Chloride and Iron Concentrate. **Minerals**, v. 10, n. 4, p. 352, 15 abr. 2020.

XUE-YI, G. U. O. et al. Leaching behavior of metals from limonitic laterite ore by high pressure acid leaching. **Transactions of Nonferrous Metals Society of China**, v. 21, n. 1, p. 191–195, 2010.

YAM, B. J. Y. et al. Recycling of magnesium waste into magnesium hydroxide aerogels. **Journal of Environmental Chemical Engineering**, v. 8, n. 5, p. 104101, out. 2020.

YANFEI, X. et al. Recovery of rare earths from weathered crust elution-deposited rare earth ore without ammonia-nitrogen pollution: I. leaching with magnesium sulfate. **Hydrometallurgy**, v. 153, p. 58–65, 2015.

YANG, J. et al. Recovery of Magnesium from Ferronickel Slag to Prepare Magnesium Oxide by Sulfuric Acid Leaching. **Minerals**, v. 11, n. 12, p. 1375, 6 dez. 2021.

YANG, Z. et al. Catalytic partial oxidation of coke oven gas to syngas in an oxygen permeation membrane reactor combined with NiO/MgO catalyst. **Renewable Energy**, v. 35, n. 12, p. 6239–6247, 2010.

YAROSHEVSKY, A. A. Abundances of Chemical Elements in the Earth's Crust. **Geochemistry International**, v. 44, n. 1, p. 48–55, 2006.

YÖRÜKOĞLU, A.; OBUT, A.; GIRGIN, I. Effect of thiourea on sulphuric acid leaching of bastnaesite. **Hydrometallurgy**, v. 68, n. 1–3, p. 195–202, 2003.

ZHAI, X. et al. Intensification of sulphation and pressure acid leaching of nickel laterite by microwave radiation. **Hydrometallurgy**, v. 99, n. 3–4, p. 189–193, 2009.

ZHANG, B. et al. Remediation of the vanadium slag processing residue and recovery of the valuable elements. **Process Safety and Environmental Protection**, v. 128, p. 362–371, 1 ago. 2019.

ZHANG, W.; ZHU, Z.; CHENG, C. Y. A literature review of titanium metallurgical processes. **Hydrometallurgy**, v. 108, n. 3–4, p. 177–188, jul. 2011.

ZHANG, X. et al. Density functional theory study on the mechanism of calcium sulfate reductive decomposition by carbon monoxide. **Industrial and Engineering Chemistry Research**, v. 51, n. 18, p. 6563–6570, 2012.

ZHANG, X. et al. Density functional theory study on the mechanism of calcium sulfate reductive decomposition by methane. **Fuel**, v. 110, p. 204–211, 2013.

ZHAO, Q. et al. Recovery of calcium and magnesium bearing phases from iron– and steelmaking slag for CO2 sequestration. **Process Safety and Environmental Protection**, v. 135, p. 81–90, 2020.

ZHENG, G. et al. Study on kinetics of the pyrolysis process of aluminum sulfate. **Phosphorus, Sulfur and Silicon and the Related Elements**, v. 195, n. 4, p. 285–292, 2020.

ZHU, F. L. et al. Behavior of titanium dioxide in alumina carbothermic reduction-chlorination process in vacuum. **Transactions of Nonferrous Metals Society of China (English Edition)**, v. 21, n. 8, p. 1855–1859, ago. 2011.

ZHU, T. et al. Innovative Vacuum Distillation for Magnesium Recycling. In: **Essential Readings in Magnesium Technology**. Cham: Springer International Publishing, 2016. p. 157–162.

8.2. Attachment 2

Analysis of the influence rate of heating and hydration of magnesium sulfate in its decomposition.

Bruno Souza [a],Nathalli Mello[a], Artur Rego [a], Rodrigo Souza[a], Eduardo Brocchi [a].

[a] Pontifícia Universidade Católica do Rio de Janeiro (PUC-Rio), Departamento de Engenharia Química e de Materiais (DEQM), Rio de Janeiro, RJ, Brasil

Abstract

The thermal decomposition of magnesium sulfate, despite being a well-known reaction, does not present much kinetic data in the literature. Therefore, this work is willing to evaluate, through kinetic modeling, the influence of the heating rate and the degree of hydration of $MgSO_4$ in its thermogravimetric decomposition. For this, four heating rates (5, 10, 15, and 20 $K.min^{-1}$) and three sulfates (anhydrous, monohydrate, and heptahydrate) were used. The kinetic modeling followed the model proposed by Speyer (1994) and Vachuška and Vobořil (1971) and presented R^2 values > 0.99 in all experiments. The orders found were around 1.8 for all tests. The heating rate was not shown to be a factor that directly influenced the reaction, while the hydration of $MgSO_4$ represented an increase in the Ea values of the decomposition of heptahydrate sulfate (433.3 $KJ.mol^{-1}$) to the others (407 and 404.5 $KJ.mol^{-1}$, for the anhydrous and the monohydrate respectively).

Keywords: Thermal decomposition kinetics, magnesium oxide, magnesium sulfate.

1. Introduction

The first major global conference to debate proposals in favor of the environment celebrates its 50th anniversary in 2022 and its realization placed the search for more sustainable development in the global focus. Despite nearly five decades, much remains to be done in this area. In this

context, the term green chemistry appears in the late 2000s, with works in the United Kingdom, Germany and the United States. This concept appears more focused on the fields of industrial chemistry and synthetic chemistry and entails a search for chemical processes that generate less waste and use renewable substances (LENOIR; SCHRAMM; LALAH, 2020; UNITED NATIONS, 1973).

In this quest, by replacing toxic and/or non-renewable substances with renewable substances that do not harm the environment, fossil fuels and greenhouse gases are great villains. According to Ali *et al*. (2017), to achieve the goals outlined in the Paris Agreement signed in 2015, a large number of different minerals will be needed. In response to this, the European Union monitors, since 2011, some raw materials considered essential. Among the raw materials highlighted in this survey is magnesium. According to the European Union study, magnesium is a critical and essential raw material due to its production concentration in some countries (China, Russia and the USA) and its low recycling rate (13%) (EUROPEAN COMMISSION, 2020). The recycling and reuse of waste that would otherwise be discarded appears as an alternative to the growing need for magnesium (ALI et al., 2017; EUROPEAN COMMISSION, 2020; THE WORLD BANK, 2017).

Despite the concentration of magnesium production, the processing of many ores has some magnesium compound as a by-product or waste. In the literature, it is possible to find residues with magnesium compounds in Aluminum, Tin, Lithium, Nickel, Gold, Titanium, Vanadium and Zinc ores (BARBOSA; GONZÁLEZ; DEL CARMEN RUIZ, 2015; BROCCHI; MOURA, 2008; CHENG et al., 2010; GUAN et al., 2016; HARVEY; HANNAH; VAUGHAN, 2011; JENA; DRESLER; REILLY, 1995; LI et al., 2018; LIU; NAIDU, 2014; MACCARTHY et al., 2016; MOODLEY et al., 2012; OZGA; RIESENKAMPF, 1996; WANDERLEY, 2018; WANG et al., 2016b; ZHANG et al., 2019).

In addition to appearing in the processing of other metals of interest, magnesium is also commonly found in textile industry waste, in electrical

furnace dust, in industrial wastewater, from mines and desalination plants, and in seawater (BOYD, 2020; DONG et al., 2018; DOU et al., 2017; MANN; BAVOR, 1993; PAUL; CHAVAN; KHAMBE, 2012; PICKLES, 2009; SANTOS et al., 2015; SILVA; LIMA; LEÃO, 2012; TAIT et al., 2009; TOLONEN; RÄMÖ; LASSI, 2015). Several of these processes have, in addition to Mg^{+2}, SO_4^{-2} in their tailings, thus $MgSO_4$ becomes one of the possible compounds present in the waste (DOU et al., 2017; SCHEIDEMA; TASKINEN, 2011; TAIT et al., 2009; TOLONEN; RÄMÖ; LASSI, 2015).

Among magnesium compounds, its oxide was the most consumed compound in the United States in recent years (CURRY; VAN OSS, 2020; U.S. GEOLOGICAL SURVEY, 2021), it can be obtained by the simple decomposition of the $MgSO_4$ (ROCHE; PRASAD, 2009). MgO can be used as a soil pH regulator, as a dye trap in industrial tailings, as an antibacterial agent, in cement applications, and the treatment of acid mine tailings. (ASENCIOS; ASSAF, 2013; CARABALLO et al., 2009; JIN; AL-TABBAA, 2014; LEE et al., 2004; MOUSSAVI; MAHMOUDI, 2009; PILARSKA; KLAPISZEWSKI; JESIONOWSKI, 2017; TOMAZ; ANDRADE; CANDIDO, 2011; UNLUER; AL-TABBAA, 2013, 2014; WANG et al., 2016a).

This work aimed to evaluate the effect of different levels of hydration of magnesium sulfate and different heating rates on the kinetics of the thermal decomposition of $MgSO_4$. Through the analysis of thermogravimetric data obtained from twelve decomposition tests involving magnesium sulfates with three different degrees of hydration and four different heating rates.

2. Decomposition kinetics of magnesium sulphate

Before evaluating the decomposition kinetics of magnesium sulfate, it was necessary to perform a literature search to find works related to the subject. Through this search, it was possible to determine that the most present magnesium sulfates in the literature are anhydrous, monohydrate and heptahydrate, thus these were the sulfates chosen for the analysis (KARIDAKIS; AGATZINI-LEONARDOU; NEOU-SYNGOUNA, 2005; LI et

al., 2010; MELLO et al., 2020; OKHRIMENKO et al., 2017, 2020; PAULIK; PAULIK; ARNOLD, 1981; RAMALINGOM; PODDER; NARAYANA KALKURA, 2001; SOUZA et al., 2020).

For the analysis to be done correctly, it was necessary to determine the moment when it would be done, to standardize the process. In the literature, several works demonstrate that for hydrated sulfates, the water molecules detach before the decomposition of these sulfates, equation 1 (OKHRIMENKO et al., 2017, 2020; PAULIK; PAULIK; ARNOLD, 1981; SOUZA et al., 2020; ZHENG et al., 2020). Thus, the moment defined for the analysis was the moment when the decomposition reaction starts, equation 2.

$$MgSO_4.nH_2O \rightarrow MgSO_4 + nH_2O_{(g)} \quad (1)$$

$$MgSO_4 \rightarrow MgO + SO_{2(g)} + 0{,}5O_{2(g)} \quad (2)$$

In the literature, few studies present kinetic values for the decomposition of $MgSO_4$. Hulbert (1968) in his article obtained a value of 311.7 ± 12.5 kJ.mol^{-1} for the activation energy (Ea) of the decomposition of $MgSO_4$, coming from a $MgSO_4.7H_2O$. L'vov e Ugolkov (2004), investigated the decomposition of $MgSO_4$ in a vacuum and found an Ea value of 335.7 ± 1.7 kJ.mol^{-1}. Recently Mello *et al* (2020), calculated the Ea of the decomposition of $MgSO_4$ heptahydrate to be 368.2 kJ.mol^{-1}.

3. Materials and methods

3.1. Chemicals

In this work, anhydrous magnesium sulfate > 97% from Merck, magnesium sulfate monohydrate 97% from Merck, and magnesium sulfate heptahydrate > 99% from Merck was used in the tests performed in the TGA. These tests were carried out in an inert atmosphere, using Linde's 99.9% Nitrogen gas.

3.2. Thermodynamics assessment

Thermodynamic assessment was performed before the TGA tests to evaluate the behavior of the reaction system of the decompositions evaluated in this work. Through it, it was possible to identify the products of this system and the operating ranges to be adopted. The analysis of the equilibrium compositions of the compounds was made considering the possible species of gaseous and solid phases present in the reaction system. This analysis was performed using the HSC Chemistry 10 program (ROINE, 2021)

3.3. Thermogravimetric analyses

For this study, thermogravimetric tests were performed using magnesium sulfates (anhydrous, monohydrate, and heptahydrate) separated and in a pure form. Each magnesium sulfate was used in a set of four experiments, each with one of the heating rates.

These thermogravimetric analyzes were performed on the Netzsch STA 449 F3 Jupiter® simultaneous thermal analyzer. The experiments were carried out in a temperature range from 298 K to 1673 K and with heating rates of 5, 10, 15, and 20 K.min^{-1}. The experiments were all carried out with a mass of close to 10 mg of sample, to make them uniform.

3.4. Kinetics modeling

The kinetic modeling of the data resulting from the thermogravimetric curves is presented by the mathematical model developed by Speyer (1994) and Vachuška and Vobořil (1971), through equation 3.

$$(\varphi t + T_r)^2 \frac{\frac{d^2f}{dt^2}}{\frac{df}{dt}} = -n\left[\frac{(\varphi t+T_r)^2\left(\frac{df}{dt}\right)}{1-f}\right] + \frac{E_a\varphi}{R} \quad (3)$$

Were f, $\frac{df}{dt}$ e $\frac{d^2f}{dt^2}$ can be calculated from the thermogravimetric curve and its derivatives, as shown in Figure 1.

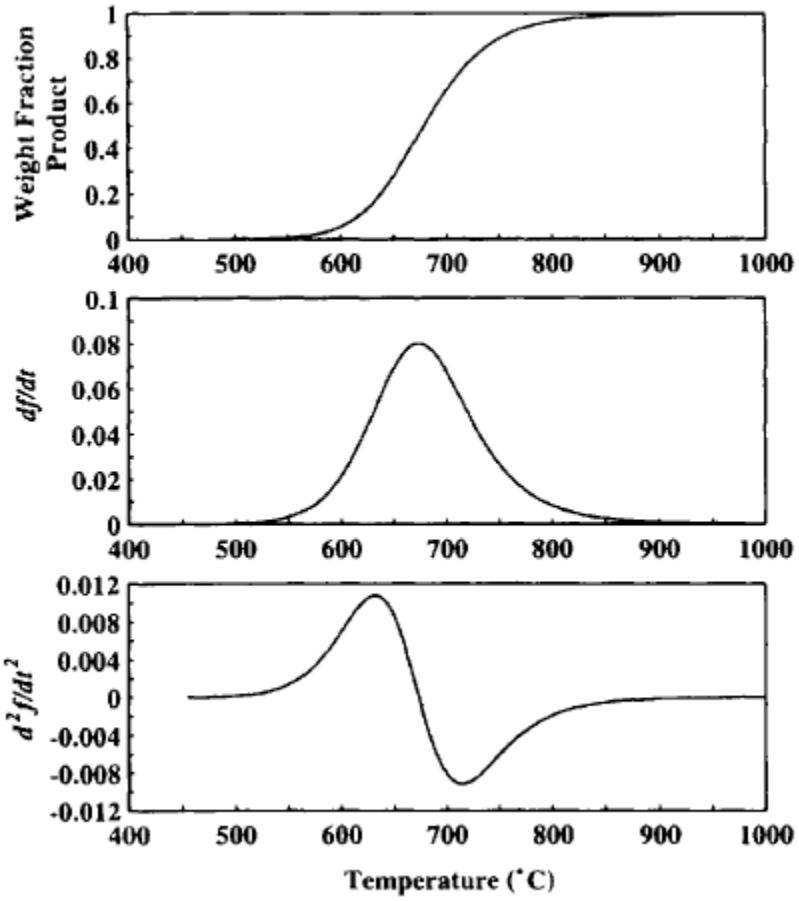

Figure 1 - Method of determination of f, $\frac{df}{dt}$ e $\frac{d^2f}{dt^2}$ (SPEYER, 1994).

To determine the derivatives, a sigmoidal function was used (equation 4), through a code in MATLAB R2021a (THE MATHWORKS INC, 2021). With the same code, the activation energy (Ea) and the order of reaction of each test were determined.

$$f(x) = \frac{1}{1+\exp(-a_1(t-a_2))} \quad (4)$$

4. Results and discussion

4.1. Thermodynamics assessment

The thermodynamic analysis was carried out to identify the possible compounds formed during the entire operational range, with this, equilibrium

species distribution graphs were constructed. Figures 2 to 4 show these graphics.

The figures 2 to 4 indicate that in the decomposition of the three sulfates the only product containing magnesium after decomposition is MgO. The formation of this MgO occurs from 1223 K onwards and from 1473 K onwards it becomes the only solid compound present in the system. In figures 2 and 4 the sulfate is hydrated and in both cases, dehydration occurs before the start of sulfate decomposition, these two figures indicate that the dehydration process causes decomposition to occur at lower temperatures than in the case of anhydrous sulfate. The thermodynamic analysis is in line with the behavior indicated in the literature.

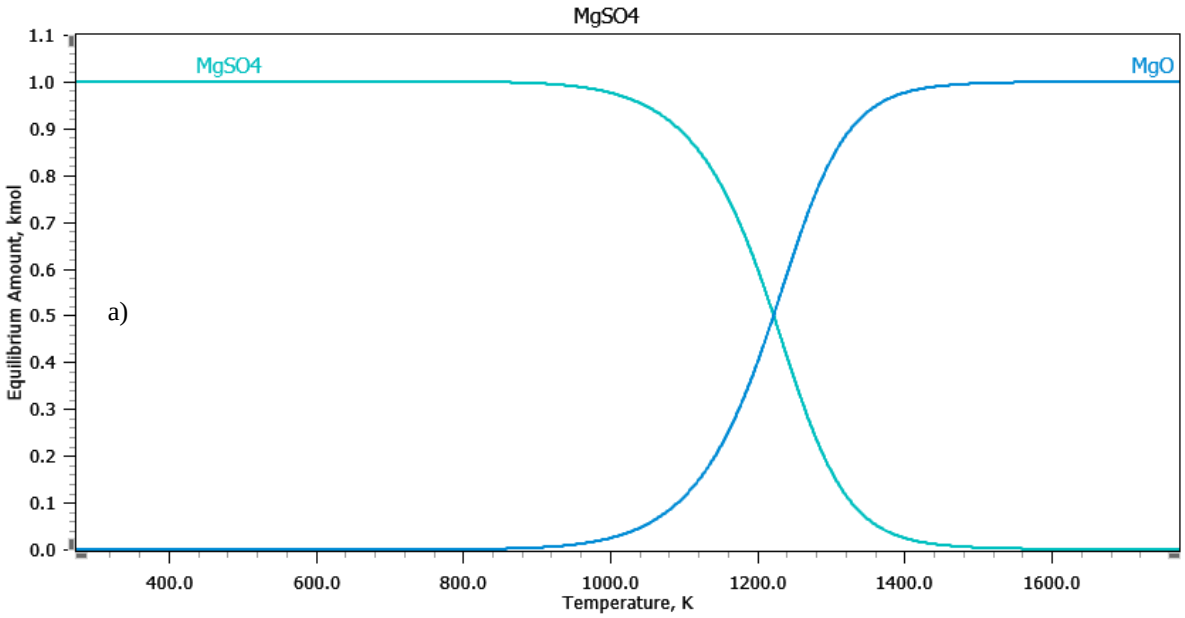

a)

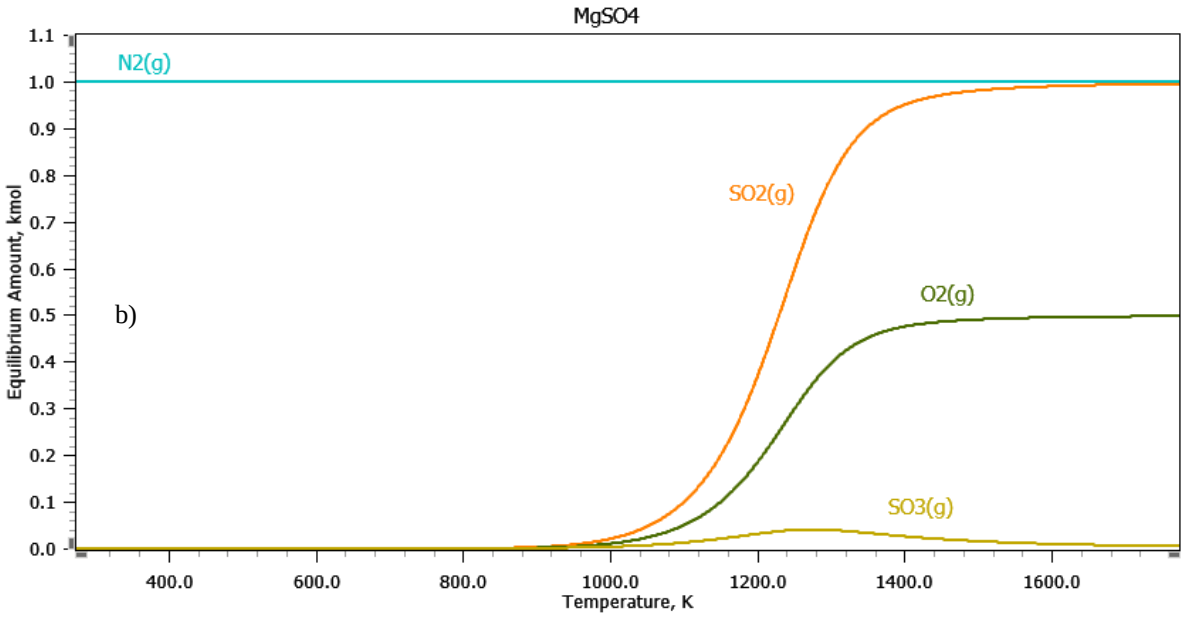

b)

Figure 2 - Equilibrium species distribution diagram for the thermal decomposition of anhydrous $MgSO_4$, constructed by the author using HSC Chemistry 10, being a) for the solid phase and b) for the gas phase.

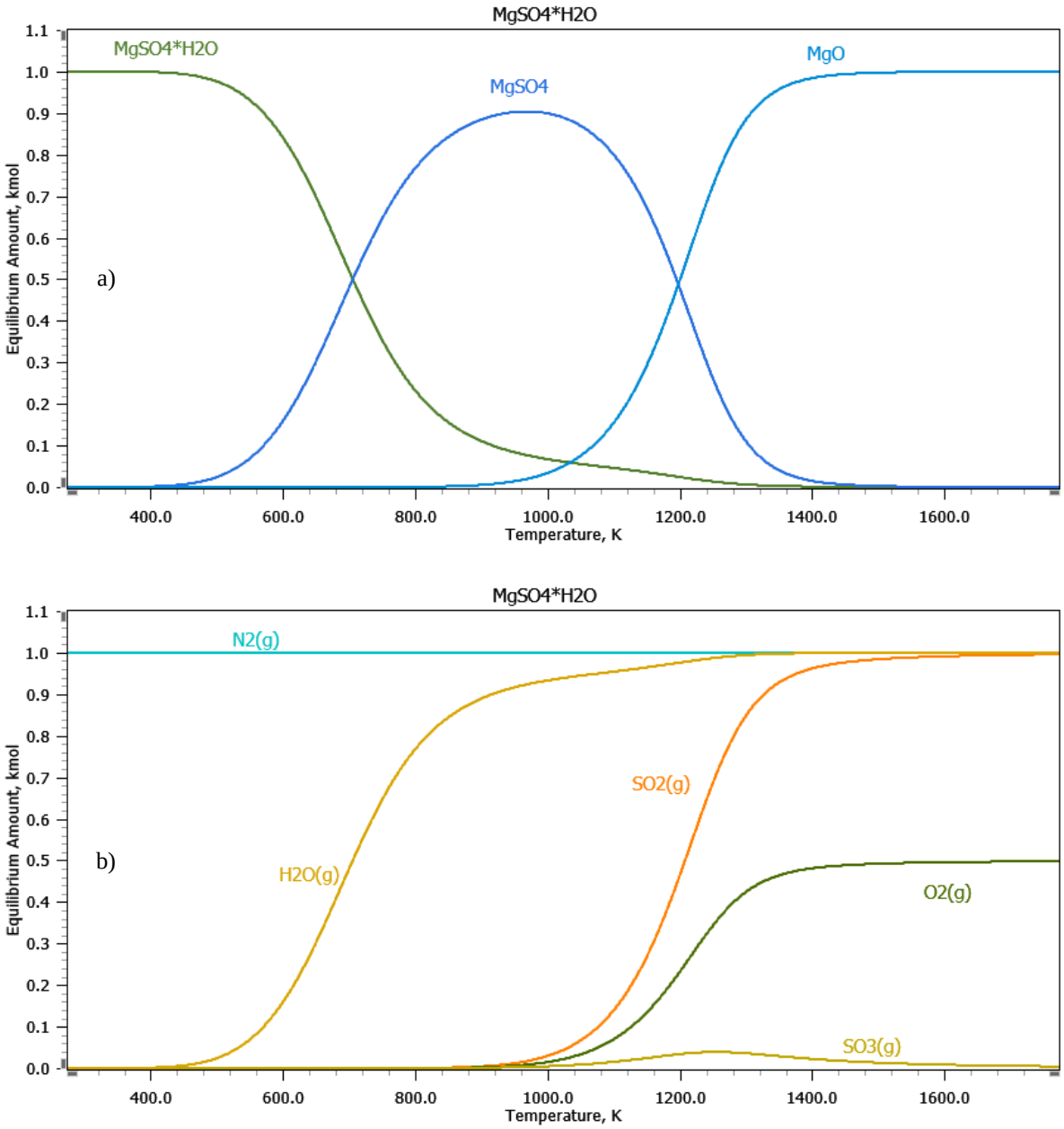

Figure 3 - Equilibrium species distribution diagram for the thermal decomposition of $MgSO_4$ monohydrate, constructed by the author using HSC Chemistry 10, being a) for the solid phase and b) for the gas phase.

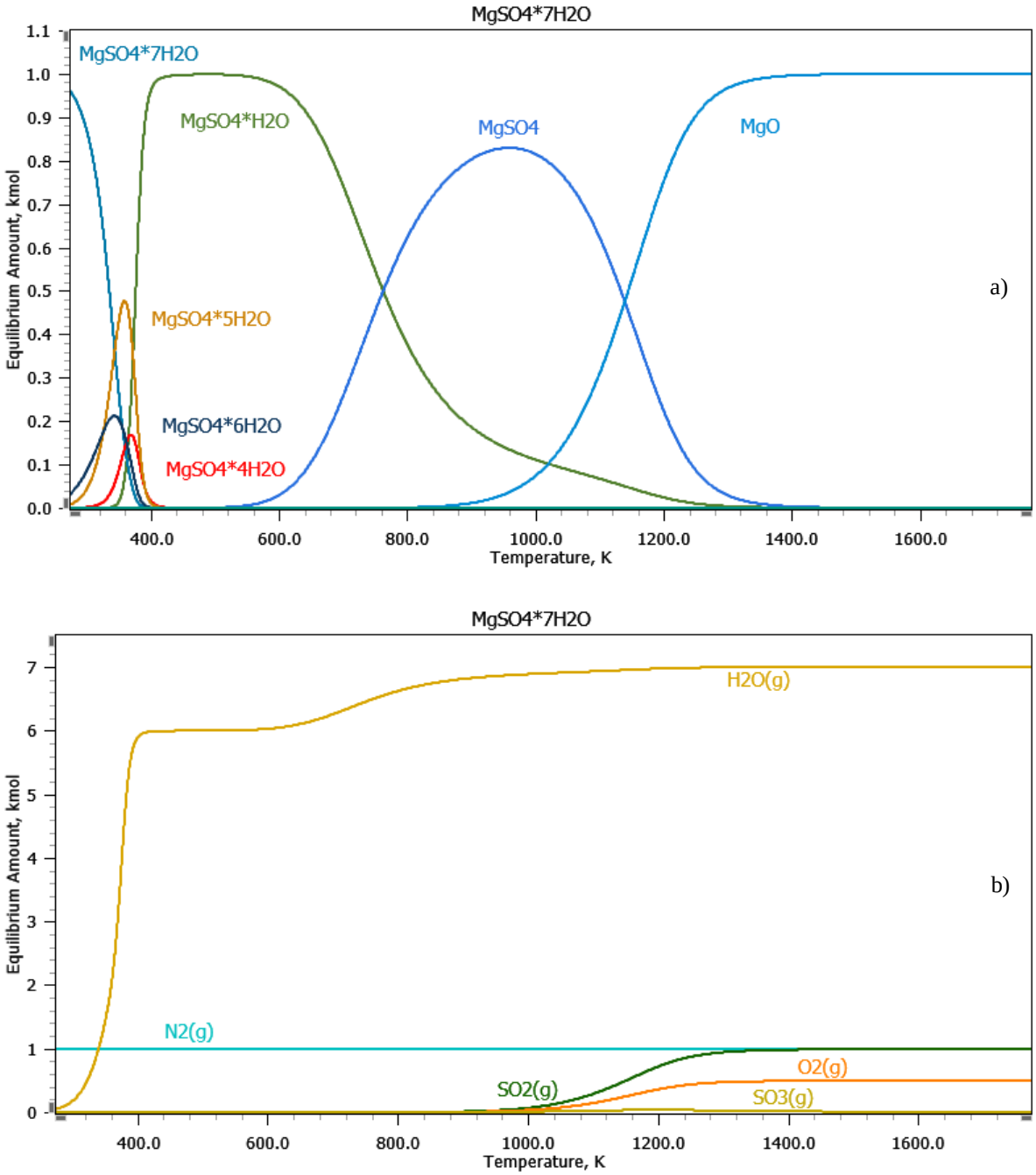

Figure 4 - Equilibrium species distribution diagram for the thermal decomposition of $MgSO_4$ heptahydrate, constructed by the author using HSC Chemistry 10, being a) for the solid phase and b) for the gas phase.

4.2. Thermogravimetric analyses

As described in item 3.3. , twelve thermogravimetric tests were performed. Each sulfate was submitted to four tests with heating rates from 5 $K.min^{-1}$ to 20 $K.min^{-1}$. Analyzing figures 5 to 7 it is possible to observe that in the three cases the curves follow an order according to the heating rates

of the tests. The test curves with a heating rate of 5 K.min^{-1} present a temperature for the beginning of magnesium sulfate decomposition that is lower than the other curves, being followed by the curves with a rate of 10 K.min^{-1}, 15 K.min^{-1}, and 20 K.min^{-1}.

Figure 5 shows the results of the TGAs of anhydrous magnesium sulfate, through which it is possible to observe that the initial decomposition temperature of the test with 5 K.min^{-1} is at least 70 K lower than the other curves. Since the onset of decomposition occurs at approximately 1183 K in the assay with a rate of 5 K.min^{-1}, while it occurs between 1253 and 1273 K with the other rates. The final decomposition temperature follows the same pattern as the initial one, with the lowest final temperatures in the tests with the lowest heating rates, however, the difference between the final temperatures of the curves is smaller than that of the initial temperatures. The final temperature of the rate curve 5 K.min^{-1} is approximately 1293 K and the others are between 1428 and 1458 K.

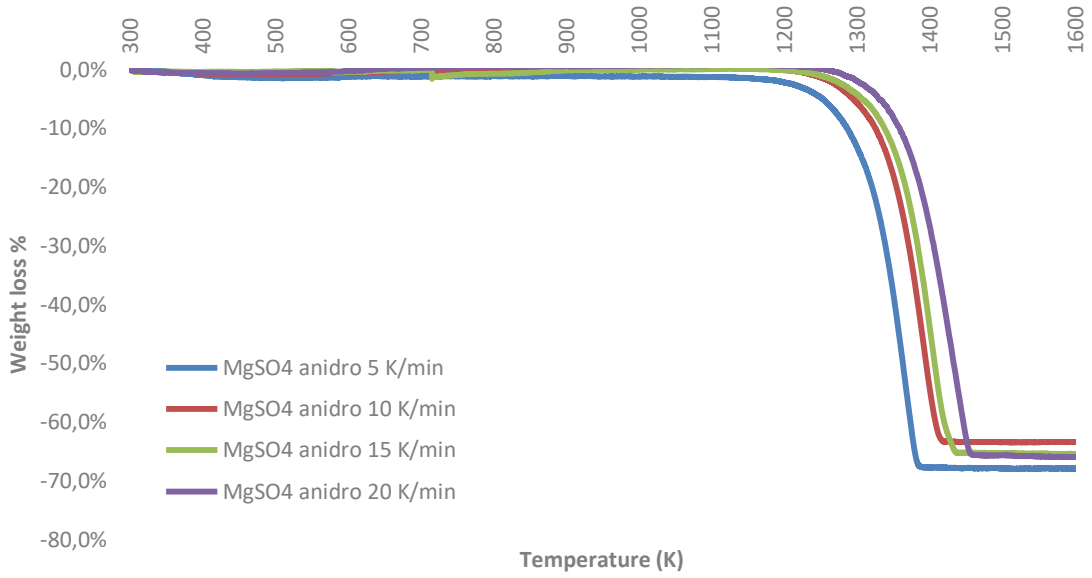

Figure 5 - Thermogravimetric analysis of anhydrous magnesium sulfate.

The figure 6 presents the results of the TGAs of magnesium sulfate monohydrate and as in the figure 5 the initial and final temperatures of sulfate decomposition follow the pattern according to heating rates, the lower the heating rate, the lower these temperatures. Unlike the tests with

anhydrous sulfate, the temperature variations between the tests of the monohydrate sulfate have similar behavior for the initial and final temperatures of decomposition. In both cases, temperatures vary around 25 K for each heating rate. Initial decomposition temperatures are 910 K (5 $K.min^{-1}$), 935 K (10 $K.min^{-1}$), 952 K (15 $K.min^{-1}$) and 981 K (20 $K.min^{-1}$) and the final decomposition temperatures are 1083 K (5 $K.min^{-1}$), 1117 K (10 $K.min^{-1}$), 1136 K (15 $K.min^{-1}$) and 1165 K (20 $K.min^{-1}$).

The big difference between figures 5 and 6 is the presence of water in the magnesium sulfate molecule. In the four tests, dehydration occurs in the same temperature range, between 40 K and 330 K, regardless of the heating rate of the test.

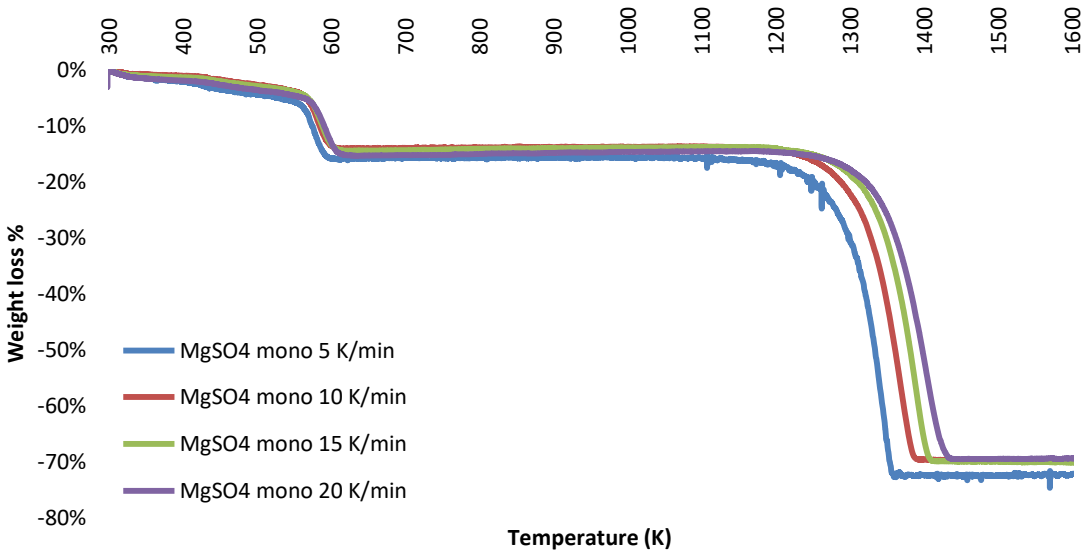

Figure 6 - Thermogravimetric analysis of magnesium sulfate monohydrate.

The figure 7 presents the results of the TGAs of magnesium sulfate heptahydrate. The decompositions are shown in this figure follow the same pattern as those shown in figures 5 and 6, showing lower initial and final decomposition temperatures for experiments with lower heating rates. As the initial decomposition temperatures are of 920 K (5 $K.min^{-1}$), 942 K (10 $K.min^{-1}$), 965 K (15 $K.min^{-1}$) and 976 K (20 $K.min^{-1}$) and the final decomposition temperatures are 1072 K (5 $K.min^{-1}$), 1092 K (10 $K.min^{-1}$),

1115 K (15 K.min^{-1}) and 1131 K (20 K.min^{-1}). Dehydration occurs between 40 K and 300 K, regardless of heating rates.

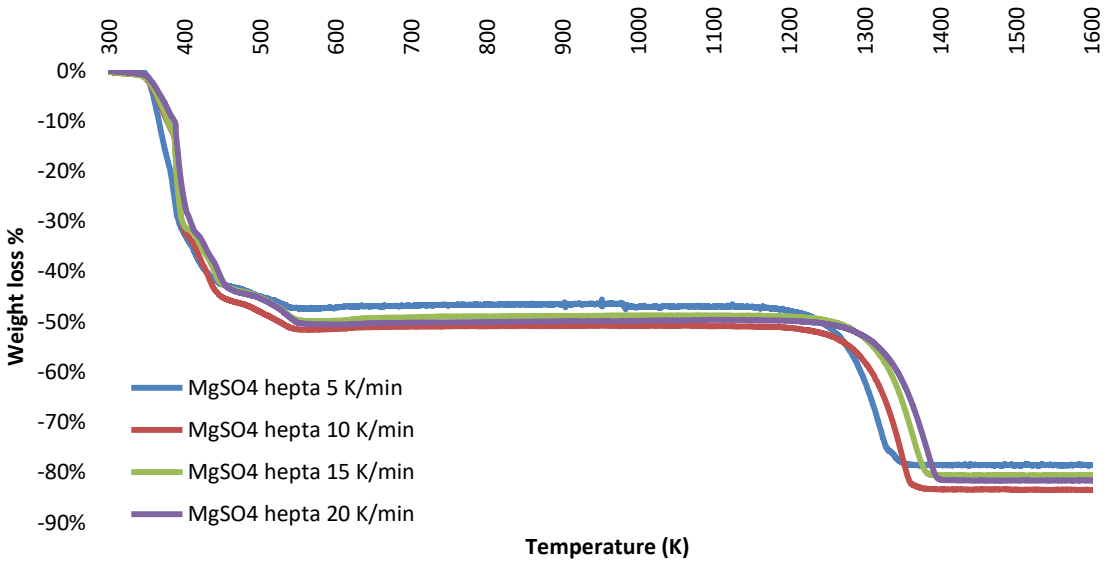

Figure 7 - Thermogravimetric analysis of magnesium sulfate heptahydrate.

4.3. Kinetics modeling

To analyze the kinetic parameters of magnesium sulfate decomposition, the data resulting from the thermogravimetric analyzes were processed by the kinetic model. Since sulfates have different levels of hydration, it was important to determine the intervals of the tests in which decompositions occur, so figure 8 shows these intervals in red in the thermogravimetric curves with a heating rate of 5 K.min^{-1}.

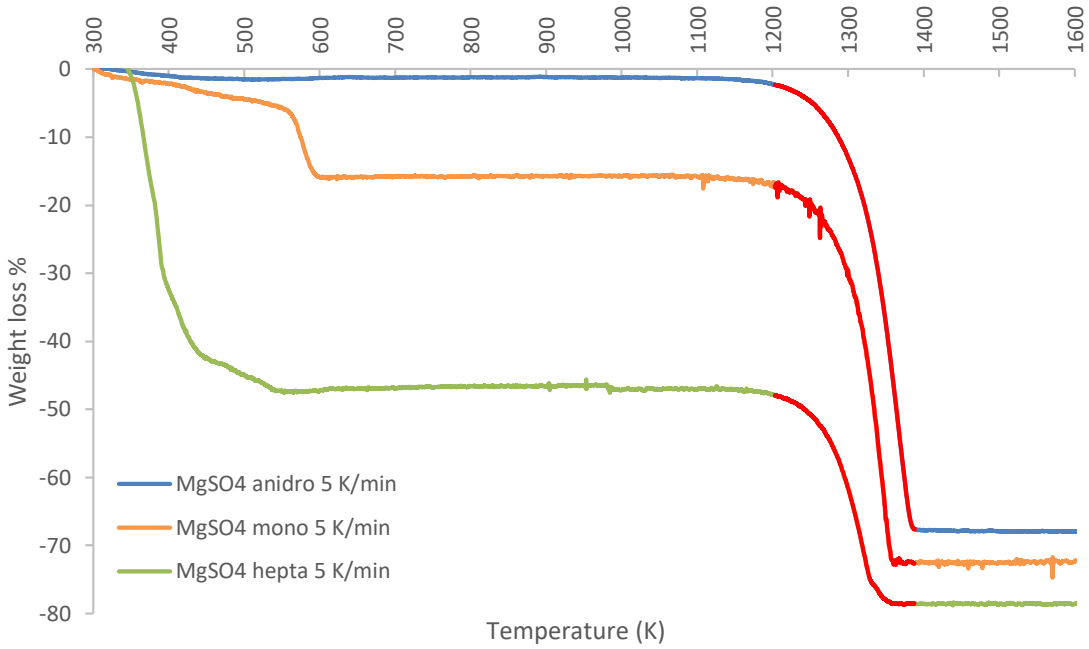

Figure 8 - Intervals analyzed by the kinetic model.

The figure 8 demonstrates that in the case of hydrated sulfates, the curves present two moments with loss of mass, so the identification of the interval where decomposition occurs was important for the kinetic modeling to be applied correctly. After determining the temperature ranges in each thermogravimetric curve, the data were applied in kinetic modeling.

The figure 9 displays the results of the linear regressions obtained for the data from the thermogravimetric curves of the decompositions of anhydrous $MgSO_4$. Through it, it was possible to observe that the experimental data and the model data were very close, a fact that can also be seen from the values of the coefficients of determination (R^2) shown in table 1. In addition to the values of R^2, table 1 presents the values of the order of reaction (n) and activation energy (Ea) of the decompositions of anhydrous magnesium sulfate. Despite the different heating rates employed in the experiments, the order of reaction was approximately 1.8 in all experiments. The activation energies of the tests were between 386 and 430 $kJ.mol^{-1}$, showing a variation between the lowest and the highest value of 11.5%. The lowest value was found in the test with the lowest heating rate.

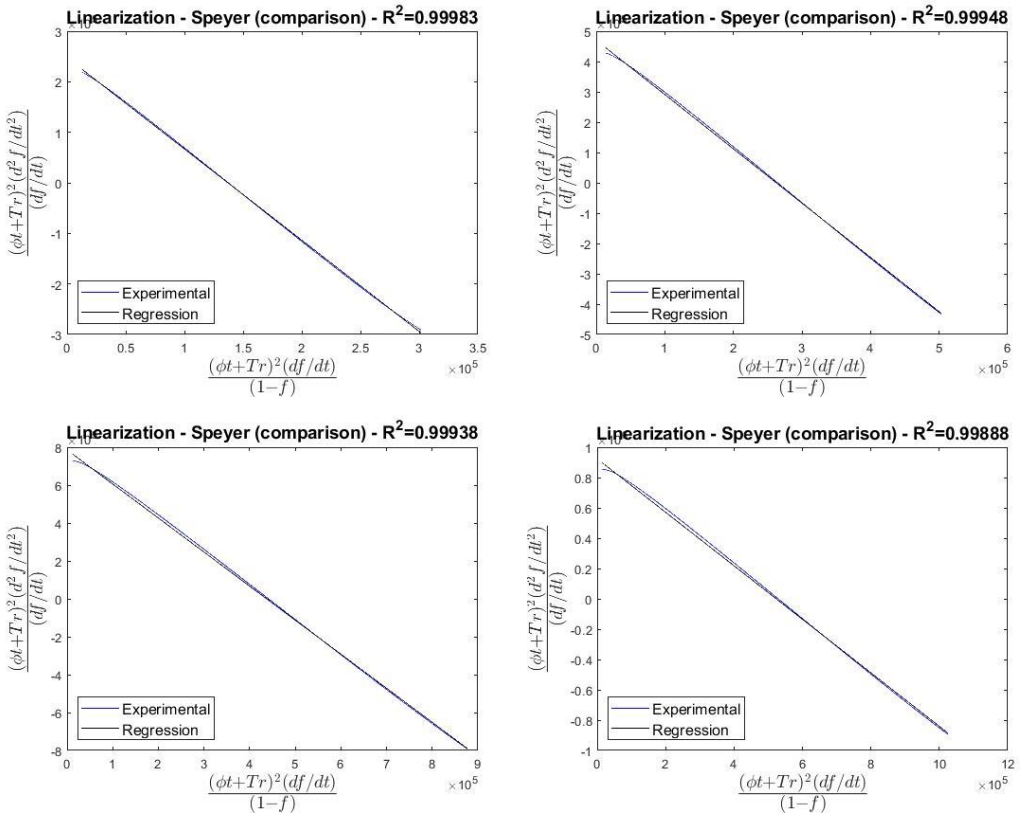

Figure 9 – Linear regression obtained for anhydrous $MgSO_4$ decompositions.

Table 1 - Kinetic data from the kinetic modeling of anhydrous $MgSO_4$ TGA curves.

Reagent	n	E_a (kJ.mol^{-1})	R^2
Anhydrous $MgSO_4$ 5K.min^{-1}	1,807	386,46	0,9998
Anhydrous $MgSO_4$ 10K.min^{-1}	1,799	412,60	0,9995
Anhydrous $MgSO_4$ 15K.min^{-1}	1,796	430,92	0,9994
Anhydrous $MgSO_4$ 20K.min^{-1}	1,773	398,05	0,9989

The figure 10 presents the linear regressions resulting from the modeling of thermogravimetric curves of the decomposition of $MgSO_4.H_2O$. It demonstrates that the modeling was efficient since experimental data and kinetic data were very close. Another factor that identifies that the modeling was efficient is the R^2 values present in table 2. The other values shown in table 2 indicate that the order of the decomposition reaction was in the range of 1.8 for the four heating rates and that the activation energies were between 387 and 417 kJ.mol^{-1}, showing a variation between the lowest and

the highest value of 7.8%. The lowest value was recorded again in the test with a heating rate of 5 K.min^{-1}.

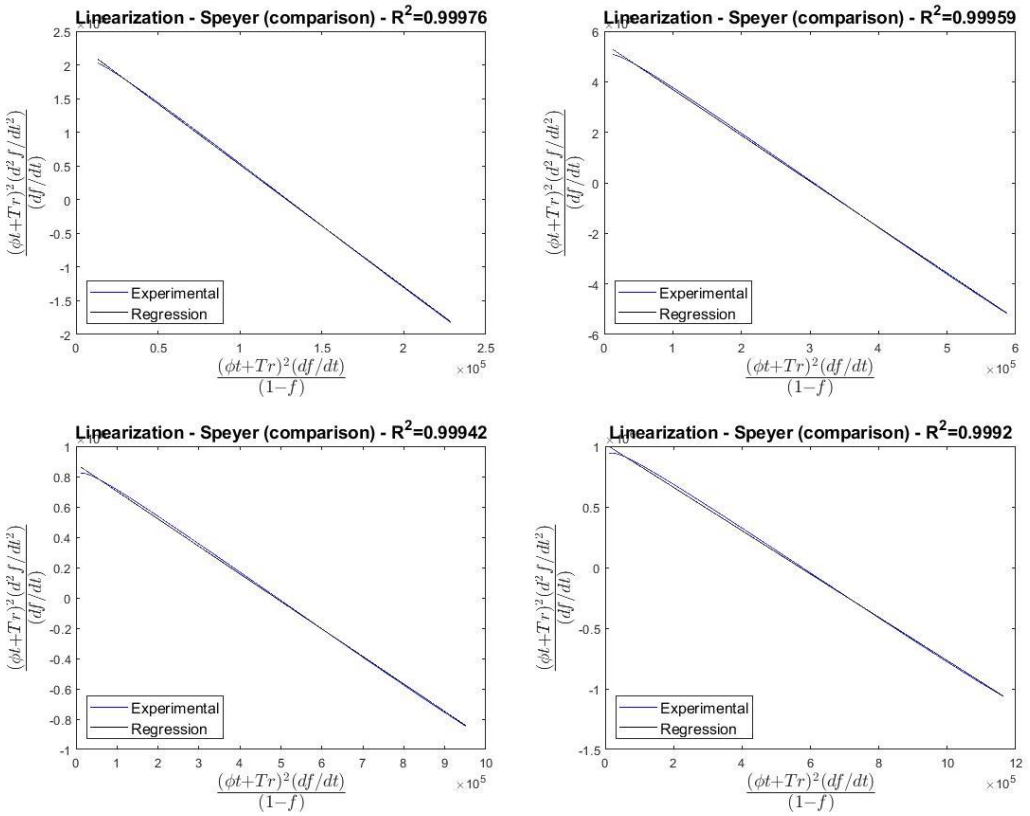

Figure 10 – Linear regression obtained for monohydrate $MgSO_4$ decompositions.

Table 2 - Kinetic data from kinetic modeling of TGA curves of $MgSO_4$ monohydrate.

Reagent	n	E_a (kJ.mol^{-1})	R^2
$MgSO_4$ monohydrate 5K.min^{-1}	1,811	387,14	0,9998
$MgSO_4$ monohydrate 10K.min^{-1}	1,797	397,07	0,9996
$MgSO_4$ monohydrate 15K.min^{-1}	1,792	416,57	0,9994
$MgSO_4$ monohydrate 20K.min^{-1}	1,786	417,24	0,9992

The analysis of figure 11 together with table 3, shows that the kinetic modeling was also efficient for heptahydrate sulfates, presenting data close to the experimental ones and R^2 values above 0.999 for all heating rates. Once again, the values of the order of reactions were around 1.8. The difference in the results is due to the Ea values that were a little higher than the anhydrous and monohydrated sulfates, being in the range of 422 and 445 kJ.mol^{-1}, being the group of tests with the most uniform values. Unlike previous analyses, the 5 K.min^{-1} rate assay was the one with the highest Ea value.

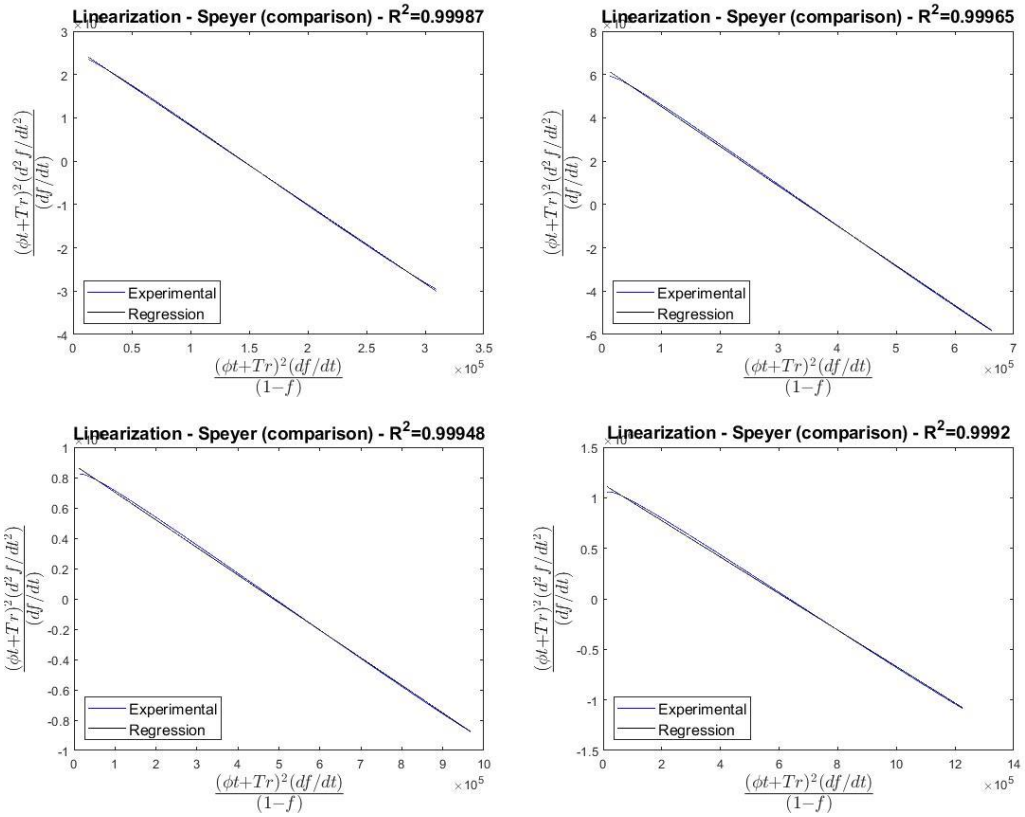

Figure 11 – Linear regression obtained for heptahydrate $MgSO_4$ decompositions.

Table 3 - Kinetic data from kinetic modeling of TGA curves of $MgSO_4$ heptahydrate.

Reagent	n	E_a (kJ.mol^{-1})	R^2
$MgSO_4$ heptahydrate 5K.min^{-1}	1,831	445,73	0,9999
$MgSO_4$ heptahydrate 10K.min^{-1}	1,809	422,73	0,9996
$MgSO_4$ heptahydrate 15K.min^{-1}	1,803	434,66	0,9995
$MgSO_4$ heptahydrate 20K.min^{-1}	1,791	422,42	0,9992

5. Final remarks

The thermodynamic and kinetic analyzes employed in the experimental and theoretical data presented in this work allowed the investigation of the effects of magnesium sulfate hydration and the heating rate in its thermal decomposition. Kinetic modeling was applied to the experimental data of the twelve thermogravimetric analyses, presenting an R^2 value greater than 0.99 in all cases, indicating that the modeling is adequate for the studied reaction.

The heating rate was not shown as a variable that directly influences the decomposition of $MgSO_4$, since the values of activation energies in the

experiments did not show a pattern to the rates. The thermodynamic analysis about the hydration of the sulfate indicated that the highest level of hydration would facilitate its decomposition, however, the kinetic analysis showed an average Ea value close to the anhydrous and monohydrated sulfates (407 and 404.5 $KJ.mol^{-1}$ respectively) and an above value for sulfate heptahydrate (433.3 $KJ.mol^{-1}$). The values of the orders of reactions of the twelve trials were close to 1.8.

6. Acknowledgments

The authors are grateful to Coordination for the Improvement of Higher Education Personnel (CAPES) for their financial support throughout the research.

7. References

ACHAR, B. N. N.; BRINDLEY, G. W.; SHARP, J. H. **Kinetics and mechanism of dehydroxylation processes. III Applications and limitations of Dynamic methods**. Proceedings of the International Clay Conference. **Anais**...Jerusalem: 1966

AGATZINI-LEONARDOU, S. et al. Hydrometallurgical process for the separation and recovery of nickel from sulphate heap leach liquor of nickeliferrous laterite ores. **Minerals Engineering**, v. 22, n. 14, p. 1181–1192, 2009.

AINA, V. et al. Magnesium- and strontium-co-substituted hydroxyapatite: the effects of doped-ions on the structure and chemico-physical properties. **Journal of Materials Science: Materials in Medicine**, v. 23, n. 12, p. 2867–2879, 2012.

AL-TABBAA, A. Reactive magnesia cement. In: **Eco-Efficient Concrete**. [s.l.] Elsevier, 2013. p. 523–543.

ALI, S. H. et al. Mineral supply for sustainable development requires resource governance. **Nature**, v. 543, n. 7645, p. 367–372, 2017.

ANM. **Anuário Mineral Brasileiro: principais substâncias metálicas**

2020. Brasília: [s.n.]. Disponível em: <www.anm.gov.br>. Acesso em: 29 dez. 2021.

APHANE, M. E.; VAN DER MERWE, E. M.; STRYDOM, C. A. Influence of hydration time on the hydration of MgO in water and in a magnesium acetate solution. **Journal of Thermal Analysis and Calorimetry**, v. 96, n. 3, p. 987–992, 2009.

ASENCIOS, Y. J. O.; ASSAF, E. M. Combination of dry reforming and partial oxidation of methane on NiO-MgO-ZrO2 catalyst: Effect of nickel content. **Fuel Processing Technology**, v. 106, p. 247–252, 2013.

ASENCIOS, Y. J. O.; NASCENTE, P. A. P.; ASSAF, E. M. Partial oxidation of methane on NiO-MgO-ZrO 2 catalysts. **Fuel**, v. 97, p. 630–637, 2012.

AVRAMI, M. Granulation, Phase Change, and Microstructure Kinetics of Phase Change. **The Journal of Chemical Physics**, v. 9, n. December, p. 177–184, 1941.

BARBOSA, L. I.; GONZÁLEZ, J. A.; DEL CARMEN RUIZ, M. Extraction of lithium from β-spodumene using chlorination roasting with calcium chloride. **Thermochimica Acta**, v. 605, p. 63–67, 10 abr. 2015.

BARIN, I.; SCHULER, W. On the kinetics of the chlorination of titanium dioxide in the presence of solid carbon. **Metallurgical Transactions B**, v. 11, n. 2, p. 199–207, jun. 1980.

BARTLEY, J. K. et al. Simple method to synthesize high surface area magnesium oxide and its use as a heterogeneous base catalyst. **Applied Catalysis B: Environmental**, v. 128, p. 31–38, 2012.

BOOSTER, J. L.; SANDWIJK, A. VAN; REUTER, M. A. MAGNESIUM REMOVAL IN THE ELECTROLYTIC ZINC INDUSTRY. **Minerals Engineering**, v. 13, n. 5, p. 517–526, 2000.

BOYD, C. E. **Water Quality**. Third Edit ed. Cham: Springer International

Publishing, 2020.

BRANCATO, V. et al. MgSO4·7H2O filled macro cellular foams: An innovative composite sorbent for thermo-chemical energy storage applications for solar buildings. **Solar Energy**, v. 173, n. February, p. 1278–1286, 2018.

BROCCHI, E. A.; MOURA, F. J. Chlorination methods applied to recover refractory metals from tin slags. **Minerals Engineering**, v. 21, n. 2, p. 150–156, jan. 2008.

BROWN, R. E. Magnesium recycling yesterday, today, and tomorrow. **The Minerals, Metals and Materials Society, Warrendale**, p. 1318–1329, 2000.

BROWNELL, W. E. Reactions Between Alkaline-Earth Sulfates and. **Journal of The American Ceramic Society**, v. 46, n. 3, p. 125–128, 1951.

BURTON, M. **Oferta menor de magnésio da China ameaça empregos na Europa**. Disponível em: <https://www.bloomberglinea.com.br/2021/10/23/oferta-menor-de-magnesio-da-china-ameaca-empregos-na-europa/>. Acesso em: 8 dez. 2021.

CALDAS, T. D. P. **Análise de Trincas e Coating em Pelotas de Minério de Ferro por Processamento Digital de Imagens**. [s.l.] Pontifícia Universidade Católica do Rio de Janeiro, 2019.

CALO, J. M.; PERKINS, M. T. A heterogeneous surface model for the “steady-state” kinetics of the boudouard reaction. **Carbon**, v. 25, n. 3, p. 395–407, 1987.

CARABALLO, M. A. et al. Field multi-step limestone and MgO passive system to treat acid mine drainage with high metal concentrations. **Applied Geochemistry**, v. 24, n. 12, p. 2301–2311, 2009.

CARDOSO, J. H. **Decomposição redutora de MgSO4.7H2O na presença de H2(g) Dissertação**. [s.l.] Pontifícia Universidade Católica do Rio de Janeiro, 2018.

CHENG, C. Y. et al. Recovery of nickel and cobalt from laterite leach solutions using direct solvent extraction: Part 1 - Selection of a synergistic SX system. **Hydrometallurgy**, v. 104, n. 1, p. 45–52, 2010.

CHENG, C. Y. et al. Synergistic solvent extraction of nickel and cobalt: A review of recent developments. **Solvent Extraction and Ion Exchange**, v. 29, n. 5–6, p. 719–754, 2011.

CHIPERA, S. J.; VANIMAN, D. T. Experimental stability of magnesium sulfate hydrates that may be present on Mars. **Geochimica et Cosmochimica Acta**, v. 71, n. 1, p. 241–250, 2007.

CIPOLLINA, A. et al. Reactive crystallisation process for magnesium recovery from concentrated brines. **Desalination and Water Treatment**, v. 55, p. 2377–2388, 2015.

COATS, A. W.; REDFERN, J. P. Kinetic Parameters from Thermogravimetric Data. **Nature**, v. 201, p. 68–69, 1964.

COSTA, R. H. **Recovery of magnesium sulfate from a zinc ore flotation tailing using hydrometallurgical route.** São Paulo: Universidade de São Paulo, 1 dez. 2020.

COURTIAL, M.; CABRILLAC, R.; DUVAL, R. Recycling of magnesium slags in construction block form. **Studies in Environmental Science**, v. 60, n. C, p. 599–604, 1994.

CURRY, K. C.; VAN OSS, H. G. 2017 Minerals Yearbook: Magnesium Compounds. **US Geological Survey, Washington DC**, n. March, 2020.

DA SILVA, A. M. V. **Estudos sobre a recuperação do titânio contido no rejeito da concentração de magnetita**. [s.l.] Pontifícia Universidade Católica do Rio de Janeiro , 2018.

DĄBROWSKI, A. et al. Selective removal of the heavy metal ions from waters and industrial wastewaters by ion-exchange method. **Chemosphere**, v. 56, n. 2, p. 91–106, 2004.

DALY, T. **China Oct magnesium exports rebound to 19-month high**. Disponível em: <https://www.reuters.com/markets/commodities/china-oct-magnesium-exports-rebound-19-month-high-2021-11-22/>. Acesso em: 10 dez. 2021.

DAMAYANTI, R.; KHAERUNISSA, H. COMPOSITION AND CHARACTERISTICS OF RED MUD: A CASE STUDY ON TAYAN BAUXITE RESIDUE FROM ALUMINA PROCESSING PLANT AT WEST KALIMANTAN. **INDONESIAN MINING JOURNAL**, v. 19, n. 3, p. 179–190, 2016.

DENISENKO, Y. G. et al. Thermal decomposition of europium sulfates Eu2(SO4)3·8H2O and EuSO4. **Journal of Solid State Chemistry**, v. 255, n. August, p. 219–224, 2017.

DHARWADKAR, S. R.; CHANDRASEKHARAIAH, M. S.; KARKHANAVALA, M. D. Evaluation of kinetic parameters from thermogravimetric curves. **Thermochimica Acta**, v. 25, p. 372–375, 1978.

DING, K. et al. Thermochemical reduction of magnesium sulfate by natural gas: Insights from an experimental study. **Geochemical Journal**, v. 45, n. 2, p. 97–108, 2011.

DONG, H. et al. Synthesis of reactive MgO from reject brine via the addition of NH4OH. **Hydrometallurgy**, v. 169, p. 165–172, 2017.

DONG, H. et al. Investigation of the properties of MgO recovered from reject brine obtained from desalination plants. **Journal of Cleaner Production**, v. 196, p. 100–108, 20 set. 2018.

DOU, W. et al. Sulfate removal from wastewater using ettringite precipitation: Magnesium ion inhibition and process optimization. **Journal of Environmental Management**, v. 196, p. 518–526, 2017.

DUPONT, C.; CAMPAGNE, A.; CONSTANT, F. Efficacy and Safety of a Magnesium Sulfate-Rich Natural Mineral Water for Patients With Functional Constipation. **Clinical Gastroenterology and Hepatology**, v. 12, n. 8, p. 1280–1287, 2014.

EUROPEAN COMMISSION. **COMMITTEE AND THE COMMITTEE OF THE REGIONS Critical Raw Materials Resilience: Charting a Path towards greater Security and Sustainability. COM(2020) 474 final**. [s.l: s.n.]. Disponível em: <http://info.worldbank.org/governance/wgi/.>.

FAN, C. et al. Leaching behavior of metals from chlorinated limonitic nickel laterite. **International Journal of Mineral Processing**, v. 110–111, p. 117–120, jul. 2012.

FERNANDES, F. R. C. et al. **TENDÊNCIAS TECNOLÓGICAS BRASIL 2015 - Geociências e Tecnologia Mineral**. Rio de Janeiro, Brazil: CETEM - Centro de Tecnologia Mineral, 2007.

FREEMAN, E. S.; CARROLL, B. The Application of Thermoanalytical Techniques to Reaction Kinetics: The Thermogravimetric Evaluation of the Kinetics of the Decomposition of Calcium Oxalate Monohydrate. **The Journal of Physical Chemistry**, v. 62, n. 4, p. 394–397, 1958.

FREITAS, E. V. DE S. et al. Indução da fitoextração de chumbo por ácido cítrico em solo contaminado por baterias automotivas. **Revista Brasileira de Ciência do Solo**, v. 33, n. 2, p. 467–473, abr. 2009.

GALLAGHER, P. K.; JOHNSON, D. W.; SCHREY, F. Thermal Decomposition of Iron (II) Sulfates. **Journal of The American Ceramic Society**, v. 53, n. 12, p. 666–670, 1970.

GAO, F. et al. Recovery of magnesium from ferronickel slag to prepare hydrated magnesium sulfate by hydrometallurgy method. **Journal of Cleaner Production**, v. 303, p. 127049, 2021.

GARCES-GRANDA, A.; LAPIDUS, G. T.; RESTREPO-BAENA, O. J. The effect of calcination as pre treatment to enhance the nickel extraction from

low-grade laterites. **Minerals Engineering**, v. 120, n. November 2017, p. 127–131, 2018.

GENCELI, F. E. et al. Crystallization and Characterization of a New Magnesium Sulfate Hydrate MgSO4·11H2O. **Crystal Growth & Design**, v. 7, n. 12, p. 2460–2466, 2007.

GRIGOROVA, D.; PAUNOVA, R. Thermodynamic and kinetic investigation of carbothermic reduction of electric arc furnace dust. **Metalurgija**, v. 61, n. 1, p. 189–192, 2022.

GUAN, Q. JUN et al. Recovery of cobalt and nickel in the presence of magnesium and calcium from sulfate solutions by Versatic 10 and mixtures of Versatic 10 and Cyanex 301. **Transactions of Nonferrous Metals Society of China (English Edition)**, v. 26, n. 3, p. 865–873, 2016.

HABASHI, F. **Handbook of Extractive Metallurgy - Vol. 2**. Weinheim - Chicester - New Youk - Toronto - Brisbane - Singapore: WILEY-VCH, 1997.

HAJBI, F. et al. Thermodynamic study of magnesium sulfate crystallization: application of Pitzer model and quinary diagrams. **Desalination and Water Treatment**, p. 12, 2015.

HAN, D. et al. A review on ignition mechanisms and characteristics of magnesium alloys. **Journal of Magnesium and Alloys**, v. 8, n. 2, p. 329–344, 2020.

HARVEY, R.; HANNAH, R.; VAUGHAN, J. Selective precipitation of mixed nickel-cobalt hydroxide. **Hydrometallurgy**, v. 105, n. 3–4, p. 222–228, 2011.

HIGHFIELD, J. et al. RSC Advances Activation of serpentine for CO2 mineralization by flux extraction of soluble magnesium salts using ammonium sulfate. **The Royal Society of Chemistry**, v. 2, p. 6535–6541, 2012.

HLABELA, P. S. et al. Thermal reduction of barium sulphate with carbon monoxide-A thermogravimetric study. **Thermochimica Acta**, v. 498, n. 1–2, p. 67–70, 2010.

HOTEIT, A. et al. Sulfate decomposition from circulating fluidized bed combustors bottom ash. **Chemical Engineering Science**, v. 62, n. 23, p. 6827–6835, 1 dez. 2007.

HUANG, P. et al. A sustainable process to utilize ferrous sulfate waste from titanium oxide industry by reductive decomposition reaction with pyrite. **Thermochimica Acta**, v. 620, p. 18–27, 2015.

HULBERT, S. F. Effect of processing parameters on the kinetics of decomposition of magnesium sulphate. **Materials Science and Engineering**, v. 2, n. 5, p. 262–268, 1968.

INEICH, T. et al. Utilization efficiency of lime consumption during magnesium sulfate precipitation. **Hydrometallurgy**, v. 173, n. September, p. 241–249, 2017.

IONASHIRO, M. **Princípios Básicos da Termogravimetria e Análise Térmica Diferencial/ Calorimetria Exploratória Diferencial**. [s.l: s.n.].

JAVAID, A. et al. LITERATURE REVIEW ON MAGNESIUM RECYCLING. **Magnesium Technology**, p. 7–12, 2006.

JENA, B. C.; DRESLER, W.; REILLY, I. G. Extraction of titanium, vanadium and iron from titanomagnetite deposits at pipestone lake, Manitoba, Canada. **Minerals Engineering**, v. 8, n. 1–2, p. 159–168, jan. 1995.

JIANG, M. et al. Mechanism of sodium sulfate in promoting selective reduction of nickel laterite ore during reduction roasting process. **International Journal of Mineral Processing**, v. 123, p. 32–38, 2013.

JIAO, F. et al. Recovery of chromium and magnesium from spent magnesia-chrome refractories by acid leaching combined with alkali

precipitation and evaporation. **Separation and Purification Technology**, v. 227, n. June, p. 115705, 2019.

JIN, F.; AL-TABBAA, A. Strength and hydration products of reactive MgO-silica pastes. **Cement and Concrete Composites**, v. 52, p. 27–33, 2014.

JOHNSON, D. W.; GALLAGHER, P. K. Kinetics of the Decomposition of Freeze-Dried Aluminum Sulfate and Ammonium Aluminum Sulfate. **Journal of the American Ceramic Society**, v. 54, n. 9, p. 461–465, 1971.

KANARI, N. et al. Thermal Behavior of Hydrated Iron Sulfate in Various Atmospheres. **Metals**, v. 8, n. 12, p. 1084, 2018.

KANARI, N.; GABALLAH, I. Chlorination and carbochlorination of magnesium oxide. **Metallurgical and Materials Transactions B**, v. 30, n. 3, p. 383–391, jun. 1999.

KARIDAKIS, T.; AGATZINI-LEONARDOU, S.; NEOU-SYNGOUNA, P. Removal of magnesium from nickel laterite leach liquors by chemical precipitation using calcium hydroxide and the potential use of the precipitate as a filler material. **Hydrometallurgy**, v. 76, n. 1–2, p. 105–114, 2005.

KATO, H. et al. Decomposition of carbon dioxide to carbon by hydrogen-reduced Ni(II)-bearing ferrite. **Journal of Materials Science**, v. 29, n. 21, p. 5689–5692, 1994.

KAYA, S.; TOPKAYA, Y. A. High pressure acid leaching of a refractory lateritic nickel ore. **Minerals Engineering**, v. 24, n. 11, p. 1188–1197, 2011.

KHAIRUL, M. A.; ZANGANEH, J.; MOGHTADERI, B. The Composition, Recycling and Utilisation of Bayer Red Mud. **Conservation and Recycling**, v. 141, n. February, p. 483–498, 2019.

KHOO, J. Z.; HAQUE, N.; BHATTACHARYA, S. Process simulation and

exergy analysis of two nickel laterite processing technologies. **International Journal of Mineral Processing**, v. 161, p. 83–93, 2017.

KIM, B. S. et al. A kinetic study of the carbothermic reduction of zinc oxide with various additives. **Materials Transactions**, v. 47, n. 9, p. 2421–2426, 2006.

KIM, J.; AZIMI, G. Resources, Conservation & Recycling Selective Precipitation of Titanium, Magnesium, and Aluminum from the Steelmaking Slag Leach Liquor. **Resources, Conservation & Recycling**, v. 180, n. January, p. 106177, 2022.

KOBERTZ, D.; MÜLLER, M. Experimental studies on NiSO4 by thermal analysis and calorimetry. **Calphad: Computer Coupling of Phase Diagrams and Thermochemistry**, v. 45, p. 55–61, 2014.

KONGOLO, K. et al. Cobalt and zinc recovery from copper sulphate solution by solvent extraction. **Minerals Engineering**, v. 16, n. 12, p. 1371–1374, 2003.

KOVACHEVA, P.; DJINGOVA, R. Ion-exchange method for separation and concentration of platinum and palladium for analysis of environmental samples by inductively coupled plasma atomic emission spectrometry. **Analytica Chimica Acta**, v. 464, n. 1, p. 7–13, 2002.

KURBAN, G. V. T. et al. Thermodynamics and Kinetic Modeling of the ZnSO4·H2O Thermal Decomposition in the Presence of a Pd/Al2O3 Catalyst. **Energies**, v. 15, n. 2, p. 548, 2022.

KUUSIK, R.; SALKKONEN, P.; NIINISTÖ, L. Thermal decomposition of calcium sulphate in carbon monoxide. **Journal of Thermal Analysis**, v. 30, n. 1, p. 187–193, 1985.

L'VOV, B. V.; UGOLKOV, V. L. Kinetics of free-surface decomposition of magnesium and barium sulfates analyzed thermogravimetrically by the third-law method. **Thermochimica Acta**, v. 411, n. 1, p. 73–79, 2004.

LAHIJANI, P. et al. Conversion of the greenhouse gas CO2 to the fuel gas CO via the Boudouard reaction: A review. **Renewable and Sustainable Energy Reviews**, v. 41, p. 615–632, 2015.

LAUREIRO, Y. et al. Kinetic parameters for the thermal decomposition reactions of CrO3 in AIR. **Thermochimica Acta**, v. 143, n. C, p. 347–350, maio 1989.

LEE, E. K. et al. Magnesium oxide as an effective catalyst in catalytic wet oxidation of H2S to sulfur. **Reaction Kinetics and Catalysis Letters**, v. 82, n. 2, p. 241–246, 2004.

LEMOS, F.; ANGORA, M.; MASSON, I. Lixiviação sob pressão de minérios lateríticos. p. 131–136, 2007.

LENOIR, D.; SCHRAMM, K. W.; LALAH, J. O. Green Chemistry: Some important forerunners and current issues. **Sustainable Chemistry and Pharmacy**, v. 18, n. September, p. 100313, 2020.

LI, H. et al. Investigation on the recovery of gold and silver from cyanide tailings using chlorination roasting process. **Journal of Alloys and Compounds**, v. 763, p. 241–249, 30 set. 2018.

LI, J. et al. Preparation of boric acid from low-grade ascharite and recovery of magnesium sulfate. **Transactions of Nonferrous Metals Society of China (English Edition)**, v. 20, n. 6, p. 1161–1165, 2010.

LI, X. MING et al. Improvement of carbothermic reduction of nickel slag by addition of CaCO3. **Transactions of Nonferrous Metals Society of China (English Edition)**, v. 29, n. 12, p. 2658–2666, 2019a.

LI, Z. et al. Efficient and Sustainable Removal of Magnesium from Brines for Lithium/Magnesium Separation Using Binary Extractants. **ACS Sustainable Chemistry and Engineering**, v. 7, p. 19225–19234, 2019b.

LIU, X. W. et al. Recovery of valuable metals from a low-grade nickel ore using an ammonium sulfate roasting-leaching process. **International**

Journal of Minerals, Metallurgy and Materials, v. 19, n. 5, p. 377–383, 2012.

LIU, Y. et al. Magnesium ammonium phosphate formation , recovery and its application as valuable resources: a review. **Journal of Chemical Technology & Biotechnology**, v. 88, n. May, p. 181–189, 2013.

LIU, Y.; NAIDU, R. **Hidden values in bauxite residue (red mud): Recovery of metalsWaste Management**, 2014.

LÜDKE, M. C. **A ROTA METALÚRGICA DO SILÍCIO: DA EXTRAÇÃO DO QUARTZO À OBTENÇÃO DO SILÍCIO DE GRAU FOTOVOLTAICO**. [s.l.] UNIVERSIDADE FEDERAL DE SANTA CATARINA, 2018.

LUO, A. A.; SACHDEV, A. K. **Applications of magnesium alloys in automotive engineering**. [s.l.] Woodhead Publishing Limited, 2012.

LV, X. et al. Non-isothermal kinetics study on carbothermic reduction of nickel laterite ore. **Powder Technology**, v. 340, p. 495–501, 2018.

MA, X. et al. One-step synthesis of basic magnesium sulfate whiskers by atmospheric pressure reflux. **Particuology**, v. 24, p. 191–196, 2016.

MACCARTHY, J. et al. Atmospheric acid leaching mechanisms and kinetics and rheological studies of a low grade saprolitic nickel laterite ore. **Hydrometallurgy**, v. 160, p. 26–37, 2016.

MACINGOVA, E.; LUPTAKOVA, A. Recovery of metals from acid mine drainage. **Chemical Engineering Transactions**, v. 28, n. 3, p. 109–114, 2012.

MAHMUD, N. et al. Magnesium recovery from desalination reject brine as pretreatment for membraneless electrolysis. **Desalination**, v. 525, n. August 2021, p. 115489, 2022.

MANN, R. A.; BAVOR, H. J. Phosphorus removal in constructed wetlands using gravel and industrial waste substrata. **Water Science and Technology**, v. 27, n. 1, p. 107–113, 1993.

MARCHI, J. et al. Influence of Mg-substitution on the physicochemical properties of calcium phosphate powders. **Materials Research Bulletin**, v. 42, n. 6, p. 1040–1050, 2007.

MCDONALD, R. G.; WHITTINGTON, B. I. Atmospheric acid leaching of nickel laterites review. Part II. Chloride and bio-technologies. **Hydrometallurgy**, v. 91, n. 1–4, p. 56–69, 2008.

MEHRA, D.; MAHAPATRA, M. M.; HARSHA, S. P. Processing of RZ5-10wt%TiC in-situ magnesium matrix composite. **Journal of Magnesium and Alloys**, v. 6, n. 1, p. 100–105, 2018.

MELLO, N. M. et al. Effect of an alumina supported palladium catalyst on the magnesium sulfate decomposition kinetics. **Materials Research**, v. 23, n. 6, 2020.

MENG, L. et al. Recovery of Ni, Co, Mn, and Mg from nickel laterite ores using alkaline oxidation and hydrochloric acid leaching. **Separation and Purification Technology**, v. 143, p. 80–87, 2015.

MME. **Boletim do Setor Mineral 2020**. Brasília, DF: [s.n.].

MO, L.; DENG, M.; TANG, M. Effects of calcination condition on expansion property of MgO-type expansive agent used in cement-based materials. **Cement and Concrete Research**, v. 40, n. 3, p. 437–446, 2010.

MONTEIRO, F. Z. R. **Estudo da decomposição térmica da fibra do coco verde na presença de um catalisador nano estruturado**. [s.l.] Pontifícia Universidade Católica do Rio de Janeiro, 2017.

MOODLEY, S. et al. **Chlorination of titania feedstocks**. TMS Annual Meeting. **Anais**...Hoboken, NJ, USA: John Wiley & Sons, Inc., 15 maio 2012Disponível em: <https://onlinelibrary.wiley.com/doi/10.1002/9781118364987.ch12>

MORCALI, M. H.; KHAJAVI, L. T.; DREISINGER, D. B. Extraction of nickel and cobalt from nickeliferous limonitic laterite ore using borax containing

slags. **International Journal of Mineral Processing**, v. 167, p. 27–34, 2017.

MOUSSAVI, G.; MAHMOUDI, M. Removal of azo and anthraquinone reactive dyes from industrial wastewaters using MgO nanoparticles. **Journal of Hazardous Materials**, v. 168, n. 2–3, p. 806–812, 2009.

NARAYAN, R.; TABATABAIE-RAISSI, A.; ANTAL JR, M. J. A Study of Zinc Sulfate Decomposition at Low Heating Rates. **Industrial & Engineering Chemistry Research**, v. 27, n. 6, p. 1050–1058, 1988.

NETZSCH. **Simultaneous Thermal Analyzer – STA 449 F3 Jupiter®**, 2022.

NKOSI, S. et al. **A comparative study of vanadium recovery from titaniferous magnetite using salt, sulphate, and soda ash roast-leach processes**. The Southern African Institute of Mining and Metallurgy. **Anais**...Pretoria: 2017Disponível em: <http://www.mintek.co.za/Pyromet/Files/2017Nkosi.pdf>. Acesso em: 7 fev. 2019

NURUNNABI, M. et al. Additive effect of noble metals on NiO-MgO solid solution in oxidative steam reforming of methane under atmospheric and pressurized conditions. **Applied Catalysis A: General**, v. 299, n. 1–2, p. 145–156, 2006.

OBERLE, B. et al. **Global Resources Outlook 2019: Natural Resources for the Future We Want.Global Resources Outlook 2019**. Nairobi, Kenya: UN, 16 set. 2020. Disponível em: <https://www.un-ilibrary.org/content/books/9789280737417>.

OKHRIMENKO, L. et al. Thermodynamic study of MgSO4 – H2O system dehydration at low pressure in view of heat storage. **Thermochimica Acta**, v. 656, n. August, p. 135–143, 2017.

OKHRIMENKO, L. et al. New kinetic model of the dehydration reaction of magnesium sulfate hexahydrate: Application for heat storage.

Thermochimica Acta, v. 687, n. July 2019, p. 178569, 2020.

OKUMURA, S. et al. Recovery of CaO by Reductive Decomposition of Spent Gypsum in a CO-CO 2-N2 Atmosphere. **Industrial and Engineering Chemistry Research**, v. 42, n. 24, p. 6046–6052, 2003.

OSLANEC, P.; IŽDINSKÝ, K.; SIMANČÍK, F. Possibilities of magnesium recycling. **Material Science and Technology**, v. 4, p. 83–88, 2008.

OSTROFFT, A. G.; SANDERSON, R. T. THERMAL STABILITY OF SOME METAL Department of Chemistry , State University of Iowa , Iowa City Abstract--The thermal decomposition of eleven (If) sulphates has been studied by a combination of thermogravimetric and differential thermal anlaysis . The re. **Journal of Inorganic and Nuclear Chemistry**, v. 9, p. 45–50, 1959.

OXLEY, A.; BARCZA, N. Hydro-pyro integration in the processing of nickel laterites. **Minerals Engineering**, v. 54, p. 2–13, 2013.

ÖZDEMIR, M.; ÇAKIR, D.; KIPÇAK, Í. Magnesium recovery from magnesite tailings by acid leaching and production of magnesium chloride hexahydrate from leaching solution by evaporation. **The International Journal of Mineral Processing**, v. 93, p. 209–212, 2009.

OZGA, P.; RIESENKAMPF, W. Effect of zinc sulphide concentrate composition and roasting temperature on magnesium distribution in zinc calcine. **Canadian Metallurgical Quarterly**, v. 35, n. 3, p. 235–244, 1996.

PAN, F.; YANG, M.; CHEN, X. A Review on Casting Magnesium Alloys: Modification of Commercial Alloys and Development of New Alloys. **Journal of Materials Science & Technology**, v. 32, n. 12, p. 1211–1221, 2016.

PAUL, S. A.; CHAVAN, S. K.; KHAMBE, S. D. Studies on characterization of textile industrial waste water in Solapur city. **International Journal of Chemical Sciences**, v. 10, n. 2, p. 635–642, 2012.

PAULIK, J.; PAULIK, F.; ARNOLD, M. Dehydration of magnesium sulphate heptahydrate investigated by quasi isothermal-quasi isobaric TG. **Thermochimica Acta**, v. 50, n. 1–3, p. 105–110, 1981.

PICKLES, C. A. Thermodynamic analysis of the selective chlorination of electric arc furnace dust. **Journal of Hazardous Materials**, v. 166, n. 2–3, p. 1030–1042, 30 jul. 2009.

PILARSKA, A. A.; KLAPISZEWSKI, Ł.; JESIONOWSKI, T. Recent development in the synthesis, modification and application of Mg(OH)2 and MgO: A review. **Powder Technology**, v. 319, p. 373–407, 2017.

PLEWA, J.; STEINDOR, J. Kinetics of reduction of magnesium sulfate by carbon oxide. **Journal of Thermal Analysis**, v. 32, n. 6, p. 1809–1820, 9 nov. 1987.

POMIRO, F. J. et al. Study of the Reaction Stages and Kinetics of the Europium Oxide Carbochlorination. **Metallurgical and Materials Transactions B: Process Metallurgy and Materials Processing Science**, v. 46, n. 1, p. 304–315, 2014.

RAM, A. **China's magnesium supply for rest of 2021 to lag demand: sources**. Disponível em: <https://www.spglobal.com/platts/en/market-insights/latest-news/metals/110321-chinas-magnesium-supply-for-rest-of-2021-to-lag-demand-sources>. Acesso em: 10 dez. 2021.

RAMALINGOM, S.; PODDER, J.; NARAYANA KALKURA, S. Crystallization and characterization of orthorhombic β-MgSO4·7H2O. **Crystal Research and Technology**, v. 36, n. 12, p. 1357–1364, 2001.

REGO, A. S. C. et al. KAl(SO4)2 thermal decomposition kinetics modeling through graphical and PSO methods. **Journal of Materials Research and Technology**, v. 14, n. 3, p. 1975–1984, set. 2021.

RIVA, L. et al. A study of densified biochar as carbon source in the silicon and ferrosilicon production. **Energy**, v. 181, p. 985–996, 15 ago. 2019.

ROCHE, E. G.; PRASAD, J. **Magnesium Oxide Recovery**USA, 2009.

RODE, H.; HLAVACEK, V. Detailed kinetics of titanium nitride synthesis. **AIChE Journal**, v. 41, n. 2, p. 377–388, fev. 1995.

RODRIGUES, R. **Modelagem Cinética e de Equilíbrio Combinadas para Simulação de Processos de Gaseificação**. [s.l.] UNIVERSIDADE FEDERAL DO RIO GRANDE DO SUL, 2015.

ROINE, A. O. **HSC Chemistry 10**Pori, Finland, 2021.

ROSITA, W. et al. Recovery of rare earth elements and Yttrium from Indonesia coal fly ash using sulphuric acid leaching. **AIP Conference Proceedings**, v. 2223, n. April, 2020.

SABATIER, M. et al. Influence of the consumption pattern of magnesium from magnesium-rich mineral water on magnesium bioavailability. **British Journal of Nutrition**, v. 106, n. 3, p. 331–334, 2011.

SAHOO, R. N.; NAIK, P. K.; DAS, S. C. Leaching of manganese from low-grade manganese ore using oxalic acid as reductant in sulphuric acid solution. **Hydrometallurgy**, v. 62, n. 3, p. 157–163, 2001.

SAKAKIBARA, M. et al. Kinetic Analysis of Thermogravimetric Data. **Nippon Kagaku Kaishi**, v. 1989, n. 10, p. 1729–1732, 1989.

SANCHEZ, M. E. et al. Thermogravimetric kinetic analysis of the combustion of biowastes. **Renewable Energy journal**, v. 34, p. 1622–1627, 2009.

SANTOS, F. et al. Behavior of Zn and Fe Content in Electric Arc Furnace Dust as Submitted to Chlorination Methods. **Metallurgical and Materials Transactions B**, v. 46, n. 4, p. 1729–1741, 21 ago. 2015.

SCHEIDEMA, M. **The reaction mechanism and operating window for the decomposition of hydrated magnesium sulfate under reducing conditions**. Helsinki: School of Chemical Technology, 2015.

SCHEIDEMA, M. N.; TASKINEN, P. Decomposition thermodynamics of magnesium sulfate. **Industrial and Engineering Chemistry Research**, v. 50, n. 16, p. 9550–9556, 2011.

SCHEIDEMA, M.; TASKINEN, P.; METSÄRINTA, M. L. Reductive decomposition of magnesium sulfate. **Proceedings - European Metallurgical Conference, EMC 2011**, v. 3, n. January, p. 1021–1032, 2011.

SETIAWAN, A. et al. Kinetics and Mechanisms of Carbothermic Reduction of Weathered Ilmenite Using Palm Kernel Shell Biomass. **Journal of Sustainable Metallurgy**, 2021.

SILVA, A. M.; LIMA, R. M. F.; LEÃO, V. A. Mine water treatment with limestone for sulfate removal. **Journal of Hazardous Materials**, v. 221–222, p. 45–55, 2012.

SILVA, L. R. DA. Magnesita. In: **Sumário Brasileiro Mineral 2018**. [s.l: s.n.]. p. 3.

SIRIWARDANE, R. V. et al. Decomposition of the sulfates of copper, iron (II), iron (III), nickel, and zinc: XPS, SEM, DRIFTS, XRD, and TGA study. **Applied Surface Science**, v. 152, n. 3, p. 219–236, 1999.

SOTO-DÍAZ, O. et al. Metal sulfate decomposition using green Pd-based catalysts supported on ΓAl2O3 and SiC: A common step in sulfur-family thermochemical cycles. **International Journal of Hydrogen Energy**, v. 4, p. 12309–12314, 2019.

SOUZA, A. D. et al. Kinetics of sulphuric acid leaching of a zinc silicate calcine. **Hydrometallurgy**, v. 89, n. 3–4, p. 337–345, 2007.

SOUZA, B. et al. MgSO4 carbothermic reductive decomposition to produce a highly reactive MgO powder. **Journal of Materials Research and Technology**, p. 9, 16 jan. 2020.

SOUZA, R. et al. Potassium alum thermal decomposition study under non-

reductive and reductive conditions. **Journal of Materials Research and Technology**, v. 8, n. 1, p. 745–751, 2019.

SPEYER, R. **Thermal Analysis of Materials**. 1st Editio ed. Boca Raton: CRC Press, 1994.

STOPIC, S.; FRIEDRICH, B. Hydrometallurgical processing of nickel lateritic ores. **Vojnotehnicki glasnik**, v. 64, n. 4, p. 1033–1047, 2016.

STOPIC, S.; FRIEDRICH, B.; FUCHS, R. Sulphuric acid leaching of the Serbian nickel lateritic ore. **Erzmetall: Journal for Exploration, Mining and Metallurgy**, v. 56, n. 4, p. 204–209, 2003.

SUK, N. I.; KOTELNIKOV, A. R.; KOVALSKII, A. M. Iron-magnesium minerals from differentiated rocks of Lovozersky alkaline massif. **Geochemistry, Mineralogy and Petrology.**, v. 47, p. 97–107, 2009.

TAIT, S. et al. Removal of sulfate from high-strength wastewater by crystallisation. **Water Research**, v. 43, n. 3, p. 762–772, 2009.

TANG, X. et al. Prospect of recovering phosphorus in magnesium slag-packed wetland filter. **Environmental Science and Pollution Research**, v. 24, p. 22808–22815, 2017.

THE ECONOMIST. **Why it matters that magnesium is in short supply**. Disponível em: <https://www.economist.com/the-economist-explains/2021/11/15/why-it-matters-that-magnesium-is-in-short-supply>. Acesso em: 8 dez. 2021.

THE MATHWORKS INC. **MATLAB R2021a**, 2021.

THE WORLD BANK. **The Growing Role of Minerals and Metals for a Low Carbon Future**. [s.l.] World Bank, Washington, DC, 2017.

TOLONEN, E. T.; RÄMÖ, J.; LASSI, U. The effect of magnesium on partial sulphate removal from mine water as gypsum. **Journal of Environmental Management**, v. 159, p. 143–146, 2015.

TOMAZ, M. A.; ANDRADE, F. V.; CANDIDO, A. D. O. Ph , Cálcio E Magnésio Influenciados Pelo Uso De Resíduos Industriais Utilizados Como Corretivos , Em Lavoura De Café Conilon Ph , Calcium and Magnesium Influenced By the Use of Industrial Waste Used As Correctives in Conilon Coffee Plantation. 2011.

U.S. GEOLOGICAL SURVEY. **Mineral Commodity Summaries 2021**. [s.l: s.n.].

UN DEPARTMENT OF ECONOMICS AND SOCIAL AFFAIRS. **World Population Prospects - Population Division - United Nations**. Disponível em: <https://population.un.org/wpp2019/>. Acesso em: 1 dez. 2021.

UNITED NATIONS. **United Nations Conference on the Human Environment**. Water Research. **Anais**...Stockholm: United Nations, 1973Disponível em: <https://linkinghub.elsevier.com/retrieve/pii/0043135473900778>

UNITED NATIONS. **World Population Prospects 2019: Highlights**. New York: [s.n.]. Disponível em: <http://www.ncbi.nlm.nih.gov/pubmed/12283219>.

UNLUER, C.; AL-TABBAA, A. Impact of hydrated magnesium carbonate additives on the carbonation of reactive MgO cements. **Cement and Concrete Research**, v. 54, p. 87–97, 2013.

UNLUER, C.; AL-TABBAA, A. Enhancing the carbonation of MgO cement porous blocks through improved curing conditions. **Cement and Concrete Research**, v. 59, p. 55–65, 2014.

UROSEVIC, D. M. et al. Recovery of copper from copper slag and copper slag flotation tailings by oxidative leaching. **Physicochemical Problems of Mineral Processing**, v. 51, n. 1, p. 73–82, 2015.

VACHUŠKA, J.; VOBOŘIL, M. Kinetic data computation from non-isothermal thermogravimetric curves of non-uniform heating rate.

Thermochimica Acta, v. 2, n. 5, p. 379–392, 1971.

VEDABOURISWARAN, G.; ARAVINDAN, S. Development and characterization studies on magnesium alloy (RZ 5) surface metal matrix composites through friction stir processing. **Journal of Magnesium and Alloys**, v. 6, n. 2, p. 145–163, 2018.

WANDERLEY, K. B. **Recuperação de magnésio do licor de lixiviação de minério limonítico por cristalização.** São Paulo: Universidade de São Paulo, 24 maio 2018.

WANDERLEY, K. B. et al. Kinetic and thermodynamic study of magnesium obtaining as sulfate monohydrate from nickel laterite leach waste by crystallization. **Journal of Cleaner Production**, v. 272, 2020.

WANG, F. et al. Three-year performance of in-situ mass stabilised contaminated site soils using MgO-bearing binders. **Journal of Hazardous Materials**, v. 318, p. 302–307, 2016a.

WANG, Q. et al. Selective chlorination of CaO from titania slag by CO+Cl2 mixtures in fluidized bed. **Thermochimica Acta**, v. 640, p. 66–73, 2016b.

WANG, Y. et al. Kinetic study on preparation of substoichiometric titanium oxide via carbothermal process. **Journal of Thermal Analysis and Calorimetry**, v. 122, n. 2, p. 635–644, 2015.

WANG, Y.; AKAISHI, M.; YAMAOKA, S. Diamond formation from graphite in the presence of anhydrous and hydrous magnesium sulfate at high pressures and high temperatures. **Diamond and Related Materials**, v. 8, n. 1, p. 73–77, 1999.

WEBMINERAL. **www.webmineral.com**. Disponível em: <www.webmineral.com>. Acesso em: 6 abr. 2022.

WHITTINGTON, B. I. Characterization of scales obtained during continuous nickel latérite pilot-plant leaching. **Metallurgical and Materials Transactions B: Process Metallurgy and Materials Processing**

Science, v. 31, n. 6, p. 1175–1186, 2000.

WHITTINGTON, B. I.; MUIR, D. Pressure Acid Leaching of Nickel Laterites: A Review. **Mineral Processing and Extractive Metallurgy Review: An International Journal**, v. 21, n. 6, p. 527–599, out. 2000.

XIA, X. et al. Recovery of CaO from CaSO4 via CO reduction decomposition under different atmospheres. **Journal of Environmental Management**, v. 301, n. June 2021, p. 113855, 2022.

XIAO, J. et al. Extraction of Nickel from Garnierite Laterite Ore Using Roasting and Magnetic Separation with Calcium Chloride and Iron Concentrate. **Minerals**, v. 10, n. 4, p. 352, 15 abr. 2020.

XUE-YI, G. U. O. et al. Leaching behavior of metals from limonitic laterite ore by high pressure acid leaching. **Transactions of Nonferrous Metals Society of China**, v. 21, n. 1, p. 191–195, 2010.

YAM, B. J. Y. et al. Recycling of magnesium waste into magnesium hydroxide aerogels. **Journal of Environmental Chemical Engineering**, v. 8, n. 5, p. 104101, out. 2020.

YANFEI, X. et al. Recovery of rare earths from weathered crust elution-deposited rare earth ore without ammonia-nitrogen pollution: I. leaching with magnesium sulfate. **Hydrometallurgy**, v. 153, p. 58–65, 2015.

YANG, J. et al. Recovery of Magnesium from Ferronickel Slag to Prepare Magnesium Oxide by Sulfuric Acid Leaching. **Minerals**, v. 11, n. 12, p. 1375, 6 dez. 2021.

YANG, Z. et al. Catalytic partial oxidation of coke oven gas to syngas in an oxygen permeation membrane reactor combined with NiO/MgO catalyst. **Renewable Energy**, v. 35, n. 12, p. 6239–6247, 2010.

YAROSHEVSKY, A. A. Abundances of Chemical Elements in the Earth's Crust. **Geochemistry International**, v. 44, n. 1, p. 48–55, 2006.

YÖRÜKOĞLU, A.; OBUT, A.; GIRGIN, I. Effect of thiourea on sulphuric

acid leaching of bastnaesite. **Hydrometallurgy**, v. 68, n. 1–3, p. 195–202, 2003.

ZHAI, X. et al. Intensification of sulphation and pressure acid leaching of nickel laterite by microwave radiation. **Hydrometallurgy**, v. 99, n. 3–4, p. 189–193, 2009.

ZHANG, B. et al. Remediation of the vanadium slag processing residue and recovery of the valuable elements. **Process Safety and Environmental Protection**, v. 128, p. 362–371, 1 ago. 2019.

ZHANG, W.; ZHU, Z.; CHENG, C. Y. A literature review of titanium metallurgical processes. **Hydrometallurgy**, v. 108, n. 3–4, p. 177–188, jul. 2011.

ZHANG, X. et al. Density functional theory study on the mechanism of calcium sulfate reductive decomposition by carbon monoxide. **Industrial and Engineering Chemistry Research**, v. 51, n. 18, p. 6563–6570, 2012.

ZHANG, X. et al. Density functional theory study on the mechanism of calcium sulfate reductive decomposition by methane. **Fuel**, v. 110, p. 204–211, 2013.

ZHAO, Q. et al. Recovery of calcium and magnesium bearing phases from iron– and steelmaking slag for CO2 sequestration. **Process Safety and Environmental Protection**, v. 135, p. 81–90, 2020.

ZHENG, G. et al. Study on kinetics of the pyrolysis process of aluminum sulfate. **Phosphorus, Sulfur and Silicon and the Related Elements**, v. 195, n. 4, p. 285–292, 2020.

ZHU, F. L. et al. Behavior of titanium dioxide in alumina carbothermic reduction-chlorination process in vacuum. **Transactions of Nonferrous Metals Society of China (English Edition)**, v. 21, n. 8, p. 1855–1859, ago. 2011.

ZHU, T. et al. Innovative Vacuum Distillation for Magnesium Recycling. In:

Essential Readings in Magnesium Technology. Cham: Springer International Publishing, 2016. p. 157–162.

8.3. Code used in attachments 1 and 2

```
% Código de ajuste do Matlab para curvas de TG utilizando o modelo de
% Speyer (1995)

clear all
close all
clc

Rcte = 8.314;        % J/mol.K
```

```
data_total = load('MgSO4 Hepta + C 10C.txt');

data_local = data_total(8270:10696, :);


[tr, phi] = calc_tr_phi(data_total);   % Calcula parâmetros Tr e phi do modelo


temp = data_local(:, 1) + 273.15; % Temperatura

t = data_local(:, 2);   % Tempo

dm = data_local(:, 3);  % Perda de massa local

nexp = length(dm);      % Número de pontos experimentais


dm0 = data_local(1, 3);     % Primeiro ponto de perda de massa

dmf = data_local(end, 3);    % Último ponto de perda de massa


f = zeros(length(dm), 1);

for i = 1:length(dm)

    f(i) = (dm(i) - dm0) / (dmf - dm0);   % Calcula o 'weight fraction'

    if f(i) < 0

        f(i) = 0;

    end

    if f(i) > 1

        f(i) = 1;

    end

end
```

```
[fcalc, dfcalc, d2fcalc, fobj] = ajustasigmoide(t,f); % Ajusta os parâmetros da curva sigmoide segundo os daods experimentais

x_speyer = ((phi * t + tr) .^ 2 .* dfcalc) ./ (1 - fcalc);  % Linearização do modelo do Speyer (coeficiente angular)

y_speyer = ((phi * t + tr) .^ 2 .* d2fcalc) ./ (dfcalc);  % Linearização do modelo do Speyer (coeficiente linear)

[x_speyer_smooth, y_speyer_smooth] = data_smooth(x_speyer, y_speyer);  % Suavização dos dados da linearização de Speyer

[par, n, Ea] = ajuste_dados(x_speyer_smooth,y_speyer_smooth, phi, Rcte);  % Calcula os coeficientes angular e linear, além da energia de ativação e ordem da reação

ycalc = par(1) * x_speyer_smooth + par(2);

[m, b, r_speyer] = reglin(x_speyer_smooth, y_speyer_smooth); % Qualidade da regressão do modelo

[m, b, r_sigmoid] = reglin(f, fcalc); % Qualidade da sigmoide feita

% GRÁFICOS
```

```
figure(1)

plot(temp, f, 'b-')

hold on

plot(temp, fcalc, 'k-')

xlabel('Temperature (K)', 'FontSize', 16)

ylabel('$f$','Interpreter','latex', 'FontSize', 16)

legend('Experimental', 'Sigmoid', 'FontSize', 12, 'Location', 'Southeast')

title(['Weight fraction - R^2 = ', num2str(r_sigmoid), ' - SSE = ', num2str(fobj)], 'FontSize', 14)

axis([temp(1) temp(end) 0 1])

saveas(gcf,'1.fig')% I want to save the g as *.tif sequencly exp. A1,A2,A3....


figure(2)

plot(f, fcalc, 'ko', 'MarkerSize', 3)

hold on

plot([0 1], [0 1], 'k--')

xlabel('Experimental', 'FontSize', 16)

ylabel('Sigmoid', 'FontSize', 16)

title(['Comparative plot - Experimental vs. Sigmoid - R^2=', num2str(r_sigmoid)], 'FontSize', 14)

axis([0 1 0 1])

saveas(gcf,'2.fig')% I want to save the g as *.tif sequencly exp. A1,A2,A3....
```

```
figure(3)

plot(x_speyer_smooth, y_speyer_smooth, 'b-')

hold on

plot(x_speyer_smooth, ycalc, 'k-')

xlabel('$\frac{(\phi t+Tr)^2(df/dt)}{(1-f)}$','Interpreter','latex', 'FontSize', 20)

ylabel('$\frac{(\phi t+Tr)^2(d^2f/dt^2)}{(df/dt)}$','Interpreter','latex',
'FontSize', 20)

legend('Experimental', 'Regression', 'FontSize', 12, 'Location', 'Southwest')

title(['Linearization - Speyer (comparison) - R^2=', num2str(r_speyer)],
'FontSize', 14)

saveas(gcf,'3.fig')% I want to save the g as *.tif sequencly exp. A1,A2,A3....
```